

This is to certify that the  
dissertation entitled

MOLECULAR DESIGN AND CHARACTERIZATION OF  
*THERMOANAEROBACTER ETHANOLICUS* 39E  
SECONDARY ALCOHOL DEHYDROGENASE FOR CHIRAL  
AROMATIC ALCOHOL SYNTHESIS AND COFACTOR  
SPECIFICITY CHANGE

presented by

Karla Iris Ziegelmann-Fjeld

has been accepted towards fulfillment  
of the requirements for the

Ph.D.

degree in

Biochemistry and Molecular  
Biology

A handwritten signature in cursive script, appearing to read "J. J. Ziegelmann-Fjeld".

Major Professor's Signature

5/15/07

Date

**PLACE IN RETURN BOX** to remove this checkout from your record.  
**TO AVOID FINES** return on or before date due.  
**MAY BE RECALLED** with earlier due date if requested.

DATE DUE	DATE DUE	DATE DUE

**MOLECULAR DESIGN AND CHARACTERIZATION OF  
*THERMOANAEROBACTER ETHANOLICUS* 39E SECONDARY  
ALCOHOL DEHYDROGENASE FOR CHIRAL AROMATIC  
ALCOHOL SYNTHESIS AND COFACTOR SPECIFICITY CHANGE**

By

Karla Iris Ziegelmann-Fjeld

A DISSERTATION

Submitted to  
Michigan State University  
in partial fulfillment of the requirements  
for the degree of

DOCTOR OF PHILOSOPHY

Department of Biochemistry and Molecular Biology

2007



## **ABSTRACT**

### **MOLECULAR DESIGN AND CHARACTERIZATION OF *THERMOANAEROBACTER ETHANOLICUS* 39E SECONDARY ALCOHOL DEHYDROGENASE FOR CHIRAL AROMATIC ALCOHOL SYNTHESIS AND COFACTOR SPECIFICITY CHANGE**

**By**

**Karla Iris Ziegelmann-Fjeld**

There is an increasing demand for environmentally friendly industrial technologies. Many current industrial chemical processes use harsh conditions (i.e., high temperature or extremes of pH), create toxic waste, and require non-renewable resources. The use of biocatalysts, such as isolated enzymes, to replace these harsh processes is a field of intense study.

Many enzymes are not well suited to industrial processes because of their lack of stability or lack of specificity. Advances in the field of enzyme engineering have allowed for the alteration of enzyme characteristics, such increased thermostability or tailored substrate specificity, to meet the needs of a specific industrial process.

In this thesis we will describe the alteration of the substrate specificity of a secondary alcohol dehydrogenase from *Thermoanaerobacter ethanolicus* (TeSADH) by rational design to include phenyl-substituted alcohols and ketones for industrial use. The W110A mutation was introduced to increase the size of the active site. W110A TeSADH uses (S)-1-phenyl-2-propanol, (S)-4-phenyl-2-butanol, and the corresponding ketones as substrates. W110A TeSADH's kinetic parameters on these substrates are in the same range as those of TeSADH on 2-butanol, making W110A TeSADH an excellent catalyst. In particular, W110A TeSADH is twice as efficient on benzylacetone as TeSADH is on

2-butanol, and it produces (S)-4-phenyl-2-butanol from benzylacetone with an enantiomeric excess above 99%. W110A TeSADH is active on aryl derivatives of phenylacetone and benzylacetone, making this enzyme a potentially useful catalyst for the chiral synthesis of aryl derivatives of alcohols.

We also describe attempts to change the cofactor specificity of TeSADH from NADP(H) to NAD(H). NADP(H) is more unstable and more costly than NAD(H), which makes it less economically feasible to use. We use both rational design and directed evolution to accomplish our goals. We constructed a triple mutant, GCY, by site-directed mutagenesis to use as our parent for directed evolution. This mutant had a 9-fold increase in  $K_m$  compared to TeSADH with  $NAD^+$ , but its  $V_{max}$  is comparable to TeSADH with  $NADP^+$ .

Two rounds of directed evolution were performed. Kinetic parameters of the first generation mutant,  $\Omega E3$ , were better than those of its parent, GCY, for  $NAD^+$ . Its  $K_m$  for  $NAD^+$  decreased nearly 2-fold and its  $V_{max}$  decreased only 1.1 times compared to GCY.

The kinetic parameters of the second generation mutant, 2E, were almost identical to those of its parent,  $\Omega E3$ , for  $NAD^+$ , with a 0.92-fold decrease in  $K_m$  and 1.1-fold decrease in  $V_{max}$ . However, the  $K_m$  of 2E for  $NADP^+$  increased by 662.5 times, and the  $V_{max}$  decreased by 16 times compared to wild-type TeSADH. 2E has a 7.4-fold higher  $V_{max}$  with  $NAD^+$  than with  $NADP^+$ , and a 7.3-fold higher catalytic efficiency with  $NAD^+$  than with  $NADP^+$ . These results show that the cofactor preference of 2E TeSADH has changed from  $NADP^+$  to  $NAD^+$ .

To Christopher, Declan, and our families

## **Acknowledgements**

I would like to thank my advisor Dr. J. Gregory Zeikus, and my committee members, Dr. R. Michael Garavito, Dr. Rawle Hollingsworth, Dr. R. Mark Worden, and Dr. Honggao Yan, for their patience and guidance. I would also like to thank Dr. Robert Phillips and Musa M. Musa, from the Department of Chemistry, University of Georgia-Athens, who added an additional dimension to the work done on this project. I would like to gratefully acknowledge Dr. Claire Vieille for her years of guidance and assistance with all my writings. I also gratefully acknowledge Maris Laivenieks for his years of guidance and technical assistance. I would also like to acknowledge former Zeikus lab members, Dr. James B. McKinlay and Dr. Harini Krishnamurthy, and postdoctoral researcher, Dr. Pil Kim, and former fellow graduate students Dr. Darrell R. Boverhof, and Dr. Clarisa M. Bejar for valuable discussions and friendship. I would also like to thank all the friends that I have made during my time at MSU, who have made this an even more enjoyable experience. I would like to thank our families, especially my sister-in-law Mary, who have always been there for us during the time we have spent away from home.

Finally, would like to thank my husband, Christopher, and my son, Declan, for all the support and love that they have provided during my years as a graduate student. Without them, none of this would have been possible.

## Table of Contents

<b>List of Tables</b> .....	ix
<b>List of Figures</b> .....	x
<b>List of Schemes</b> .....	xii
<b>List of Abbreviations</b> .....	xiii
<b>CHAPTER I</b> .....	1
1.1 Biocatalysis in industry .....	2
1.2 Limitations and Developments of Enzymes for Industrial Purposes .....	4
1.3 Thermostable Enzymes .....	10
1.4 ADHs .....	13
1.5 Stereospecificity of ADHs .....	19
1.6 TeSADH .....	23
1.7 NADH vs. NADPH .....	25
1.8 Objectives .....	31
1.9 Acknowledgements .....	32
1.10 References .....	33
<b>CHAPTER II: A <i>Thermoanaerobacter ethanolicus</i> secondary alcohol dehydrogenase mutant derivative highly active and stereoselective on phenylacetone and benzylacetone</b> .....	40
2.1 Abstract .....	41
2.2 Introduction .....	43
2.3 Materials and methods .....	48
2.3.1 Chemicals .....	48
2.3.2 Syntheses of phenylacetone, and (S)- and (R)-4-phenyl-2- butanol .....	48
2.3.3 Modeling .....	49
2.3.4 Mutagenesis .....	50
2.3.5 Protein expression and purification .....	52
2.3.6 Enzyme assays .....	52
2.3.7 Asymmetric reduction of benzylacetone to the corresponding <i>sec</i> -alcohol .....	54
2.3.8 Stability assays .....	54
2.4 Results and discussion .....	56
2.4.1 Modeling and mutagenesis .....	56
2.4.2 Activity and substrate specificity .....	67
2.4.3 Effect of pH on enzyme activity .....	68
2.4.4 W110A TeSADH's enantioselectivity .....	68
2.4.5 Effects of temperature on W110A TeSADH activity and stability .....	72

2.4.6	W110A TeSADH activity on aryl derivatives of phenylacetone and benzylacetone .....	75
2.4.7	Effect of solvent on W110A TeSADH stability .....	78
2.4.8	Validation of our modeling approach .....	80
2.5	Conclusions .....	81
2.6	Acknowledgements .....	82
2.7	References .....	83

### **CHAPTER III: Molecular Design and Characterization of *Thermoanaerobacter ethanolicus* 39E Secondary Alcohol Dehydrogenase for**

Cofactor Specificity Change .....	86
3.1 Abstract .....	87
3.2 Introduction .....	88
3.3 Materials and methods .....	95
3.3.1 Strains and plasmids .....	95
3.3.2 Structural and sequence comparisons .....	95
3.3.3 Site directed mutagenesis .....	96
3.3.4 Error prone PCR .....	97
3.3.5 Screening .....	98
3.3.6 Protein expression and purification .....	99
3.3.7 Enzyme assays .....	101
3.3.8 TeSADH NAD <sup>+</sup> inhibition .....	104
3.4 Results and discussion .....	105
3.4.1 TeSADH inhibition .....	105
3.4.2 Construction and characterization of a TeSADH G198D/Y218F double mutant .....	108
3.4.3 Structural and sequence comparisons .....	108
3.4.4 Site directed mutagenesis .....	112
3.4.5 Directed evolution .....	112
3.4.6 Enzyme activity .....	118
3.5 Conclusions .....	121
3.6 References .....	122

### **CHAPTER IV**

Conclusions and directions for future research .....	125
4.1 W110A TeSADH .....	126
4.2 Future work with W110A TeSADH .....	127
4.3 Changing TeSADH cofactor specificity .....	128
4.4 Future work to increase NAD(H) specificity of TeSADH .....	129
4.5 References .....	131

### **APPENDIX A**

Asymmetric reduction and oxidation of aromatic ketones and alcohols using W110A secondary alcohol dehydrogenase from

<i>Thermoanaerobacter ethanolicus</i> .....	134
A.1 Abstract .....	135

A.2	Introduction .....	137
A.3	Results and discussion .....	141
A.4	Conclusions .....	152
A.5	Experimental section .....	153
A.5.1	General procedures .....	153
A.5.2	Materials .....	153
A.5.3	Gene expression and purification of W110A TESADH .....	153
A.5.4	General procedure for asymmetric reduction of phenyl rRing- containing ketones with W110A TESADH .....	153
A.5.5	(+)-(2 <i>S</i> ,3 <i>R</i> )-3-Chloro-4-(4-chlorophenyl)-2-butanol ((+)- (2 <i>S</i> ,3 <i>R</i> )-6b) .....	154
A.5.6	General Procedure for Kinetic Resolution of Phenyl Ring- Containing Racemic Alcohols with W110A TESADH .....	154
A.5.7	Synthesis of (-)-(2 <i>S</i> ,3 <i>S</i> )-4-(4-Chlorophenyl)-2,3-epoxybutane ((-)-(2 <i>S</i> ,3 <i>S</i> )-6c) .....	155
A.5.8	Determination of absolute configuration .....	155
A.6	Acknowledgements .....	156
A.7	Supporting information .....	157
A.8	References .....	158

## APPENDIX B

Sol-gel encapsulated W110A secondary alcohol dehydrogenase from

*Thermoanaerobacter ethanolicus* performs asymmetric reduction

of hydrophobic ketones in organic solvent .....	161
B.1 Introduction, results and discussion .....	162
B.2 Experimental section .....	172
B.3 References .....	174
B.4 Asymmetric synthesis .....	176

## List of Tables

1-1	Potential benefits of using thermostable proteins as industrial catalysts .....	5
1-2	Kinetic parameters for G198D and Y218F TeSADH mutants .....	30
2-1	Specific activities of wild-type TeSADH and W110A TeSADH on multiple substrates .....	69
2-2	Kinetic parameters of W110A TeSADH on multiple substrates .....	70
2-3	Activity of W110A TeSADH on (1 mM) aryl derivatives .....	76
3-1	TeSADH and G198D and Y218F TeSADH kinetic parameters .....	93
3-2	All mutants constructed by SDM and tested for activity .....	113
3-3	Kinetic parameters of TeSADH, G198D TeSADH, GCY TeSADH, and TeSADH DE mutants ΩE3 and 2E for NAD <sup>+</sup> and 2-butanol .....	114
3-4	Mutations in the DE parent and resulting enzymes .....	114
3-5	Locations of mutated residues in DE mutants .....	115
3-6	Specific activities of TeSADH, SDM mutant GCY, and DE mutants ΩE3 and 2E .....	119
3-7	Kinetic parameters of TeSADH with NAD <sup>+</sup> , and TeSADH DE mutant 2E for NAD <sup>+</sup> and NADP <sup>+</sup> .....	119
A-1	Asymmetric Reduction of Phenyl Ring-Containing Ketones Using W110A TeSADH .....	142
A-2	Enantiospecific Kinetic Resolution of Phenyl Ring-Containing <i>rac</i> -Alcohols Using W110A TeSADH .....	148
B-1	Asymmetric reduction of 1a by using sol-gel-encapsulated W110A TeSADH in different media .....	165
B-2	Asymmetric reduction of phenyl-ring-containing ketones by using sol-gel W110A TeSADH in organic solvents .....	168



## List of Figures

**Images in this dissertation are presented in color**  
**Stereo images are presented in “wall-eyed” mode**

1-1	Hydride transfer of the <i>pro</i> R hydrogen of cofactor NAD(P)(H) during alcohol reduction or ketone/aldehyde oxidation .....	14
1-2	The ordered bi bi reaction mechanism carried out by HLADH .....	15
1-3	Residues His51 and Ser48 bound to the nicotinamide ribose of the NAD <sup>+</sup> of HLADH .....	20
1-4	Sequence comparison of the Zn binding sites of HLADH and TeSADH .....	24
1-5	Sequence comparison of HLADH, TeSADH, and YADH .....	29
2-1	TbSADH active site in CPK representation, based on PDB # 1YKF .....	45
2-2	Modeling of the TbSADH•(S)-2-butanol and the TbSADH•(S)-NADP <sup>+</sup> binary complexes into a single, TbSADH•(S)-2-butanol•(S)-NADP <sup>+</sup> model .....	57
2-3	Modeling of (S)-1-phenyl-2-propanol in the catalytic sites of TeSADH and W110A TeSADH using the HLADH•BRB•NAD <sup>+</sup> ternary complex as the template .....	59
2-4	Geometry of hydride transfer in HLADH .....	61
2-5	NAD <sup>+</sup> hydrogen bonded with HLADH, and NADP <sup>+</sup> from TeSADH .....	62
2-6	(S)-1-Phenyl-2-propanol modeled in the TbSADH•(S)-2-butanol•NADP <sup>+</sup> ternary complex .....	64
2-7	Effect of pH on W110A TeSADH activity .....	71
2-8	Temperature activity profiles of W110A TeSADH .....	73
2-9	Kinetic stability of W110A TeSADH versus TeSADH .....	74

2-10	Solvent stability of W110A TeSADH .....	79
3-1	Kinetics of NADP <sup>+</sup> reduction by 2E TeSADH with 2-butanol as the oxidation substrate at pH 8.0 and 60°C .....	103
3-2	Inhibition of TeSADH by NAD <sup>+</sup> shown as a Lineweaver-Burke plot .....	106
3-3	Inhibition of TeSADH by NAD <sup>+</sup> .....	107
3-4	Comparison of the TeSADH, YADH, and HLADH NAD(P)(H) binding residues .....	109
3-5	Superimposed TeSADH and HLADH cofactor binding sites .....	110
3-6	Locations of all mutations in DE mutant 2E .....	116
A-1 -	Prelog's rule for predicting the stereochemistry of alcohols formed from their corresponding ketones by asymmetric reduction with ADHs .....	139
A-2 -	GC chromatograms illustrating (a) the products of NaBH <sub>4</sub> reduction .....	145

## List of Schemes

1-1	Proton transfer/deprotonation system of HLADH .....	21
3-1	NAD(P)(H), PMS and NBT reaction to produce formazan dye .....	100
A-1	Conversion of (+)-(2 <i>S</i> ,3 <i>R</i> )-6b into (-)-(2 <i>S</i> ,3 <i>S</i> )-6c .....	146

## Abbreviations

ADH	Alcohol dehydrogenase
<i>adhB</i>	Gene encoding the <i>T. ethanolicus</i> secondary alcohol dehydrogenase
BLA	<i>Bacillus licheniformis</i> $\alpha$ -amylase
BRB	p-bromobenzyl alcohol
CmFDH	<i>Candida methylica</i> formate dehydrogenase
DE	Directed evolution
E	Enantiomeric ratio
ee	Enantiomeric excess
EXAFS	Extended X-ray Absorption Fine Structure
FDH	Formate dehydrogenase
G198D TeSADH	TeSADH containing the mutation G198D
GCY TeSADH	TeSADH containing the mutations G198D/C203K/Y218P
GO	Galactose oxidase
HLADH	Primary alcohol dehydrogenase from horse liver
ICP-AES	Inductively coupled plasma - atomic emission spectroscopy
IDH	Isocitrate dehydrogenase
IMDH	Isopropylmalate dehydrogenase
L-Tle	L- <i>tert</i> -leucine
NBT	nitroblue tetrazolium
NMR	Nuclear magnetic resonance
PMS	phenazine methosulfate
SADH	Secondary alcohol dehydrogenase

ScFDH	<i>S. cerevisiae</i> formate dehydrogenase
SDM	Site-directed mutagenesis
TeSADH	Secondary alcohol dehydrogenase from <i>Thermoanaerobacter ethanolicus</i> 39E
TbSADH	Secondary alcohol dehydrogenase from <i>Thermoanaerobacter brockii</i>
W110A TeSADH	TeSADH containing the mutation W110A
Y218F TeSADH	TeSADH containing the mutation Y218F
Y267G TeSADH	TeSADH containing the mutation Y267G
YADH	Primary alcohol dehydrogenase I from <i>Saccharomyces cerevisiae</i>
1HLD	PDB code for horse liver alcohol dehydrogenase structure complexed with p-bromobenzyl alcohol and NAD <sup>+</sup>
1BXZ	PDB code for <i>T. ethanolicus</i> secondary alcohol dehydrogenase complexed with 2-butanol
1YKF	PDB code for <i>T. ethanolicus</i> secondary alcohol dehydrogenase complexed with NADP <sup>+</sup>
2E TeSADH	TeSADH containing the mutations G198D/C203K/Y218P/D186V/I49V/N54S/D315N
ΩE3 TeSADH	TeSADH containing the mutations G198D/C203K/Y218P/D186V

# **CHAPTER I**

## **Literature Review**

**By**

**Karla Iris Ziegelmann-Fjeld**

## **1.1 Biocatalysts in industry**

Biocatalytic processes were first implemented in industry many decades ago and there has since been an ever expanding interest in the use of biocatalysts (57). The shift to enzymes in industrial synthesis, rather than the use of traditional chemical synthesis, is a reflection of the growing need for “cleaner” technology that creates less waste, uses fewer harsh chemicals that are not environmentally friendly, and uses fewer non-renewable resources (2).

The shift to enzyme catalysis also reflects an increased industrial demand for chiral purity of compounds to produce safer and purer products for consumption. This is particularly true for pharmaceutical production due to FDA mandates requesting that compounds must either be enantiomerically pure, or that extensive toxicity testing be performed to ensure that the contaminating enantiomer is not biologically detrimental (8, 17). These extra expenses and efforts will be an increasing burden on a ballooning demand for chiral chemicals. For example, the 2000 world market for chiral pharmaceuticals exceeded \$100 billion (25). The production of pure chiral compounds by traditional chemical synthesis can only be ensured if the reaction is fed an already pure chiral feedstock due to the high cost and difficulty of racemate separation (8).

Numerous industrial-scale chemical syntheses (i.e., of polymer intermediates, pharmaceuticals, agrochemicals, and specialty chemicals) are hindered by low-selectivity processes, and by the production of undesirable byproducts (16). Enzymatic reactions can be carried out at neutral or close to neutral pH, and ambient temperatures and pressures, which can reduce the incidence of undesirable isomerization, racemization, epimerization, and rearrangement reactions. Enzymatic reactions can replace some

classical organic chemical reactions that are difficult to conduct, or replace a multi-step chemical reaction with a single enzymatic reaction. Enzymatic reactions are typically highly regio- and stereospecific (31, 43). This specificity eliminates the need for tedious blocking and deblocking steps typically required in chemical synthesis, and also eliminates many byproducts (56). The use of enzymes as catalysts also eliminates the need for expensive chemical catalysts, which can be difficult to produce, regenerate, and separate from the final product (31).

One well-known immobilized enzyme process that has been in use since 1973 is the production of the  $\beta$ -lactam antibiotic precursor 6-aminopenicillanic acid (6APA) using penicillin amidase from penicillin G or V. Most  $\beta$ -lactam antibiotics, penicillins and cephalosporins, are prepared from one of three precursors: 6APA, 7-aminocephalosporanic acid (7ACA), or 7-amino-des-acetoxyccephalosporanic acid (7ADCA). In this case, the use of a single enzyme reaction replaces several chemical steps and eliminates the need for organic solvents, low temperatures ( $-40^{\circ}\text{C}$ ) and completely anhydrous conditions (31).

In conventional acrylamide synthesis, nitriles are hydrated by copper salt catalysts. This process is problematic in that preparing the copper catalysts is a very complex process, regenerating the copper catalysts is difficult, and separating and purifying the acrylamide both from the remaining substrate and the spent catalysts is difficult as well. In the biocatalytic process, acetonitrile conversion to acrylamide is nearly 100%, which eliminates the need for the separation of the substrate and product. Also, because using immobilized cells eliminates the need for the copper catalysts, the removal of copper ions from the product is no longer needed. Finally the bioprocess's



mild reaction conditions prove to be more economical than those of the copper-catalyzed reaction. This immobilized cell process has been used by the Nitto Tire Corporation since 1985 to produce about 6000 tons of acrylamide per year (31).

In the food industry, the use of xylanase for the separation of soluble and insoluble xylans in the production of wheat flour uses much less water than the previous chemical processes, and consequently produces much less waste water. Also, an amylolytic step to break down starch has replaced the strong acid and high temperature treatment that was previously needed for starch processing (2). The food industry also uses xylose isomerase to catalyze the isomerization of D-glucose to D-fructose for the production of high fructose corn syrup (56).

Other examples of current enzymatic processes are the use of acylases, hydantoinases, and aminopeptidases for the production of optically pure amino acids (57). The bulk chemical industry employs peroxidases to catalyze the synthesis of phenolic resins to replace conventional phenol-formaldehydes (56).

Due to poor stability in harsh reaction conditions, mesophilic enzymes are often not well suited for industrial synthesis (16). For this reason, thermostable enzymes are a target of industrial interest. The many potential benefits of using thermostable proteins in industry versus using mesophilic enzymes are listed in Table 1.

## **1.2 Limitations and Developments of Enzymes for Industrial Purposes**

Economic factors must be taken into account in any industrial-scale process. High conversion rates, specificity and selectivity, catalyst stability, and space-time yield must be considered during the scale-up of any reaction (69).

**Table 1-1. Potential benefits of using thermostable proteins as industrial catalysts**

	Benefit	Reference
Increased reaction temperature	▪ Reduced viscosity of the reaction mixture	(10)
	▪ Increased solubility of some reactants to allow for the use of higher concentrations	(10)
	▪ Easier removal of volatile products under light vacuum conditions, which can also decrease the build-up of inhibitory byproducts	(10)
	▪ Reduced bioreactor cooling costs	(10)
	▪ Reduced risks of growth of mesophilic contaminants	(10)
	▪ Increased diffusion coefficient of organic compounds	(40)
Other benefits gained from using thermostable enzymes	▪ These enzymes are more resistant to detergents and solvents that are often used as substrates, produced as products, or are reaction contaminants	(10)
	▪ Immobilized enzyme reactors have a longer period of operation, which reduces production costs	(10)
	▪ Enzymes can be purified at room temperature	(10)
	▪ Increased enzyme solvent stability allows for the addition of organic solvents to the reaction to increase the solubility of poorly water-soluble substrates/products	(59)
	▪ Increased shelf-life and longer life during use	(54)

Substrate cost can be a limiting factor in the industrial costs of biocatalysts. One such case is the production of L-phenylalanine. L-Phenylalanine can be produced in two ways: reductive amination of phenylpyruvate by L-phenylalanine dehydrogenase, or by fermentation with glucose and ammonia. Because phenylpyruvate is prohibitively expensive, L-phenylalanine commercial production is carried out by fermentation (70).

Extremophilic organisms can be difficult to grow, they can have low enzyme yields, and they can produce toxic or corrosive metabolites during large scale production. For example, many hyperthermophiles are anaerobic and can produce H<sub>2</sub>, CO<sub>2</sub> and sometimes H<sub>2</sub>S as fermentation products during growth. Other issues are also that extremophiles often have slow growth rates, and genetic tools are only poorly developed for these organisms, so extremophilic enzymes can hardly be overexpressed in their original host. This problem is typically solved by overexpressing extremophilic enzymes of interest in mesophilic hosts (i.e. *Escherichia coli*) for large scale production (62).

Another limitation to the use of enzyme catalysis in industry has been the lack of enzyme specificity for desired substrates and the lack of selectivity for products (72). Also, although an enzyme may use one substrate with high enantiospecificity, the addition or subtraction of a single functional group to the substrate may cause a loss of specificity or activity (37). Luckily, recent advances in molecular biology, high-throughput screening, instrumentation, and engineering have now led to the production of enzymes with enhanced stability and novel activities to create customized activity and selectivity (37, 72).

Like their mesophilic counterparts, thermostable enzymes tend to have a narrow substrate specificity that precludes their use for a wide variety of purposes (46).

Engineering of thermostable enzymes by random and site-directed mutageneses has produced enzymes with novel activities (43). Directed evolution can also be used to increase enzyme activity on native substrates that are of interest for industrial applications (14), to increase thermostable enzyme activity at mesophilic temperatures, to increase activity at different pH values (61), or to increase the thermostability of a mesophilic enzyme without sacrificing activity at mesophilic temperatures (20).

Common chemical methods of oxidizing alcohols depend on heavy metal catalysts (i.e., chromium(VI) reagents), and the reactions are often performed in organic solvents. Using these methods on an industrial scale typically gives low yields due to the reaction going one step further to produce carboxylic acid from the desired aldehyde product. Galactose oxidase (GO) has potential use in industrial chemical and pharmaceutical industries to oxidize primary alcohols to produce aldehydes and hydrogen peroxide. In particular GO is active toward guar, a polymer isolated from the guar plant, which can be enzymatically oxidized by GO to a compound called oxidized guar. Oxidized guar is used as an additive in paper manufacturing to increase the mechanical strength of paper. However, once purified, GO has such low activity that it is not economically usable in an industrial scale reaction. Directed evolution (DE) was used to increase GO's activity for use in industrial purposes. One mutant identified from the screening showed a 19-fold increase in catalytic efficiency ( $V_{\max}/K_m$ ) relative to the wild-type enzyme (14).

DE was also used to make a *Pseudomonas aeruginosa* lipase enantioselective. The wild-type enzyme had an enantiomeric ratio (E) of 1.1 towards model substrate *p*-methyldecanoic acid *p*-nitrophenyl ester. After DE and screening of thousands of

mutants, mutant enzymes were found that had increased selectivity for either the (S)-enantiomer ( $E = 51$ ), or the (R)-enantiomer ( $E = 30$ ) (25). Any  $E$  value above 20 is an acceptable resolution (19).

Site-directed mutagenesis can also be used as a method for improving the characteristics of proteins that are industrially interesting. *Bacillus licheniformis*  $\alpha$ -amylase (BLA) is a thermostable enzyme (half-life  $>4$  hours at  $90^{\circ}\text{C}$ ) from a mesophilic host, which is widely used for industrial hydrolysis of starch to maltodextrins. Although this enzyme is thermostable, BLA irreversibly unfolds when exposed to high temperatures. BLA thermostability was increased both by delaying irreversible unfolding and by preventing irreversible inactivation by mechanisms such as deamidation (12, 62).

In nature prochiral centers are often reduced to produce a chiral center by ketone reduction or reductive amination of keto groups by redox enzymes. These enzymes typically need a cofactor (i.e. NAD(P)). The need for cofactors for redox reactions has been a hurdle for the use of dehydrogenases in industrial-scale reactions. Chemical cofactor recycling methods have been developed, but they have only been used on a laboratory scale. If the cofactor cannot be recycled then a stoichiometric amount of cofactor must be used. Due to the high cost of the cofactor, this use is not economically feasible. Recent advances in enzymatic cofactor recycling systems have shown promise for larger scale uses of dehydrogenases (69).

Degussa-Hüls AG (Germany) developed an enzyme-membrane reactor (EMR) in 1981, and has since modified it to accommodate L-amino acid dehydrogenase to produce the unnatural amino acid L-*tert*-leucine (L-Tle) by reductive amination of the prochiral  $\alpha$ -keto acid, trimethyl pyruvate. In this reactor, *Candida boidinii* formate dehydrogenase

(FDH) is used to recycle the cofactor, NADH. Because L-Tle is an unnatural amino acid, its synthesis cannot be carried out by fermentation, Degussa's EMR produces L-Tle with an average conversion of 85% and a space-time yield of 638g/day, with the total cofactor turnover number of 125,000 over a two month period. Degussa operates this reactor on an industrial scale to produce high quality L-Tle (31, 69, 70). L-Tle is important because it is substituted for leucine in therapeutic peptides in which it is less prone to hydrolysis by serum proteases (69). This reactor demonstrates the possibility of an increased use of dehydrogenases in industrial settings.

Another example of the use of dehydrogenases coupled with a cofactor recycling enzyme in the pharmaceutical industry is for the production of a drug called Omapatrilat (Bristol-Meyers Squibb), a vasopeptidase inhibitor used for the treatment of hypertension. The proper side-chain chirality of an amino group in an Omapatrilat precursor was obtained by reductive amination with phenylalanine dehydrogenase. Phenylalanine dehydrogenase uses NAD(H) as a cofactor, which was efficiently recycled by the use of a formate/FDH system. In three batches, 197 kg of specific product was produced with a space-time yield of 91% and a >98% enantiomeric excess (ee) (72).

Cofactor regeneration has benefits other than reducing cost by reusing the cofactor. It reduces costs by driving the reaction to completion, which simplifies product isolation because all, or nearly all, the substrate has been converted to product. It also reduces the build up of inhibitory cofactor by-products (74).

Electrochemical recycling is another cofactor recycling method that is being researched (4, 15, 21, 27, 66). This approach would eliminate the need for and cost of a second enzyme and cosubstrate in the reaction. Removing of the second enzyme would

eliminate any side-products produced by the recycling enzyme, and the need for side-product removal. This is not a problem with the formate/FDH system as its only product, aside from NADH, is CO<sub>2</sub>. At this time, though, electrochemical reduction methods are not developed to a point that they are rapid, sturdy, or cost effective enough to be used in any large scale productions (15, 66).

Enzyme specificity for NADP(H) versus NAD(H) has also been a limitation. Per gram, NADPH is nearly ten times as expensive as NADH (\$877/g NADPH vs. \$85.10/g NADH – Sigma online catalog March 2007). NADPH is also much less stable than NADH. For example, at 30°C from pH 2 to 4.5 NADPH degrades 80% faster than NADH, and at pH 6.0 at 41°C, NADH has a half-life of 400 min, while NADPH has a half-life of only 56 min (71).

### **1.3 Thermostable Enzymes**

Moderate thermophiles grow optimally from 50 to 80°C, though they are still able to grow slowly at lower temperatures (20 to 40°C), while hyperthermophiles grow best at 80°C or above. Because of the close phylogenetic relationship to their mesophilic counterparts, moderate thermophiles may have developed thermophilicity as a secondary adaptation to hot environments (46), while hyperthermophiles are often thought to be the closest relatives known to the last common ancestor of all present-day organisms (18). Due to the stress from natural habitat of thermophiles, the cellular components of these organisms, specifically proteins, must themselves be thermostable (49).

Multiple mechanisms have been described that can be at the origin of increased protein thermostability: optimized hydrophobic interactions in the enzyme core, increased

packing efficiency, increased number of salt bridges and/or hydrogen bonds, reduction of conformational strain, loop stabilization, more hydrophilic surface, additional aromatic-aromatic interactions, decrease of main-chain flexibility from the presence of additional prolines, and shortening of surface loops. These factors can be present in any combination to increase the thermostability of an enzyme (67, 68, 73).

Thermostable enzymes typically share the same catalytic mechanisms as their mesophilic counterparts. Most retain their increased stability and chemical resistance and are correctly folded when expressed in mesophilic hosts at 37°C or lower temperatures, indicating that the thermophilic properties are genetically encoded rather than a result of the host organism's machinery (40, 73), though not all thermostable enzymes are from thermophilic hosts. There are examples of thermostable enzymes that come from mesophilic hosts, such as the  $\alpha$ -amylase from *B. licheniformis* and an ADH from *Burkholderia* sp. AUI 652 (12, 24). A continually growing number of thermostable enzymes are being cloned and expressed in mesophilic hosts for ease of growth and purification (40).

The enzymes from thermophilic organisms (thermozymes) have been shown to be inherently thermostable and active at the host organisms' optimal growth temperature. Thermozymes have been shown to be not only stable at high temperatures and extremes of pH, but also resistant to common protein denaturants, proteases, detergents, chaotropic reagents, and organic solvents (16, 40, 46). These features have elicited interest from industry for potential biotechnological applications. The synthesis of aspartame by the Holland Sweetener Company is carried out by the thermostable protein thermolysin from *Bacillus proteolicus*. Thermolysin catalyzes the reaction of L-phenylalanine methylester



with L-aspartic acid (which has a protective group attached) to form  $\alpha$ -aspartame (protected). Two further chemical steps are needed to remove the protecting group and convert the methylester to  $\alpha$ -aspartame (31, 57). Another thermostable enzyme currently used in industry is the aforementioned *Bacillus licheniformis*  $\alpha$ -amylase (BLA). This  $\alpha$ -amylase is widely used for industrial hydrolysis of starch to maltodextrins (12, 62)

Thermophilic ADHs are of great interest to the chemical synthesis industry because of their ability to produce alcohols, such as ethanol. These ADHs are also of particular interest to the pharmaceutical industry for the production of the enantiomerically pure compounds needed as building blocks for chirally pure pharmaceutical agents (46).

As of 2003, 20 thermophilic archeal and 17 thermophilic bacteria strains had been found to contain ADHs, or hypothetical ADHs. These strains have been isolated from a variety of natural and man-made environments such as hydrothermal vents, hot springs, canned peas, and sugar beet factories. Many of these species not only contain multiple ADHs, but these ADHs can be of different types. For example *Sulfolobus solfataricus* contains 13 ADHs of the same type (46), while *Thermoanaerobacter ethanolicus* contains two ADHs, which are of different types (6). The different ADHs can serve a variety of functions in survival depending upon the environment to which the organism is adapted (46).

The environment to which the organism is adapted may also dictate the type and variety of ADHs the organism has. For example, marine thermophiles are likely to have at least one iron-dependent ADH and 50% have additional types of ADHs, while 78% of terrestrial organisms have zinc-dependent ADHs and only 33% have more than one type.

The similarities among the ADHs isolated from marine organisms may be due to the fact that all the organisms were isolated from very similar environments and had similar characteristics: all were anaerobic and had optimal growth temperatures that ranged from 80 to 100°C. The only known exception to this is the archaeon *Pyrobaculum aerophilum*, which is the only known aerobic marine hyperthermophile, and the only species that does not contain an iron-activated ADH. It is speculated that known terrestrial thermophiles present more variety (i.e. most marine thermophiles had Fe-ADHs with little variety amongst them, while thermophiles from terrestrial biotopes typically have Zn-ADHs and more variety of ADH types) because terrestrial environments are more variable than marine environments and therefore require more diverse adaptations (46).

## 1.4 ADHs

Alcohol dehydrogenases (EC 1.1.1.1 or EC 1.1.1.2) catalyze the reversible reduction of ketones and aldehydes to alcohols. This catalysis takes place by a hydride transfer from the *pro*-R hydrogen of the NAD(P)H cofactor (Figure 1-1) (13, 63). The reduction/oxidation reaction follows an ordered bi bi mechanism in which the cofactor binds before the substrate, the hydride transfer occurs, the product (alcohol or ketone) is released, and finally the cofactor is released (Figure 1-2) (44).

Most ADHs are soluble, cytoplasmic enzymes but some, such as the PQQ-dependent polyvinyl alcohol ADH of a *Pseudomonas* sp. and ADHs from acid-producing bacteria *Acetobacter aceti* and *Glucobacter suboxydans*, have been shown to be membrane-bound (34).

ADHs are found in a wide variety of hosts from microorganisms to plants, fungi,

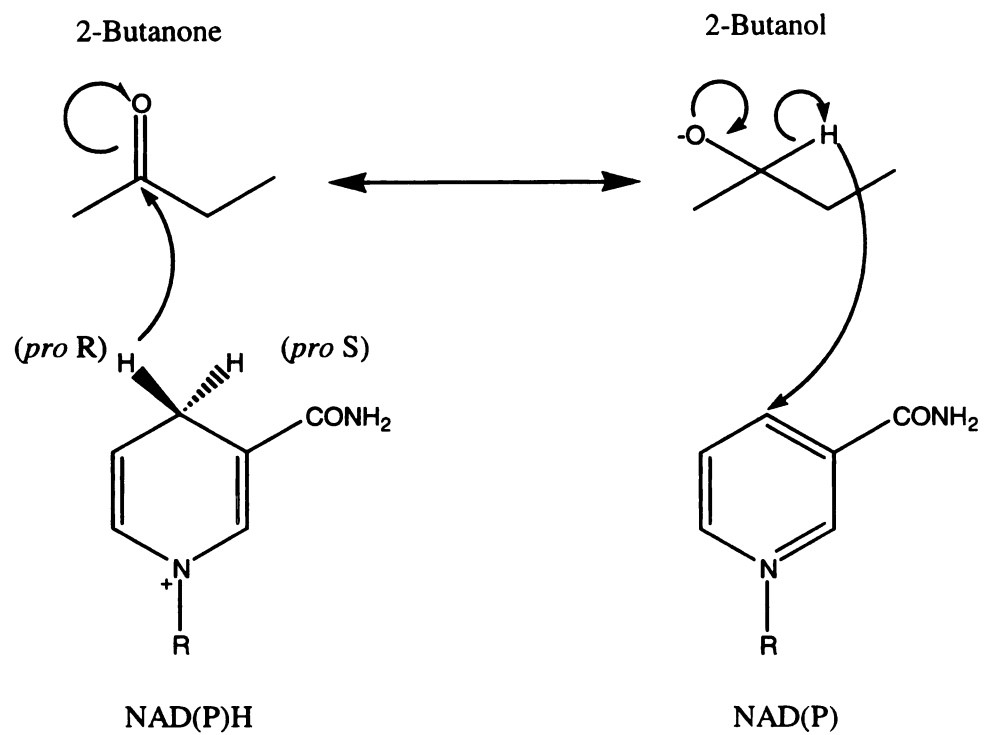


**Figure 1-1. Hydride transfer of the *pro R* hydrogen of cofactor NAD(P)(H) during alcohol reduction or ketone/aldehyde oxidation (63)**

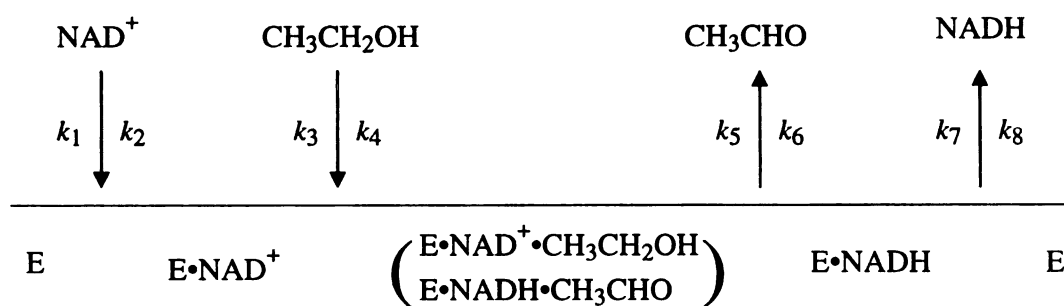


**Figure 1-2. The ordered bi bi reaction mechanism carried out by HLADH** (as shown by Plapp, 1970 (44))

and animals (3). ADHs generally have a very wide substrate range including normal and branched aliphatic and aromatic alcohols (both primary and secondary), and the corresponding aldehydes and ketones. Many organisms contain multiple ADHs with roles that can be difficult to separate from one another (50). Organisms may also have isozymes with opposing or similar functions. For example (1) *Saccharomyces cerevisiae* has two cytoplasmic ADHs, ADH-I and ADH-II. ADH-I is the common, commercially available, yeast ADH, that serves in ethanol formation, while ADH-II produces acetaldehyde from ethanol in aerobic conditions; (2) *Zymomonas mobilis* has two cytoplasmic ADHs, one of which is activated by iron, and the other is activated by zinc; and (3) *Acinetobacter calcoaceticus* has two NAD-dependent benzaldehyde dehydrogenases one of which is heat-stable, potassium activated, and induced by phenylglyoxylate, and the other is heat-labile and induced by benzyl alcohol (34).

MacKintosh and Fewson (34) classified ADHs in seven groups, based on the enzymes' substrate specificities. This classification method is seldom used and it does not reflect the enzyme's structural and mechanistic properties. For example two ADHs of very different specificities can have very similar folds and the same metal or cofactor requirement. A classification more relevant to this dissertation is the classification that groups enzymes according to their cofactor specificity: (a) NAD(P), (b) pyrroloquinoline quinine (PQQ), haem (a.k.a. heme) or cofactor F<sub>420</sub>, or (c) FAD. The groups of ADHs that use FAD and pyrroloquinoline quinine as cofactors are small, not well studied, and their presence tends to be limited to certain bacterial species (51). With only one exception from *Methanoculleus thermophilicus*, which uses F<sub>420</sub>, all known thermophilic ADHs are NAD(P)-dependent. The cofactor utilization by thermophilic ADHs is similar

to that of their mesophilic counterparts, indicating that the two groups share a common catalytic mechanism (46).

NAD(P)-dependent ADHs are typically divided into three groups: short-chain; medium-chain (also referred to as long-chain by some sources); and long-chain and/or iron-activated enzymes. The short-chain ADHs are metal-independent and typically have around 250 residues per subunit. Medium-chain ADHs are zinc-dependent and have 350-375 residues per subunit. When referred to as long-chain, these enzymes are typically specified as zinc-dependent. The last group is the iron-activated ADHs, sometimes also referred to as long-chain ADHs (3, 23, 26, 50, 51).

Metal-independent short-chain ADHs frequently have terminal transmembrane domains or signal peptides, or may even form parts of multi-enzyme complexes. Sequence identity among short-chain ADHs is low, typically only 15-30%, but available 3D structures are highly similar in their  $\alpha/\beta$  folding patterns. These enzymes also contain a Rossmann fold, which is common to other types of ADHs (41, 55).

Zinc-dependent ADHs are the best studied of the three classes and form the largest and most diverse class. Zn-dependent ADHs are either dimeric (typically found in plants and animals) or tetrameric (typically found in bacteria and yeast) (3). Within this class, ADHs from related organisms show high similarity, and thermophilic ADHs are homologous to their mesophilic counterparts. This class can be further broken down into three groups based on cofactor and substrate specificity: NAD(H)-dependant primary ADHs, NADP(H)-dependent primary ADHs, and NADP(H)-dependent secondary ADHs (46). Primary and secondary ADHs are classified based on their preference toward primary or secondary alcohols (7).

Like the zinc-dependent ADHs, iron-activated ADHs from related organisms show high similarity, and thermophilic iron-activated ADHs are homologous to their mesophilic counterparts. These ADHs have been shown to prefer NADP(H) and primary alcohols, and the biological role of these enzymes is likely to detoxify aldehydes rather than to produce alcohols (46).

Horse liver alcohol dehydrogenase (HLADH; E.C. 1.1.1.1) has been a very commonly studied ADH for many years, and much is known about its structure and function (1, 11, 29, 30, 35, 39, 42, 45, 48, 53, 58, 65). HLADH is a medium-chain, zinc-dependent ADH that catalyzes the reaction of various primary, secondary, branched, and cyclic alcohols (47), but prefers primary alcohols and aldehydes (7, 45). HLADH is a homodimer with a total molecular weight of 80,000 (47). Each subunit contains one catalytic zinc and one structural zinc. The catalytic zinc has three protein ligands (Cys46/His67/Cys174) and a fourth ligand which is either water or a substrate atom (45). Each subunit contains two domains, generally called the substrate- and the cofactor-binding domains, with the active site sitting in the cleft between the two domains (48).

The apoenzyme is in an open form, in which the active site is accessible to solvent and the fourth zinc ligand is water (11). Upon cofactor binding a rotation of about 10° of the cofactor-binding domain occurs bringing the two domains closer to each other, creating the closed form of the enzyme (48). This domain rotation facilitates the displacement of water so that the alcohol/ketone/aldehyde substrate can coordinate with the zinc to become the fourth ligand. These conformational change and substrate-zinc coordination are essential for the hydride transfer to occur (11).

In addition to the hydride transfer, protonation (deprotonation) of the ketone (alcohol) must occur. It is thought that HLADH residues His51 and Ser48 contribute to this acid/base chemistry. The proton transfer occurs through a hydrogen bond system connecting His51 to the 2'-hydroxyl group on NAD<sup>+</sup>'s nicotinamide ribose-Ser48 and the Zn-bound substrate (or H<sub>2</sub>O) (Figure 1-3 and Scheme 1-1). The hydrogen bond system relays a proton from alcohol to solvent during dehydrogenation (30, 47). An alkoxide intermediate is formed during alcohol oxidation when a proton is removed and relayed to the solvent. The alkoxide intermediate is stabilized by Ser48, before being oxidized to ketone/aldehyde by NAD<sup>+</sup> (30).

## 1.5 Stereospecificity of ADHs

A reaction is termed stereospecific if starting materials differing only in their configuration are converted into stereoisomeric products. According to this definition, a stereospecific process is necessarily stereoselective but not all stereoselective processes are stereospecific. Stereospecificity may be total (100%) or partial. The term is also applied to situations where reaction can occur with only one stereoisomer. For example the exclusive formation of *trans*-1,2-dibromocyclohexane upon bromination of cyclohexene is a stereospecific process, although the analogous reaction with (*E*)-cyclohexene has not been performed (36). So, in short, in a stereospecific synthesis, one isomer leads to one product while another isomer leads to the opposite product.

Stereoselectivity is the preferential formation of one stereoisomer over another. When the stereoisomers are enantiomers, the phenomenon is called enantioselectivity, and it is quantitatively expressed by the enantiomer excess (ee) (36). Enantiomeric



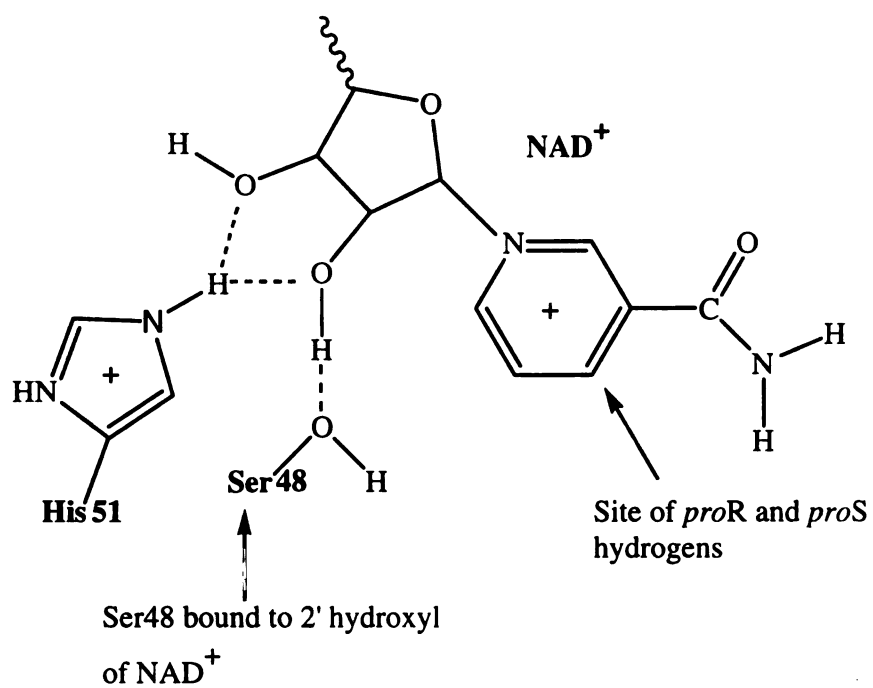
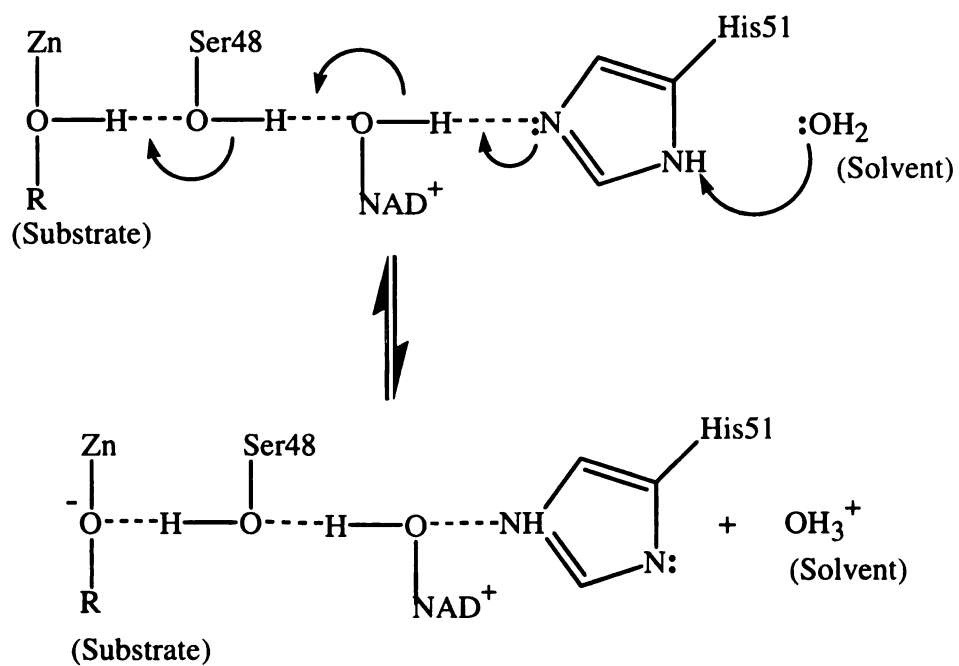


**Figure 1-3. Residues His51 and Ser48 bound to the nicotinamide ribose of the NAD<sup>+</sup> of HLADH (47)**



**Scheme 1-1. Proton transfer/deprotonation system of HLADH (30)**

excess is the percentage of one enantiomer in excess of another. So if the (S)-enantiomer is present in excess:

$$ee = (S-R)/(S+R)$$

or if the (R)-enantiomer is present in excess:

$$ee = (R-S)/(R+S)$$

So even if the ee = 2% for (S), the (S)-enantiomer is still more abundant than the (R).

Our laboratory created a *Thermoanaerobacter ethanolicus* secondary ADH mutant (W110A) that is active on 1-phenyl-2-propanol and 4-phenyl-2-butanol, and on their respective ketones phenylacetone and benzylacetone (see details in Chapter II (76) and Appendices A and B (37, 38)). The wild-type enzyme showed little to no activity with phenyl-substituted substrates. The W110A mutation was introduced to increase the size of the large substrate binding pocket and accommodate larger substrates, such as phenyl alcohols and ketones. The small binding pocket is too small to accommodate large alkyl groups, so these groups are forced into the large binding pocket, producing (S)-alcohols. The W110A mutant was shown to reduce benzylacetone to (S)-4-phenyl-2-butanol with an ee >99%.

*Lactobacillus brevis* contains an (R)-specific ADH. This ADH is a member of the short-chain ADH family, is NADP(H)-specific, and is unique in that it has been found to be magnesium-dependent, unlike most short-chain ADHs that are metal-independent. Structural studies of this enzyme show that the side of the substrate binding pocket where the target functional group binds is only large enough to allow a methyl group with reasonable distances (3.5 Å to 4 Å) between the atoms of the substrate and the surrounding side chains, Leu152, Glu144, Tyr155, and Tyr189. This local structure

forces substrates, such as acetophenone, to bind in a manner that will lead exclusively to (R)-alcohol production (55).

## **1.6 *Thermoanaerobacter ethanolicus* secondary ADH**

The secondary ADH (EC 1.1.1.2) from the thermophilic bacterium *Thermoanaerobacter ethanolicus* 39E (TeSADH) was cloned and expressed in *E. coli* by Burdette et al. (9). TeSADH is a medium chain, zinc-containing enzyme, and has a requirement for a nicotinamide cofactor, specifically NADP(H). TeSADH is 352 amino acids long, and has a total molecular mass of 160 kDa (each subunit being 40 kDa.). TeSADH was previously thought to differ from *Thermoanaerobacter brockii* SADH (TbSADH) by 3 amino acids (9), but recent sequencing results in our lab (Laivenieks, unpublished result) and *T. ethanolicus* 39E genome sequencing data (NCBI entry 2P\_00779753) show that the two enzymes are in fact identical (6).

Structural studies of HLADH showed that the catalytic Zn is bound by residues Cys46, His67, and Cys174. Sequence alignments of TeSADH and HLADH suggested that the corresponding Zn-binding residues in TeSADH were Cys37, His59, and Asp150 (Figure 1-4). EXAFS and ICP-AES experiments confirmed that TeSADH contains a single catalytic zinc that is coordinated by residues Cys37, His59, and Asp150 (7). The mutation D150C was introduced in TeSADH to mirror HLADH's catalytic Zn binding site. The TeSADH D150C mutant retained only 3% of the wild-type activity (7). Further mutations were introduced in either TeSADH or TbSADH. When each of the three zinc-chelating residues was individually replaced with the non-chelating residue alanine, TbSADH/TeSADH was no longer able to bind zinc and had no detectable activity. When

TeSADH	-MKGFAMLSIGKVGWIEK-----EKPA	21
HLADH	STAGKVIKCKAAVLWEEKKPFSEEEVEVAP	30
	* .: . . * * ** * ..	
TeSADH	PGPFDAIVRPLAVAP <b>C</b> TSDIHTVFEGAIGE	51
HLADH	PKAHEVRIKMVATGI <b>C</b> RSDDH-VVSGTLVT	59
	* ..... : : *.. * ** * *..*::	
TeSADH	RHNMILG <b>H</b> EAVGEVVEVGSEVKDFKPGDRV	81
HLADH	PLPVIAG <b>H</b> EAAGIVESIGEGVTTVRPGD-K	88
	: * ***. * * .: * . * . .:***	
TeSADH	VVPAITPDWRTSEVQRG-----YHQ	101
HLADH	VIPLFTPQCGKCRVCKHPEGNFCLKNDLSM	118
	*: * :*: : ..* :	
TeSADH	HSGGMLAGWKFSNVKDGVFGEFFHVN----	127
HLADH	PRGTMQDGTSRFTCRGKPIHHFLGTSTFSQ	148
	* * * . . : . : * : ..	
TeSADH	---DADMNLAHLPKEIPLEAAVMIP <b>D</b> MMTT	154
HLADH	YTVVDEISVAKIDAASPLEKVCLIG <b>C</b> GFST	178
	: : : * : : *** . : * : : *	

**Figure 1-4. Sequence comparison of the Zn binding sites of HLADH and TeSADH.**  
Zn binding residues are in bold:

(TeSADH/HLADH)  
Cys37/Cys46  
His59/His67  
Asp150/Cys174

the zinc-chelating residues were replaced with other zinc-chelating residues (with mutations C37S, H59Q, H59N, D150Q, and D150N, individually) activity was only detectable in the presence of excess zinc (1mM) in solution, and the mutants retained less than 1% of wild-type activity (5, 7).

## **1.7 NADH vs. NADPH**

NADPH has been shown to be less stable than NADH. Both temperature and pH have significant effects on the stability of both cofactors. At 41°C and pH 6, the half-life of NADPH is only 56 min compared to 400 min for NADH. The difference at lower pHs (41°C) is less significant, 4 min vs. 5.5 min at pH 4, and 15 min vs. 43 min at pH 5 for NADPH and NADH respectively, while the rates of degradation are nearly the same at pH 3.7 (71). At 30°C it was shown that NADPH is destroyed 80% faster than NADH at pH 2-4.5, however both are shown to be quite stable in alkaline solutions. If either NADH or NADPH was heated to 100°C for 30 min in 0.1 N NaOH the cofactors remained intact (32, 71). Concentrated (40 mM) NADH or NADPH solutions kept well at both -20°C and -85°C at any pH, but they were shown to be degraded at alkaline pH, while more dilute solutions tended to be stable at alkaline pH at 4°C and degraded at -20°C if the pH was 10.5 or above. The degradation of the more dilute samples at -20°C was thought to happen because at this temperature there is a residual water layer present where any impurities capable of degrading the reduced cofactor can concentrate to cause quicker degradation (32). These results indicate that NADH is more stable than NADPH in conditions compatible with catalysis, particularly at pHs that are favorable for ketone reduction (e.g. pH 6.5 for TeSADH, and pH 4.9 for W110A TeSADH) (76).

NADH is also significantly less expensive than NADPH, making its use more cost-effective than NADPH. According to the Sigma/Aldrich website, the current cost for 1 g of  $\beta$ -NADH (95% pure, reduced disodium salt) is \$85.10, while the cost for 1g of the commonly used  $\beta$ -NADPH (95% pure, 2-phosphate reduced tetrasodium salt) is \$877, greater than ten times the cost of the same amount of NADH.

Several groups have reported the change of enzyme cofactor specificity through rational design and mutagenesis. Both isocitrate dehydrogenase (IDH) and isopropylmalate dehydrogenase (IMDH) have been engineered to reverse their cofactor specificity, each using the other as the template for change. IDH and IMDH are homologous and structurally similar enzymes that are both involved in amino acid synthesis. The wild-type *E. coli* IDH is a NADP(H)-dependent enzyme, and the wild-type *E. coli* and *Thermus thermophilus* IMDHs are both NAD(H)-dependent. First, the sequences and crystal structures (both with cofactor bound to the enzyme) of *E. coli* IDH and *T. thermophilus* IMDH were compared. This comparison showed that six residues are conserved in NADP(H)-dependent IDHs, but that only three are conserved in NAD(H)-dependent IMDHs and confer cofactor specificity. These three NAD(H)-dependent conserved residues were mutated in IDH (K344D, Y345I, and V351A), and two additional mutations of non-conserved residues (Tyr391 and Arg395) were made to remove interactions with the ribose phosphate of NADP(H). Crystal structures show that the mutant IDH binds NAD(H) in the same manner as the wild-type IMDH binds NAD(H), forming the same hydrogen bonds, and has comparable activity (33, 75).

Similar sequence and structural comparisons were used to change the cofactor specificity of *E. coli* IMDH from NAD(H) to NADP(H). In this case, the *E. coli* and *T.*

*thermophilus* IMDHs were compared. Five additional mutations were introduced in the *E. coli* IMDH to mimic the IDH cofactor binding site (D236R, D289K, I290Y, A296V, and G337Y). *E. coli* IMDH's cofactor specificity changed from a 100-fold preference for NAD(H) to a 200-fold preference for NADP(H) (33).

Most FDHs (including the commonly used *C. boidinii* enzyme) are NAD(H)-dependent. Because FDHs are often used for cofactor recycling in redox reactions, the cofactor specificity of *Pseudomonas* sp. FDH (PseFDH) was changed from NAD(H) to NADP(H) to create an enzyme that could be used for NADP(H) recycling. The wild-type PseFDH has a  $K_m$  for NADP<sup>+</sup> above 0.4 M. In contrast, the NADP<sup>+</sup> specific mutant (amino acid substitutions not described) has a  $K_m$  of 0.15 mM for NADP<sup>+</sup>. It is commercially available from Codexis (Redwood City, CA) (formerly Jülich Fine Chemicals). Attempts have been made to change the cofactor specificity of *Candida methyllica* and *S. cerevisiae* FHDs (CmFDH and ScFDH, respectively), but the results were not as significant. The CmFDH mutant was nearly inactive with NADP<sup>+</sup> (with a  $K_m$  above 0.4 M). The ScFHD mutant had much improved activity with NADP<sup>+</sup>, but it was only 1.8 times more specific for NADP<sup>+</sup> ( $K_m$  of 4.5 mM) than for NAD<sup>+</sup> ( $K_m$  of 7.6 mM) (60, 64).

To investigate the minimal structure requirements for cofactor specificity reversal, three mutations were introduced into *Rana perezi* ADH8 (Western Palearctic water frog), which is the only known vertebrate NADP(H)-specific ADH. Mutations G223D, T224I, and H225N were chosen to mimic residues common to NAD(H)-specific vertebrate ADHs. Individually, single mutants still preferred NADP(H) to NAD(H), but double mutants G223D+T224I and T224I+H225N showed decreased catalytic efficiency with



NADP(H). The triple mutant G223D+T224I+H225N showed complete cofactor specificity reversal, with a catalytic efficiency ( $k_{\text{cat}}/K_m$ ) on NADH of  $155,00 \text{ mM}^{-1} \text{ min}^{-1}$  versus a  $k_{\text{cat}}/K_m$  of  $760 \text{ mM}^{-1} \text{ min}^{-1}$  on NADPH starting from a  $k_{\text{cat}}/K_m$  for NADPH of  $133,330 \text{ mM}^{-1} \text{ min}^{-1}$  for the wild-type enzyme (52).

Changing the cofactor specificity of TeSADH has also been attempted. Burdette et al. constructed the G198D mutant as a result of sequence comparisons with the NAD(H)-specific HLADH (7). This same Asp residue is also present in the *S. cerevisiae* NAD(H)-specific ADHI (YADH) (Figure 1-5). Crystal structures of HLADH and TbSADH were also compared. This comparison showed that in the holo-enzymes the space that would be filled by Asp in HLADH was open to accommodate the 2'-phosphate of NADP(H) in TeSADH (28). It was thought that the increase in the size of the residue would sterically exclude the phosphate group of NADP(H), and favor NAD(H). The TeSADH G198D mutant's affinity for  $\text{NADP}^+$  decreased 225 times compared to that of the wild-type enzyme (Table 2). The mutant's affinity for  $\text{NAD}^+$  increased 3 times compared to the wild-type with  $\text{NAD}^+$ . Still the G198D mutant has 47.5 times less affinity for  $\text{NAD}^+$  than the wild-type does for  $\text{NADP}^+$  (7).

Hassler et al. also attempted to change the cofactor specificity of TeSADH by constructing the Y218F mutant (Table 2). The TeSADH Y218F mutant's affinity for  $\text{NADP}^+$  decreased 213 times compared to that of the wild-type enzyme (Table 1-2). The mutant's affinity for  $\text{NAD}^+$  increased 2.4 times compared to the wild-type with  $\text{NAD}^+$ . Still the Y218F mutant has 58 times less affinity for  $\text{NAD}^+$  than the wild-type does for  $\text{NADP}^+$  (22).

HLADH	GYGSAVKVAKVTQGSTCAVFGLG-GVGLSV	207
TeSADH	GF-HGAELADIELGATVAVLGIG-PVGLMA	182
YADH	VY-KALKSANLMAGHWVAISGAAGGLGSLA	186
	: . : *.: * *: * . :*	.
HLADH	IMGCKAAGAARIIGV <b>D</b> INKDKFAKAKEVGA	237
TeSADH	VAGDKLRGAGRIIAV <b>G</b> SRPVCVDAAKYYGA	212
YADH	VQYAKAMG-YRVLGI <b>D</b> GGEGKEELFRSIGG	215
	:* * *: : : . : *	.

**Figure 1-5. Sequence comparison of HLADH, TeSADH, and YADH.** NAD(H) binding conserved residue (HLADH D223, YADH D201) and analogous NADP(H) binding residue in TeSADH (G198) in bold

**Table 1-2. Kinetic parameters for G198D and Y218F TeSADH mutants**

	NADP+		NAD+	
	Vmax (U/mg)	Km (mM)	Vmax (U/mg)	Km (mM)
Wild-type	72	0.016	4.4	2.3
G198D	18	3.6	25	0.76
Y218F	21	3.4	23	0.93

These results show a significant change in cofactor specificity in G198D and Y218F TeSADH mutants, however the  $V_{\max}$  of the mutants with  $\text{NAD}^+$  is still 3 times lower than that of the wild-type with  $\text{NADP}^+$ . These results indicate that more work is needed to optimize the activity of this enzyme with NAD(H).

There is not currently a universal approach for changing cofactor specificity in dehydrogenases (64). Consequently, methods other than rational design, such as directed evolution may need to be employed to reach the full potential of cofactor specificity change.

## 1.8 Objectives

Due to increasing interest in industrial biocatalysis and demand for compounds that are difficult to chemically produce, there is an increasing demand for novel biocatalysts. Advances in technology have allowed for enzyme engineering, using techniques such as rational design and directed evolution, to create biocatalysts with novel activities specifically tailored to a predetermined purpose. Added benefits to using these biocatalysts are often cleaner, less expensive processes than the chemical processes that they are to replace.

TeSADH is a promising enzyme for use as a biocatalyst due to its broad substrate specificity and increased global stability in comparison to mesophilic ADHs. One objective of this thesis is to engineer an industrially attractive enzyme to produce chiral *phenyl*-substituted alcohols with high enantiospecificity. The phenyl alcohol (S)-4-*phenyl*-2-butanol is important because it is a precursor to some anti-hypertensive and *spasmolytic* (anti-epileptic) drugs. Through a single point mutation (W110A), TeSADH

is now able to produce (S)-4-phenyl-2-butanol, and 4-phenyl-2-butanol and 1-phenyl-2-propanol derivatives with high enantiospecificity. Chapter II describes the results of this work.

Another objective of this thesis is to engineer TeSADH to change the cofactor specificity from NADP(H) to NAD(H). Because of the increased cost and decreased stability of NADP(H) compared to NAD(H) the change in cofactor specificity is an important step in producing an industrially attractive enzyme. So we are changing TeSADH's cofactor specificity using site-directed mutagenesis and directed evolution to make this enzyme cheaper, more economically feasible, to use. This work is presented in Chapter III.

In order to engineer and economically feasible enzyme further work needs to be done to increase the activity of TeSADH with NAD(H) and to increase the solvent stability of W110A TeSADH.

## **1.9 Acknowledgements**

This work was supported by a grant from The Michigan Technology Tri-Corridor Fund and NSF Award MCB-0445750.

## 1.10 References

1. **Adolph, H. W., P. Zwart, R. Meijers, I. Hubatsch, M. Kiefer, V. Lamzin, and E. Cedergren-Zeppezauer.** 2000. Structural basis for substrate specificity differences of horse liver alcohol dehydrogenase isozymes. *Biochemistry* **39**:12885-12897.
2. **Ahuja, S. K., G. M. Ferreira, and A. R. Moreira.** 2004. Utilization of enzymes for environmental applications. *Crit. Rev. Biotechnol.* **24**:125-154.
3. **Ammendola, S., C. A. Raia, C. Caruso, L. Camardella, S. D'Auria, M. De Rosa, and M. Rossi.** 1992. Thermostable NAD(+)-dependent alcohol dehydrogenase from *Sulfolobus solfataricus*: gene and protein sequence determination and relationship to other alcohol dehydrogenases. *Biochemistry* **31**:12514-12523.
4. **Bardea, A., E. Katz, A. F. Bückmann, and I. Willner.** 1997. NAD<sup>+</sup>-Dependent enzyme electrodes: Electrical contact of cofactor-dependent enzymes and electrodes. *J. Amer. Chem. Soc.* **119**:9114-9119.
5. **Bogin, O., M. Peretz, and Y. Burstein.** 1997. *Thermoanaerobacter brockii* alcohol dehydrogenase: characterization of the active site metal and its ligand amino acids. *Protein Sci.* **6**:450-458.
6. **Burdette, D., and J. G. Zeikus.** 1994. Purification of acetaldehyde dehydrogenase and alcohol dehydrogenases from *Thermoanaerobacter ethanolicus* 39E and characterization of the secondary-alcohol dehydrogenase (2° Adh) as a bifunctional alcohol dehydrogenase--acetyl-CoA reductive thioesterase. *Biochem. J.* **302**:163-170.
7. **Burdette, D. S., F. Secundo, R. S. Phillips, J. Dong, R. A. Scott, and J. G. Zeikus.** 1997. Biophysical and mutagenic analysis of *Thermoanaerobacter ethanolicus* secondary-alcohol dehydrogenase activity and specificity. *Biochem. J.* **326**:717-724.
8. **Burdette, D. S., V. V. Tchernajenko, and J. G. Zeikus.** 2000. Effect of thermal and chemical denaturants on *Thermoanaerobacter ethanolicus* secondary-alcohol dehydrogenase stability and activity. *Enzyme. Microb. Technol.* **27**:11-18.
9. **Burdette, D. S., C. Vieille, and J. G. Zeikus.** 1996. Cloning and expression of the gene encoding the *Thermoanaerobacter ethanolicus* 39E secondary-alcohol dehydrogenase and biochemical characterization of the enzyme. *Biochem. J.* **316**:115-122.

10. **Bustard, M. T., J. G. Burgess, V. Meeyoo, and P. C. Wright.** 2000. Novel opportunities for marine hyperthermophiles in emerging biotechnology and engineering industries. *J. Chem. Technol. Biotechnol.* **75**:1095-1109.
11. **Colby, T. D., B. J. Bahnson, J. K. Chin, J. P. Klinman, and B. M. Goldstein.** 1998. Active site modifications in a double mutant of liver alcohol dehydrogenase: structural studies of two enzyme-ligand complexes. *Biochemistry* **37**:9295-9304.
12. **Declerck, N., M. Machius, G. Wiegand, R. Huber, and C. Gaillardin.** 2000. Probing structural determinants specifying high thermostability in *Bacillus licheniformis* alpha-amylase. *J. Mol. Biol.* **301**:1041-1057.
13. **Deetz, J. S., and J. D. Rozzell.** 1988. Enzymatic catalysis by alcohol dehydrogenases in organic solvents. *Ann. N.Y. Acad. Sci.* **542**:230-234.
14. **Delagrave, S., D. J. Murphy, J. L. Pruss, A. M. Maffia, III., B. L. Marrs, E. J. Bylina, W. J. Coleman, C. L. Grek, M. R. Dilworth, M. M. Yang, and D. C. Youvan.** 2001. Application of a very high-throughput digital imaging screen to evolve the enzyme galactose oxidase. *Protein Eng.* **14**:261-267.
15. **Délécouls-Servat, K., A. Bergel, and R. Basseguy.** 2004. Membrane electrochemical reactors (MER) for NADH regeneration in HLADH-catalysed synthesis: comparison of effectiveness. *Bioprocess. Biosyst. Eng.* **26**:205-215.
16. **Demirjian, D. C., F. Moris-Varas, and C. S. Cassidy.** 2001. Enzymes from extremophiles. *Curr. Opin. Chem. Biol.* **5**:144-151.
17. **Devaux-Basseguy, R., A. Bergel, and M. Comtat.** 1997. Potential applications of NAD(P)-dependent oxidoreductases in synthesis: A survey. *Enzyme Microb. Technol.* **20**:248-258.
18. **Forterre, P.** 1996. A Hot Topic: The Origin of Hyperthermophiles. *Cell* **85**:789-792.
19. **Ghanem, A., and H. Y. Aboul-Enein.** 2005. Application of lipases in kinetic resolution of racemates. *Chirality* **17**:1-15.
20. **Giver, L., A. Gershenson, P. O. Freskgard, and F. H. Arnold.** 1998. Directed evolution of a thermostable esterase. *Proc. Natl. Acad. Sci. USA.* **95**:12809-12813.
21. **Gorton, L., and E. Domínguez.** 2002. Electrocatalytic oxidation of NAD(P)H at mediator-modified electrodes. *J. Biotechnol.* **82**:371-392.
22. **Hassler, B. L., M. Dennis, M. Laivenieks, J. G. Zeikus, and R. M. Worden.** 2007. Mutation of Tyr-218 to Phe in *Thermoanaerobacter ethanolicus* secondary

alcohol dehydrogenase: effects on bioelectronic interface performance. Appl. Biochem. Biotechnol. **In press**.

23. **Hummel, W.** 1997. New alcohol dehydrogenases for the synthesis of chiral compounds. Adv. Biochem. Eng. Biotechnol. **58**:145-184.
24. **Isobe, K., and N. Wakao.** 2003. Thermostable NAD<sup>+</sup>-dependent (*R*)-specific secondary alcohol dehydrogenase from cholesterol-utilizing *Burkholderia* sp. AIU 652. J. Biosci. Bioeng. **96**:387-393.
25. **Jaeger, K. E., and T. Eggert.** 2004. Enantioselective biocatalysis optimized by directed evolution. Curr. Opin. Biotechnol. **15**:305-313.
26. **Jornvall, H., B. Persson, and J. Jeffery.** 1987. Characteristics of alcohol/polyol dehydrogenases. The zinc-containing long-chain alcohol dehydrogenases. Eur. J. Biochem. **167**:195-201.
27. **Kim, M. H., and S. E. Yun.** 2004. Construction of an electro-enzymatic bioreactor for the production of (*R*)-mandelate from benzoylformate. Biotechnol. Lett. **26**:21-26.
28. **Korkhin, Y., A. J. Kalb (Gilboa), M. Peretz, O. Bogin, Y. Burstein, and F. Frolow.** 1998. NADP-dependent bacterial alcohol dehydrogenases: crystal structure, cofactor-binding and cofactor specificity of the ADHs of *Clostridium beijerinckii* and *Thermoanaerobacter brockii*. J. Mol. Biol. **278**:967-981.
29. **Larsson, K. M., P. Adlercreutz, and B. Mattiasson.** 1990. Studies on horse liver alcohol dehydrogenase in a microemulsion system. Ann. N.Y. Acad. Sci. **613**:791-795.
30. **LeBrun, L. A., D. H. Park, S. Ramaswamy, and B. V. Plapp.** 2004. Participation of histidine-51 in catalysis by horse liver alcohol dehydrogenase. Biochemistry **43**:3014-3026.
31. **Liese, A., K. Seelbach, and C. Wandry.** 2000. Industrial Biotransformations. Wiley-VCH, Weinheim, New York, Chichester, Brisbane, Singapore, Toronto.
32. **Lowry, O. H., J. V. Passonneau, and M. K. Rock.** 1961. The stability of pyridine nucleotides. J. Biol. Chem. **236**:2756-2759.
33. **Lunzer, M., S. P. Miller, R. Felsheim, and A. M. Dean.** 2005. The biochemical architecture of an ancient adaptive landscape. Science **310**:499-501.
34. **MacKintosh, R. W., and C. A. Fewson.** 1987. Microbial alcohol and aldehyde dehydrogenases, p. 259-273. In H. Weiner and T. G. Flynn (ed.), Progress in Clinical and Biological Research - Enzymology and Molecular Biology of Carbonyl Metabolism, vol. 232. Alan R. Liss, Inc., New York.



35. **Meijers, R., R. J. Morris, H. W. Adolph, A. Merli, V. S. Lamzin, and E. S. Cedergren-Zeppezauer.** 2001. On the enzymatic activation of NADH. *J. Biol. Chem.* **276**:9316-9321.
36. **Muller, P.** 1994. Glossary of terms used in physical organic chemistry. *Pure Appl. Chem.* **66**:1077-1184.
37. **Musa, M. M., K. I. Ziegelmann-Fjeld, C. Vieille, J. G. Zeikus, and R. S. Phillips.** 2007. Asymmetric reduction and oxidation of aromatic ketones and alcohols using W110A secondary alcohol dehydrogenase from *Thermoanaerobacter ethanolicus*. *J. Org. Chem.* **72**:30-34.
38. **Musa, M. M., K. I. Ziegelmann-Fjeld, C. Vieille, J. G. Zeikus, and R. S. Phillips.** 2007. Xerogel-encapsulated W110A secondary alcohol dehydrogenase from *Thermoanaerobacter ethanolicus* performs asymmetric reduction of hydrophobic ketones in organic solvents. *Angew. Chem. Int. Ed. Engl.* .
39. **Nadolny, C., and G. Zundel.** 1997. Fourier transform infrared spectroscopic studies of proton transfer processes and the dissociation of  $\text{Zn}^{2+}$ -bound water in alcohol dehydrogenases. *Eur. J. Biochem.* **247**:914-919.
40. **Niehaus, F., C. Bertoldo, M. Kahler, and G. Antranikian.** 1999. Extremophiles as a source of novel enzymes for industrial application. *Appl. Microbiol. Biotechnol.* **51**:711-729.
41. **Oppermann, U., C. Filling, M. Hult, N. Shafqat, X. Wu, M. Lindh, J. Shafqat, E. Nordling, Y. Kallberg, B. Persson, and H. Jornvall.** 2003. Short-chain dehydrogenases/reductases (SDR): the 2002 update. *Chem. Biol. Interact.* **143-144**:247-253.
42. **Pacaud-Mercier, K., M. Blaghen, K. M. Lee, D. Tritsch, and J. F. Biellmann.** 2007. Electron transfer from NADH bound to horse liver alcohol dehydrogenase (NAD<sup>+</sup> dependent dehydrogenase): visualisation of the activity in the enzyme crystals and adsorption of formazan derivatives by these crystals. *Bioorg. Chem.* **35**:59-67.
43. **Patel, R. N.** 2005. Biocatalysis: Synthesis of chiral intermediates for pharmaceuticals, p. Chapter 26. *In* C. T. Hou (ed.), *Handbook of Industrial Biocatalysis*. Taylor & Francis Group, Boca Raton, FL.
44. **Plapp, B. V.** 1970. Enhancement of the activity of horse liver alcohol dehydrogenase by modification of amino groups at the active sites. *J. Biol. Chem.* **245**:1727-1735.
45. **Pocker, Y., J. D. Page, H. Li, and C. C. Bhat.** 2001. Ternary complexes of liver alcohol dehydrogenase. *Chem. Biol. Interact.* **130-132**:371-381.

46. **Radianingtyas, H., and P. C. Wright.** 2003. Alcohol dehydrogenases from thermophilic and hyperthermophilic archaea and bacteria. *FEMS Microbiol. Rev.* **27**:593-616.
47. **Ramaswamy, S., H. Eklund, and B. V. Plapp.** 1994. Structures of horse liver alcohol dehydrogenase complexed with NAD<sup>+</sup> and substituted benzyl alcohols. *Biochemistry* **33**:5230-5237.
48. **Ramaswamy, S., D. H. Park, and B. V. Plapp.** 1999. Substitutions in a flexible loop of horse liver alcohol dehydrogenase hinder the conformational change and unmask hydrogen transfer. *Biochemistry* **38**:13951-13959.
49. **Razvi, A., and J. M. Scholtz.** 2006. Lessons in stability from thermophilic proteins. *Protein Sci.* **15**:1569-1578.
50. **Reid, M. F., and C. A. Fewson.** 1994. Molecular characterization of microbial alcohol dehydrogenases. *Crit. Rev. Microbiol.* **20**:13-56.
51. **Riveros-Rosas, H., A. Julián-Sánchez, R. Villalobos-Molina, J. P. Pardo, and E. Piña.** 2003. Diversity, taxonomy and evolution of medium-chain dehydrogenase/reductase superfamily. *Eur. J. Biochem.* **270**:3309-3334.
52. **Rosell, A., E. Valencia, W. F. Ochoa, I. Fita, X. Pares, and J. Farres.** 2003. Complete reversal of coenzyme specificity by concerted mutation of three consecutive residues in alcohol dehydrogenase. *J. Biol. Chem.* **278**:40573-40580.
53. **Rubach, J. K., and B. V. Plapp.** 2003. Amino acid residues in the nicotinamide binding site contribute to catalysis by horse liver alcohol dehydrogenase. *Biochemistry* **42**:2907-2915.
54. **Salazar, O., P. C. Cirino, and F. H. Arnold.** 2003. Thermostabilization of a cytochrome p450 peroxxygenase. *Chembiochem.* **4**:891-893.
55. **Schlieben, N. H., K. Niefind, J. Muller, B. Riebel, W. Hummel, and D. Schomburg.** 2005. Atomic resolution structures of *R*-specific alcohol dehydrogenase from *Lactobacillus brevis* provide the structural bases of its substrate and cosubstrate specificity. *J. Mol. Biol.* **349**:801-813.
56. **Schmid, A., J. S. Dordick, B. Hauer, A. Kiener, M. Wubbolts, and B. Witholt.** 2001. Industrial biocatalysis today and tomorrow. *Nature* **409**:258-268.
57. **Schoemaker, H. E., D. Mink, and M. G. Wubbolts.** 2003. Dispelling the myths-  
-biocatalysis in industrial synthesis. *Science* **299**:1694-7.
58. **Sekhar, V. C., and B. V. Plapp.** 1988. Mechanism of binding of horse liver alcohol dehydrogenase and nicotinamide adenine dinucleotide. *Biochemistry* **27**:5082-5088.

59. **Sellek, G. A., and J. B. Chaudhuri.** 1999. Biocatalysis in organic media using enzymes from extremophiles. *Enzyme Microb. Technol.* **25**:471-482.
60. **Serov, A. E., A. S. Popova, V. V. Fedorchuk, and V. I. Tishkov.** 2002. Engineering of coenzyme specificity of formate dehydrogenase from *Saccharomyces cerevisiae*. *Biochem. J.* **367**:841-847.
61. **Sriprapundh, D., C. Vieille, and J. G. Zeikus.** 2003. Directed evolution of *Thermotoga neapolitana* xylose isomerase: high activity on glucose at low temperature and low pH. *Protein Eng.* **16**:683-690.
62. **Synowiecki, J., B. Grzybowska, and A. Zdzienbło.** 2006. Sources, properties and suitability of new thermostable enzymes in food processing. *Crit. Rev. Food Sci. Nutr.* **46**:197-205.
63. **Testa, B.** 1995. Chapter 2: Dehydrogenation of alcohols and aldehydes, carbonyl reduction, p. 41-69. *In* B. Testa (ed.), *Biochemistry of Redox Reactions (Metabolism of Drugs and Other Xenobiotics)*. Academic Press, London.
64. **Tishkov, V. I., and V. O. Popov.** 2004. Catalytic mechanism and application of formate dehydrogenase. *Biochemistry (Moscow)* **69**:1252-1267.
65. **Tsai, S. C., and J. P. Klinman.** 2003. De novo design and utilization of photolabile caged substrates as probes of hydrogen tunneling with horse liver alcohol dehydrogenase at sub-zero temperatures: a cautionary note. *Bioorg. Chem.* **31**:172-190.
66. **van der Donk, W. A., and H. Zhao.** 2003. Recent developments in pyridine nucleotide regeneration. *Curr. Opin. Biotechnol.* **14**:421-426.
67. **Vieille, C., K. L. Epting, R. M. Kelly, and J. G. Zeikus.** 2001. Bivalent cations and amino-acid composition contribute to the thermostability of *Bacillus licheniformis* xylose isomerase. *Eur. J. Biochem.* **268**:6291-6301.
68. **Wallon, G., G. Kryger, S. T. Lovett, T. Oshima, D. Ringe, and G. A. Petsko.** 1997. Crystal structures of *Escherichia coli* and *Salmonella typhimurium* 3-isopropylmalate dehydrogenase and comparison with their thermophilic counterpart from *Thermus thermophilus*. *J. Mol. Biol.* **266**:1016-1031.
69. **Wandrey, C.** 2004. Biochemical reaction engineering for redox reactions. *The Chemical Record* **4**:254-265.
70. **Wöltinger, J., K. Drauz, and A. S. Bommarius.** 2001. The membrane reactor in the fine chemicals industry. *Applied Catalysis A: General* **221**:171-185.
71. **Wu, J. T., L. H. Wu, and J. A. Knight.** 1986. Stability of NADPH: effect of various factors on the kinetics of degradation. *Clin. Chem.* **32**:314-319.

72. **Zaks, A.** 2001. Industrial biocatalysis. *Curr. Opin. Chem. Biol.* **5**:130-136.
73. **Zeikus, J. G., C. Vieille, and A. Savchenko.** 1998. Thermozyms: biotechnology and structure-function relationships. *Extremophiles* **2**:179-183.
74. **Zhao, H., and W. A. van der Donk.** 2003. Regeneration of cofactors for use in biocatalysis. *Curr. Opin. Biotechnol.* **14**:583-589.
75. **Zhu, G., G. B. Golding, and A. M. Dean.** 2005. The selective cause of an ancient adaptation. *Science* **307**:1279-1282.
76. **Ziegelmann-Fjeld, K. I., M. M. Musa, R. S. Phillips, J. G. Zeikus, and C. Vieille.** 2007. A *Thermoanaerobacter ethanolicus* secondary alcohol dehydrogenase mutant derivative highly active and stereoselective on phenylacetone and benzylacetone. *Protein Eng. Des. Sel.* **20**:47-55.

## **CHAPTER II**

### ***A *Thermoanaerobacter ethanolicus* secondary alcohol dehydrogenase mutant derivative highly active and stereoselective on phenylacetone and benzylacetone***

**Research presented in this chapter was published as the following manuscript:**

Ziegelmann-Fjeld, K.I., Musa, M.M., Phillips, R.S., Zeikus, J.G., and Vieille, C. A *Thermoanaerobacter ethanolicus* secondary alcohol dehydrogenase mutant derivative highly active and stereoselective on phenylacetone and benzylacetone. *Protein Engineering, Design and Selection*. 2007. 20(2); 47-55. DOI:10.1093/protein/gzl052.

## 2.1 Abstract

The secondary alcohol dehydrogenase from *Thermoanaerobacter ethanolicus* 39E (TeSADH) is highly thermostable and solvent-stable, and it is active on a broad range of substrates. These properties make TeSADH an excellent template to engineer an industrial catalyst for chiral chemical synthesis. (S)-1-Phenyl-2-propanol was our target product because it is a precursor to major pharmaceuticals containing secondary alcohol groups. TeSADH has no detectable activity on this alcohol, but it is highly active on 2-butanol. The structural model we used to plan our mutagenesis strategy was based on the substrate's orientation in a horse liver alcohol dehydrogenase•p-bromobenzyl alcohol•NAD<sup>+</sup> ternary complex (PDB entry 1HLD). The W110A TeSADH mutant now uses (S)-1-phenyl-2-propanol, (S)-4-phenyl-2-butanol, and the corresponding ketones as substrates. W110A TeSADH's kinetic parameters on these substrates are in the same range as those of TeSADH on 2-butanol, making W110A TeSADH an excellent catalyst. In particular, W110A TeSADH is twice as efficient on benzylacetone as TeSADH is on 2-butanol, and it produces (S)-4-phenyl-2-butanol from benzylacetone with an enantiomeric excess above 99%. W110A TeSADH is optimally active at 87.5°C and it remains highly thermostable. W110A TeSADH is active on aryl derivatives of phenylacetone and benzylacetone, making this enzyme a potentially useful catalyst for the chiral synthesis of aryl derivatives of alcohols. As a control in our engineering approach, we used the TbSADH•(S)-2-butanol binary complex (PDB entry 1BXZ) as the template to model a mutation that would make TeSADH active on (S)-1-phenyl-2-propanol. Mutant Y267G TeSADH did not have the substrate specificity predicted in this modeling study. Our results suggest that (S)-2-butanol's orientation in the TbSADH•(S)-

2-butanol binary complex does not reflect its orientation in the enzyme-substrate-cofactor ternary complex.

Keywords: (S)-alcohol/ benzylacetone/ enantioselectivity/ phenylacetone/ secondary alcohol dehydrogenase/

## 2.2 Introduction

Up to 90% of the drugs currently being made are sold as racemic mixtures, but the FDA has been increasingly mandating chiral purity, or evidence to show that the inactive enantiomer is not harmful. Indeed, while generally only one enantiomer is biologically active for the intended purpose of the drug, the other enantiomer can be toxic (5, 8, 10). For these reasons pharmaceutical companies are looking for more efficient ways of producing enantiomerically pure compounds. Much effort has been spent in the last two decades to replace conventional chemical reactions with biological reactions. With their high substrate specificity and their high enantio- and regio-selectivities, enzymes can catalyze in one step reactions that would otherwise require costly blocking and deblocking steps. These enzyme properties also lead to fewer by-products by helping minimize undesirable side reactions such as isomerization, racemization, epimerization, and rearrangement (25, 27).

Chiral alcohols are important building blocks in a variety of high-value chemicals used in the food, fine chemical, and pharmaceutical industries (21). Alcohol dehydrogenases (ADHs) (EC 1.1.1.1 and 1.1.1.2) catalyze the reversible reduction of ketones and aldehydes to alcohols (6). Commercially available ADHs often have one or more shortcomings that prevent their use in industrial applications. Most lack long-term stability, most lack activity in organic solvents and at elevated temperatures, and their substrate specificity is often not adapted to a particular application (14). The secondary ADH (SADH) from the thermophilic bacterium *Thermoanaerobacter ethanolicus* 39E (TeSADH) has several properties that make it a promising enzyme for chiral alcohol production. It is optimally active near 90°C, thermostable (half-life of 1.7 hours at 90°C)



(5), and specific for secondary alcohols (3). TeSADH is also stable in solvents. It retains 90%, 100%, 80%, and 68% activity after a 3-hr incubation at 50°C in 100% n-dodecane, n-octane, toluene, and pyridine, respectively (3, 15, 22).

The *T. ethanolicus adhB* gene was cloned and expressed in *Escherichia coli* (6). TeSADH is a medium chain, zinc-containing, tetrameric ADH composed of identical 40 kDa subunits. This NADP(H)-dependent enzyme contains a single catalytic zinc coordinated by Cys37, His59, and Asp150 (2). TeSADH is commercially available under the name *Thermoanaerobacter* (formerly *Thermoanaerobium* (19)) *brockii* SADH (TbSADH) (Sigma, St. Louis, MO). Early sequencing results (6) suggested that TeSADH and TbSADH differed by three residues: Trp91, Pro313, and Gln325 in TeSADH versus Arg91, Arg313, and Arg325 in TbSADH. Recent *T. ethanolicus* 39E genome sequencing results (NCBI entry 2P\_00779753) and repeated sequencings in our lab (Laivenieks, unpublished results) indicate that TeSADH is identical to TbSADH. Both enzymes have very broad substrate specificities. Examples of successful synthesis with TbSADH have been reported in the literature (15).

TbSADH's three dimensional structure has been solved by X-ray crystallography in complex with NADP<sup>+</sup> (PDB entry 1YKF) (16) and in complex with (S)-2-butanol (PDB entry 1BXZ) (13). TeSADH has been structurally characterized by X-ray crystallography in the Arni lab at the Universidade de Sao Paulo, Ribeirao Preto-SP, Brazil (personal communication). Since the two enzymes are identical, the published TbSADH structures were used for our modeling studies. The TbSADH substrate-binding site is composed of a large pocket and a small pocket (Figure 2-1), whose structural and chemical makeups determine the enzyme's substrate specificity and stereospecificity

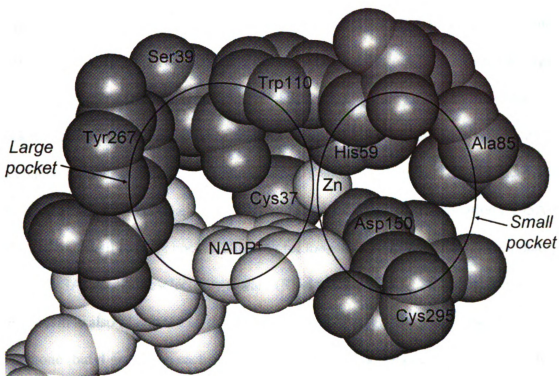


**Figure 2-1.** TbSADH active site in CPK representation, based on PDB # 1YKF. NADP<sup>+</sup> and Zn are in white, TbSADH residues are in gray. NADP<sup>+</sup>'s nicotinamide ring was rotated 90° to match the orientation of NAD<sup>+</sup>'s nicotinamide ring in the HLADH•BRB•NAD<sup>+</sup> ternary complex (PDB # 1HLD).

(12). The small pocket has a higher affinity for alkyl groups than the larger pocket does, and it can accommodate methyl, ethyl, isopropyl, and cyclopropyl groups, while anything larger is excluded. The current hypothesis explaining TeSADH's stereospecificity is that, if the larger of the alkyl groups of a ketone fits into the small alkyl-binding pocket, the enzyme will likely produce an (R)-alcohol. If the larger of the alkyl groups is too large to fit into the small pocket, the large group will be forced into the large alkyl-binding pocket, causing the enzyme to produce an (S)-alcohol (15). This substrate specificity mechanism was demonstrated by mutations S39T and C295A in the TeSADH active site. Mutation S39T decreased the size of the large alkyl-binding pocket. Mutation C295A enlarged the small binding pocket, allowing for longer alkyl chains to fit. Both mutations shifted TeSADH enantioselectivity toward (R)-alcohols (12, 29). This specificity mechanism is also illustrated by the fact that TbSADH is unable to use either 4-heptanone (butyl groups on each side of the ketone) or 5-nonanone (pentyl groups on each side of the ketone), whereas both 2-heptanone and 2-nonanone are substrates (15).

We chose TeSADH as our target enzyme to develop a catalyst able to produce 1-phenyl-2-propanol from phenylacetone. One-phenyl-2-propanol is important to the pharmaceutical industry because it is an immediate precursor to amphetamine and amphetamine derivatives (20), and no thermostable and solvent-stable ADH is known to be active on this alcohol. TeSADH is naturally inactive on phenylacetone. In this study we designed a catalytic site point mutation, W110A, that makes TeSADH active on phenylacetone, producing 1-phenyl-2-propanol. We also show that W110A TeSADH is active on benzylacetone, and that it is specific for (S)-4-phenyl-2-butanol and (S)-1-phenyl-2-propanol. Four-phenyl-2-butanol is also important to the pharmaceutical

industry because it is used as a precursor to anti-hypertensive agents and spasmolytics (anti-epileptic agents) (20).

## 2.3 Materials and Methods

### 2.3.1 Chemicals

The racemic, (S)-, and (R)-forms of 1-phenyl-2-propanol, racemic 4-phenyl-2-butanol, NaIO<sub>4</sub>, Na<sub>2</sub>Cr<sub>2</sub>O<sub>7</sub>·2H<sub>2</sub>O, and isopropenyl acetate were purchased from Aldrich (St. Louis, MO). Benzylacetone was purchased from ACROS Organics (Morris Plains, NJ). *Candida Antarctica* lipase immobilized on acrylic resin was purchased from Sigma (L4777).

### 2.3.2 Syntheses of phenylacetone, and (S)- and (R)-4-phenyl-2-butanol

Phenylacetone was synthesized from (rac)-1-phenyl-2-propanol as described (30), with the only modification that the reaction was performed at room temperature instead of 4°C. The yield was 33%. <sup>1</sup>H NMR spectra were recorded on a Varian Mercury Plus 400 spectrometer at 400 MHz <sup>1</sup>H NMR (CDCl<sub>3</sub>): δ 7.2-7.4 (m, 5H), δ 3.7 (s, 2H), δ 2.2 (s, 3H).

(S)-4-Phenyl-2-butanol was produced from (rac)-4-phenyl-2-butanol by kinetic resolution as described (7), with the exception that the ruthenium catalyst and *tert*-butoxide were omitted. (S)-4-Phenyl-2-butanol and (R)-1-methyl-3-phenylpropyl acetate were produced in quantitative yields after a 5-day reaction at room temperature. (*S*)-4-Phenyl-2-butanol {α}<sub>D</sub> +13.5 (c= 3.9, CHCl<sub>3</sub>) <sup>1</sup>H NMR (CDCl<sub>3</sub>): δ 7.2-7.4 (m, 5H), δ 3.8 (m, 1H), δ 2.8 (m, 2H), δ 1.80 (m, 3H), δ 1.3 (d, 3H). (*R*)-1-Methyl-3-phenylpropyl acetate <sup>1</sup>H NMR (CDCl<sub>3</sub>): δ 7.2-7.4 (m, 5H), δ 4.9 (m, 1H), δ 2.7 (m, 2H). δ 2.1 (s, 3H), δ 1.8 (m, 2H), δ 1.3 (d, 3H).

(R)-4-phenyl-2-butanol was then produced from (R)-1-methyl-3-phenylpropyl acetate by saponification. The yield was 90%.  $[\alpha]_D -14.9$  ( $c=3.9$ ,  $\text{CHCl}_3$ )  $^1\text{H}$  NMR ( $\text{CDCl}_3$ ):  $\delta$  7.2-7.4 (m, 5H),  $\delta$  3.8 (m, 1H),  $\delta$  2.7 (m, 2H),  $\delta$  1.8 (m, 2H),  $\delta$  1.6 (s, 1H),  $\delta$  1.3 (d, 3H).

### 2.3.3 Modeling

Modeling was done manually in InsightII (Accelrys, San Diego, CA) on a Silicon Graphics Octane 2 computer. The TbSADH•(S)-2-butanol complex (PDB # 1BXZ) was superimposed with the TbSADH• $\text{NADP}^+$  complex (PDB #1YKF) (16) in InsightII. After superposition, the entire 1BXZ structure, except for the (S)-2-butanol molecule, was removed, and the (S)-2-butanol was merged with the 1YKF structure. The result was a single TbSADH enzyme structure model containing  $\text{NADP}^+$ , zinc, and (S)-2-butanol. The 3D-structure of (S)-1-phenyl-2-propanol was generated with CORINA-Gasteiger Research. This substrate was fitted in the active site of the new TbSADH•(S)-2-butanol• $\text{NADP}^+$  model, with its reactive oxygen superimposed with that of (S)-2-butanol.

In a second modeling approach, we started from the structure of the horse liver ADH (HLADH) co-crystallized with a substrate (i.e., p-bromobenzyl alcohol, BRB) and  $\text{NAD}^+$  (PDB # 1HLD). The TbSADH•(S)-2-butanol• $\text{NADP}^+$  model was superimposed with the structure of the HLADH•BRB• $\text{NAD}^+$  complex using the conserved catalytic site residues for the alignment. Starting from the (S)-1-phenyl-2-propanol pdb file we had generated in CORINA, we generated the lowest energy conformations of this substrate using Omega (OpenEye Scientific Software, Santa Fe, NM). Individual conformations were then fitted manually into the TbSADH catalytic site, their C–OH bond superimposed with that of

BRB in HLADH. All individual conformations of (S)-1-phenyl-2-propanol were manually rotated around their C–OH bond axis to identify orientations that would minimize steric overlap between atoms of the substrate and active site residues. One of the seven (S)-1-phenyl-2-propanol conformations tested (the lowest energy conformation) created steric overlap with a single residue, Trp110, in TeSADH's catalytic site. All other (S)-1-phenyl-2-propanol conformations created overlaps with more than one residue.

The 3D structures of the mutant enzymes were modeled using the SWISS-MODEL (11, 26, 28) program with the TbSADH•NADP<sup>+</sup> complex as the template. The wild-type enzyme was also modeled as a control to detect any changes that may be modeling artifacts. The models were superimposed with the TbSADH crystal structure to determine how much if any the backbone of the mutant structure deviated from the crystal structure.

#### **2.3.4 Mutagenesis**

Mutations W110A and Y267G were introduced by site-directed mutagenesis (SDM) using PCR (4). The wild-type *adhB* gene in the pADHB1M1-kan plasmid (a pBluescript II KS+–kanamycin derivative) (4, 6) was used as the template. Primers were synthesized by the Michigan State University Macromolecular Structure Facility. For unknown reasons the *T. ethanolicus adhB* gene does not lend itself to single-step mutagenesis using protocols such as Stratagene's QuikChange® Site-Directed Mutagenesis Kit. Therefore, mutagenesis was performed in two steps using the Expand High Fidelity PCR System (Roche, Indianapolis, IN).

In step 1, primers 5'-ATCAATATGTCATATGATGAAAGGTTTTGCAATGC (**A**, where CATATG encodes a 5' *NdeI* site) and 5'-CATTCGAAAATTTTCGCGCCTGCCAGC (where CGC creates the W110A mutation) or 5'-AGGACCATCTTTAGGGTTTACAA-TATC (where AGG creates the Y267G mutation), were used to create the W110A or Y267G mutation in the 5' end of the gene, and primers 5'-GCTGGCAGGCGCGA-AATTTTAGAATG (where GCG creates the W110A mutation) or 5'-GATATTGTAAAC-CCTAAAGATGGTCCT (where CCT creates the Y267G mutation), and 5'-GTCATCTCGAGTGCTAATATTACAACAGGTTTG (**B**, where CTCGAG encodes a 3' *XhoI* site) were used to create the W110A mutation in the 3' end of the gene. In step 2 the complete *adhB* gene was reconstructed using the two PCR products from step 1 as co-templates and oligonucleotides **A** and **B** as primers.

The PCR products were subcloned into the PCR 2.1-TOPO vector (Invitrogen, Carlsbad, CA) and transformed into Chemically Competent One Shot TOP10 *E. coli* cells (Invitrogen, Carlsbad, CA). The recombinant plasmids were purified from the TOP10 cells for automated sequencing at the Michigan State University Genomics Facility. Mutant sequences were compared to the wild-type *adhB* sequence using the ClustalW multiple sequence alignment program. Genes containing only the W110A or the Y267G mutation were then subcloned into pET24a(+) (Novagen, Madison, WI) for expression. In these constructs, W110A and Y267G TeSADHs were expressed as a fusion protein with a C-terminal His<sub>6</sub> tag.



### **2.3.5 Protein expression and purification**

W110A TeSADH was expressed in HB101(DE3) cells. Cultures were grown in 500 ml LB medium (per liter: 10 g tryptone, 5 g yeast extract, 5g NaCl) containing 100 mg/l kanamycin. When the culture reached 0.6-1 OD<sub>600</sub>, W110A TeSADH expression was induced with 1 mM IPTG for 5 hours. The cells were spun down (5,000 rpm for 20 min) and resuspended in 4 volumes of lysis buffer (50 mM Tris-HCl (pH 8.5), 10 mM 2-mercaptoethanol, 1 mM phenylmethylsulfonyl fluoride) per 1 gram of cells. The cells were lysed in a French pressure cell, and the lysate was spun down (10,000 rpm for 10 min) to remove the cell debris. The crude extract was heat-treated at 85°C for 15 min to inactivate non-thermostable proteins, then spun down (10,000 rpm for 10 min) to remove the denatured proteins. The cleared crude extract was loaded on a 5 ml Ni-NTA (Qiagen, Valencia, CA) column. W110A TeSADH was purified using the Gibco BRL procedure for Protein Expression System, pRoEX-1 vector (cat. no. 10197-010, Gaithersburg, MD). Protein expression in the fractions was tested by SDS-PAGE (18). Protein concentration was quantified using the Biorad Protein Dye with bovine serum albumin as the standard. The purified protein was frozen in 250 µl aliquots at -80°C for months without affecting enzyme activity.

### **2.3.6 Enzyme assays**

Activities of the wild-type, Y267G, and W110A TeSADHs were first tested in crude extracts from 5 ml cultures as described (3) with (rac)-2-butanol, (rac)-1-phenyl-2-propanol, and (rac)-4-phenyl-2-butanol as substrates. All assays were done in the presence of 50 mM Tris-HCl pH 8.0 and 0.4 mM NADP<sup>+</sup> (alcohol oxidation), or pH 6.5

and 0.4 mM NADPH (ketone reduction). Initial velocity was measured spectrophotometrically at 60°C by following NADPH production (alcohol oxidation), or consumption (ketone reduction) at 340 nm for 1 min in a Varian Cary 300 UV/Vis spectrophotometer equipped with a Peltier heating system. In all cases the enzyme was preincubated for at least 5 min at 40°C before being added to the assay. The same conditions were used to test activity of the purified W110A TeSADH with (rac)-2-butanol; (rac)-1-phenylethan-1-ol; the (S)- and (R)-4-phenyl-2-butanol; (S)- and (R)-1-phenyl-2-propanol; acetophenone; benzylacetone; phenylacetone; and the aryl derivatives (1 mM each) 1-chloro-3-phenyl-2-propanol, 3-chloro-3-methyl-4-phenyl-2-butanone, (2-fluorophenyl) acetone, and 1-(4-bromophenyl) acetone. One unit of activity was defined as the amount of enzyme needed to consume or produce 1  $\mu$ mol of NADPH per minute.

To determine the effect of temperature on activity, enzyme assays were performed at temperatures from 5°C to 97°C, with 10 mM (rac)-1-phenyl-2-propanol as the substrate. To determine the kinetic parameters, enzyme assays were performed with (rac)-2-butanol (0.5–500 mM), (S)-1-phenyl-2-propanol (0.05–10.5 mM), (S)-4-phenyl-2-butanol (0.05–10 mM), benzylacetone (0.05–5 mM), and phenylacetone (0.05–7.5 mM) at 60°C for 1 min in 50 mM Tris-HCl pH 8.0 (alcohol oxidation) or pH 6.5 (ketone reduction) in the presence of 0.4 mM NADP(H). At least eight substrate concentrations were used for each data set and each set was performed in triplicate. The  $K_m$  and  $V_{max}$  values of W110A TeSADH were calculated using the Non-Linear Curve Fit tool of Origin 6.1 (OriginLab Corporation, Northampton, MA).

To determine the effect of pH on activity, enzyme assays were performed at pH 4.0–9.1 with 5 mM benzylacetone or (rac)-4-phenyl-2-butanol as the substrate. Ketone

reduction assays were performed in 50 mM citrate buffer (pH 4.0–7.2) and 50 mM Tris buffer (pH 7.0–7.3) in the presence of 0.4 mM NADPH. Alcohol oxidation assays were performed in 50 mM citrate buffer (pH 7.0–7.2) and 50 mM Tris buffer (pH 7.0–9.1) in the presence of 0.4 mM NADP<sup>+</sup>. Assays at each pH were performed in triplicate.

### **2.3.7 Asymmetric reduction of benzylacetone to the corresponding *sec*-alcohol**

A mixture of 0.3 mmol benzylacetone, 1.31  $\mu$ mol (0.131 mM final concentration) NADP<sup>+</sup> and 0.56 mg W110A TeSADH in 10.0 ml Tris-HCl (pH 6.5)/isopropanol (70:30) was stirred at 50°C for 12 h before being extracted with CH<sub>2</sub>Cl<sub>2</sub>. The organic layer was then concentrated under vacuum. The residual compound was purified on a silica gel column. The absolute configuration of the produced alcohol was determined by comparing the sign of the optical rotation with those reported for (S)-, and (R)-4-phenyl-2-butanol (24). The percent conversion and enantiomeric excess (ee) were determined by chiral column GC.

### **2.3.8 Stability assays**

Enzyme kinetic stability was tested as described (5) at 85°C and 90°C for W110A TeSADH, and 90°C for TeSADH. Activity assays on the heat-treated enzymes were performed with 5 mM (rac)-4-phenyl-2-butanol (W110A TeSADH) and 5 mM (rac)-2-butanol (TeSADH). Fifty  $\mu$ l of the 0.2 mg/ml W110A TeSADH inactivation solution (10  $\mu$ g enzyme) or 30  $\mu$ l of the wild-type inactivation solution (6  $\mu$ g enzyme) was added to each activity assay. Inactivation curves were performed in triplicate, and fit using the Non-Linear Curve Fit tool of Origin 6.1.

W110A TeSADH solvent stability was tested with the same procedure as the thermostability tests (5) with 30% 2-propanol in the inactivation enzyme solutions. Time points were taken every 30 min for 2 hr. Fifty  $\mu$ l of the 0.2 mg/ml W110A TeSADH (10  $\mu$ g per assay) in 30% 2-propanol (195 mM final assay concentration) inactivation solution was added to each enzyme assay. All assays were performed in 50 mM Tris-HCl (pH 8.0) and 0.4 mM NADP<sup>+</sup>. The 2-propanol present in the inactivation solution was used as the substrate.

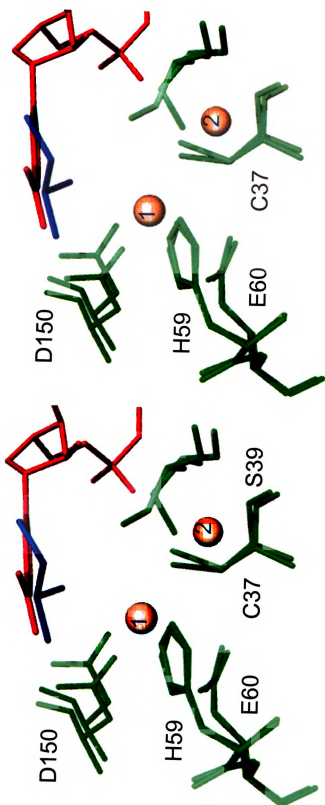
## 2.4 Results and Discussion

It has previously been shown with TbSADH that large substrates, such as 2-decanone, can be reduced to the corresponding alcohol at very low rates. In contrast, TbSADH is not significantly active on substrates containing rings with more than three carbons (15); the bulk of the ring does not fit in the active site. Mutations were decided upon to increase the size of the active site and accommodate the large phenyl ring of 1-phenyl-2-propanol.

### 2.4.1 Modeling and mutagenesis

When we superimposed the TbSADH•(S)-2-butanol and TbSADH•NADP<sup>+</sup> complexes, we noticed that the 2-butanol molecule in the TbSADH•(S)-2-butanol complex almost overlapped NADP<sup>+</sup>'s nicotinamide ring in the TbSADH•NADP<sup>+</sup> complex (Figure 2-2). In addition, the catalytic Zn<sup>2+</sup> moves by more than 1 Å between the two structures. These observations suggest that the positions in which NADP<sup>+</sup>'s nicotinamide ring is oriented in the TbSADH•NADP<sup>+</sup> complex and/or the position in which 2-butanol is oriented in the TbSADH•(S)-2-butanol complex do not reflect their orientations in an active enzyme-substrate-cofactor ternary complex. In PDB structure # 1HLD, HLADH is co-crystallized with a substrate (i.e., *p*-bromobenzyl alcohol, BRB) and NAD<sup>+</sup>. When we superimposed this structure with those of the TbSADH•(S)-2-butanol and the TbSADH•NADP<sup>+</sup> complexes (1BXZ and 1YKF, respectively; 2- 3A), we could see (i) that the orientation of (S)-2-butanol in TbSADH's catalytic site did not correspond to that of BRB in HLADH, and (ii) that NADP<sup>+</sup>'s nicotinamide ring in the

**Figure 2-2. Modeling of the TbSADH•(S)-2-butanol and the TbSADH•(S)-NADP<sup>+</sup> binary complexes into a single, TbSADH•(S)-2-butanol•(S)-NADP<sup>+</sup> model.** Green: TeSADH residues; red: NADP<sup>+</sup>; blue: 2-butanol; and orange: Zn<sup>2+</sup>. The two structures were superimposed in InsightII using the heavy atoms of catalytic site residues C37, S39, H59, E60, Asp150, L294, and C295. 1 and 2 denote the positions of the catalytic Zn<sup>2+</sup> in the TbSADH•(S)-NADP<sup>+</sup> and TbSADH•(S)-2-butanol binary complexes, respectively. Figure is shown in stereo.



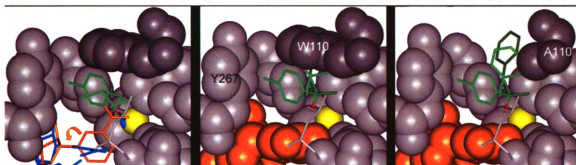


**Figure 2-3. Modeling of (S)-1-phenyl-2-propanol in the catalytic sites of TeSADH and W110A TeSADH using the HLADH•BRB•NAD<sup>+</sup> ternary complex as the template.** (A) Superposition of our TbSADH•2-butanol•NADP<sup>+</sup> model and HLADH•BRB•NAD<sup>+</sup> (pdb #1HLD). The proteins were aligned using the backbones of the Zn<sup>2+</sup>-binding residues, C36, H67, and C174 in HLADH, and C37, H59, and D150 in the TbSADH complexes. (B) Modeling of (S)-1-phenyl-2-propanol in TbSADH catalytic site, with its reactive hydroxyl group superimposed with that of BRB. Two orientations of (S)-1-phenyl-2-propanol are shown. (C) W110A mutation showing how (S)-1-phenyl-2-propanol can be a substrate of W110A TeSADH. Only residues in the TbSADH catalytic site are shown (in gray, CPK representation); Leu294 is not in CPK representation to allow a view into the catalytic site. Blue: NAD<sup>+</sup> (sticks) and catalytic zinc (CPK) in 1HLD; orange: NADP<sup>+</sup> in 1YKF (sticks in A, CPK in B and C); yellow: catalytic zinc in 1YKF; and atom colors (carbon in green and oxygen in red): substrates (BRB in 1HLD and 2-butanol in 1BXZ in A; BRB in 1HLD and (S)-1-phenyl-2-propanol in 1YKF in B and C). The orange arrow in (A) indicates the direction in which NADP<sup>+</sup>'s nicotinamide ring was rotated in (B) and (C) to match the orientation in PDB #1HLD.



TbSADH•NADP<sup>+</sup> complex is rotated by almost 90° in comparison to NAD<sup>+</sup>'s nicotinamide ring in the HLADH•BRB•NAD<sup>+</sup> ternary complex. The orientation of the NAD<sup>+</sup> allows for hydrogen bonding with residues of the HLADH. The orientation of the NADP<sup>+</sup> in the TeSADH does not allow for the same hydrogen bonds to be made (Figure 2-4). The hydrogen bonded NAD<sup>+</sup> is in proper position for the hydride transfer with the substrate, *p*-bromobenzyl alcohol (Figure 2-5) (1).

Because HLADH is a primary ADH that is only very poorly active on secondary alcohols, it is unclear how well the orientation of the substrate in TeSADH should match that in HLADH. For this reason, we decided to adopt two modeling and mutagenic strategies: one based on the orientation of (S)-2-butanol in a TbSADH•(S)-2-butanol•NADP<sup>+</sup> ternary model (construction described in the Materials and Methods) and one based on the orientation of BRB in the HLADH•BRB•NAD<sup>+</sup> ternary complex.

(S)-1-Phenyl-2-propanol was fitted manually into the TbSADH•(S)-2-butanol•NADP<sup>+</sup> model with the reactive hydroxyl group superimposed with that of (S)-2-butanol. As seen in Figure 2-6, the phenyl ring of (S)-1-phenyl-2-propanol is in close proximity (1.69 Å) with the C $\beta$  of Y267. This steric clash potentially excludes (S)-1-phenyl-2-propanol from being a substrate for TeSADH. To remove this steric overlap, we constructed the Y267G mutant to increase the depth of the large pocket enough to accommodate the phenyl ring of (S)-1-phenyl-2-propanol.

In our second modeling approach, all seven Omega-generated conformations of (S)-1-phenyl-2-propanol were manually fitted into the TbSADH catalytic site, with their C–OH bond superimposed with that of BRB in HLADH. (S)-1-phenyl-2-propanol individual conformations were manually rotated around their C–OH bond axis to identify

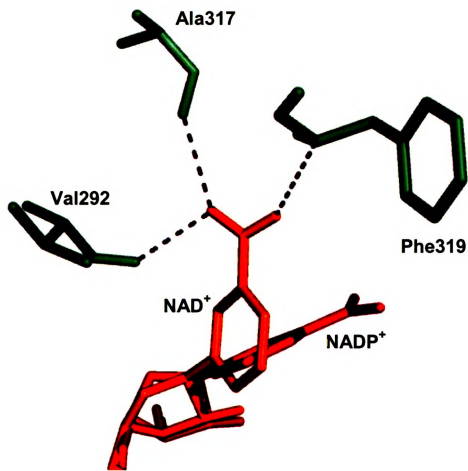


**Figure 2-4. NAD<sup>+</sup> hydrogen bonded with HLADH, and NADP<sup>+</sup> from TeSADH**  
 Green: HLADH residues; orange: NAD<sup>+</sup> of HLADH; red: NADP<sup>+</sup> of TeSADH

**Figure 2-5. Geometry of hydride transfer in HLADH**

Green: HLADH residues; orange:  $\text{NAD}^+$ ; yellow: catalytic zinc; blue: *p*-bromobenzyl alcohol

Arrow indicates the hydride transfer from *p*-bromobenzyl alcohol to the nicotinamide ring of  $\text{NAD}^+$

Figure is shown in stereo.

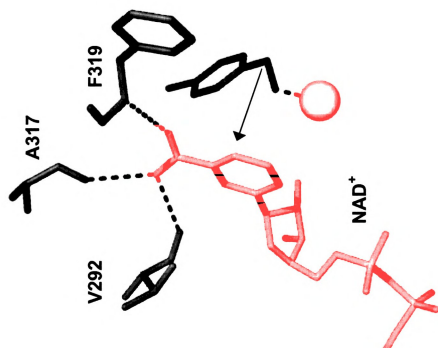
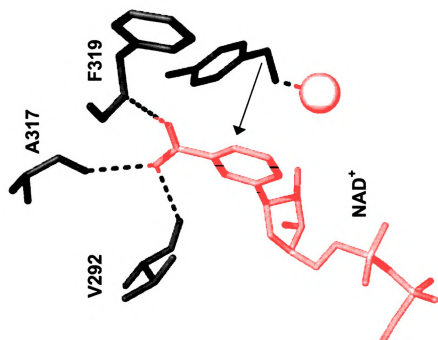
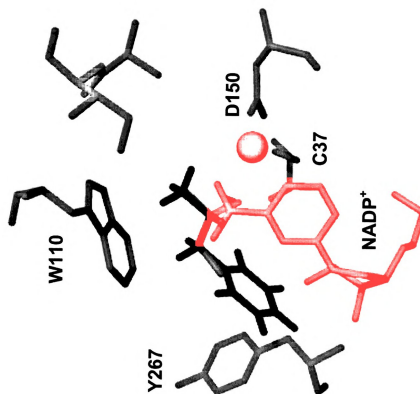
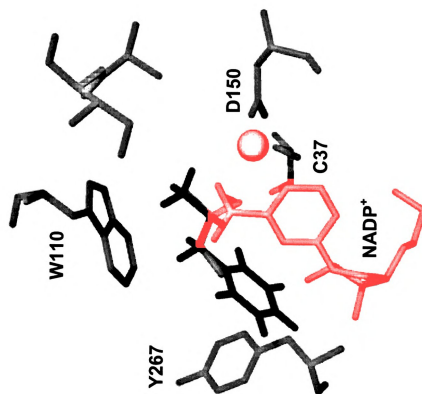


**Figure 2-6. (S)-1-Phenyl-2-propanol modeled in the TbSADH•(S)-2-butanol•NADP<sup>+</sup> ternary complex.** Green: TeSADH residues; red: NADP<sup>+</sup>; orange: Zn<sup>2+</sup>; pink: 2-butanol; and blue: (S)-1-phenyl-2-propanol.  
Figure is shown in stereo.



orientations that would minimize steric overlap between atoms of the substrate and active site residues. Two orientations of one (S)-1-phenyl-2-propanol conformation tested (the lowest energy conformation) created steric overlap with a single residue, Trp110, in TeSADH's catalytic site (Figure 2-3B). All other (S)-1-phenyl-2-propanol conformations created overlaps with more than one residue (not shown). We constructed the W110A mutant to remove the steric overlap between (S)-1-phenyl-2-propanol and Trp110 (Figure 2-3C).

The Y267G and W110A mutations were individually modeled into TbSADH using SWISS-MODEL to predict changes in the mutant structure in comparison to the TbSADH crystal structure. Wild-type TbSADH was also modeled to check for possible artifacts in the modeling process. In both mutant 3D-models the backbones of the mutated residues, Y267G and W110A, remained unchanged with the same ( $\phi, \psi$ ) angles as in the wild-type crystal structure. In both mutant models the catalytic zinc shifted by 0.78 Å, and the side-chains of zinc-binding residues, His59, Cys37, Asp150, were slightly reoriented. Because these changes also occurred in the wild-type (control) model they were discounted as modeling artifacts.

Mutations W110A and Y267G were introduced into *T. ethanolicus adhB* by site-directed mutagenesis. The mutant TeSADHs were expressed in *E. coli* as fusion proteins with a C-terminal His<sub>6</sub> tag. Both mutant enzymes were abundantly expressed as soluble proteins. They were stable during a 15-min heat treatment at 85°C suggesting that they were properly folded despite the active site mutations.

#### **2.4.2 Activity and substrate specificity**

The activity of Y267G TeSADH was tested on heat-treated crude extracts with (rac)-2-butanol, (rac)-1-phenyl-2-propanol, and (rac)-4-phenyl-2-butanol as substrates. Results were compared to those of heat-treated crude extracts of TeSADH. TeSADH's and Y267G TeSADH's relative concentrations in heat-treated crude extracts were estimated by SDS-PAGE (not shown). Y267G TeSADH showed a slight decrease in specific activity on (rac)-2-butanol (~33 U/mg protein) when compared to the wild-type enzyme (~41 U/mg protein). Y267G TeSADH had no activity on (rac)-1-phenyl-2-propanol or (rac)-4-phenyl-2-butanol, and was not further studied.

Activity assays with heat-treated crude extracts suggested that W110A TeSADH is much less active on 2-butanol than TeSADH is, and that it is inactive on 1-phenylethan-1-ol and acetophenone. In contrast, W110A TeSADH showed significant activity on (rac)-1-phenyl-2-propanol, phenylacetone, and (rac)-4-phenyl-2-butanol, substrates on which wild-type TeSADH showed no activity. W110A TeSADH also showed significant activity with benzylacetone, on which wild-type TeSADH showed only slight activity (Table 2-1). W110A TeSADH was purified to homogeneity and characterized. Initial activity assays with purified W110A TeSADH agreed with previous assays on crude extracts (Table 2-1): W110A TeSADH showed ten-fold lower activity on (rac)-2-butanol than TeSADH did; it showed almost no activity on (rac)-1-phenylethan-1-ol and acetophenone; and it showed high activity levels on phenylacetone, benzylacetone, (S)-1-phenyl-2-propanol, and (S)-4-phenyl-2-butanol (Table 2-1). Further assays showed that W110A TeSADH is not active on (R)-1-phenyl-2-propanol and (R)-4-phenyl-2-butanol.



Table 2-2 highlights W110A TeSADH's kinetic parameters. W110A TeSADH's  $V_{\max}$  on (rac)-2-butanol only decreased by about 20%, while its affinity for (rac)-2-butanol decreased by more than two orders of magnitude. The low affinity for 2-butanol explains why we detected low specific activity for W110A TeSADH on 10 mM (rac)-2-butanol (Table 2-1). In contrast W110A TeSADH's kinetic parameters on (S)-1-phenyl-2-propanol, phenylacetone, (S)-4-phenyl-2-butanol, and benzylacetone are of the same order of magnitude as those of TeSADH on (rac)-2-butanol, making W110A TeSADH an excellent catalyst on these substrates. It is interesting to note that W110A TeSADH's  $V_{\max}$  and  $K_m$  values on benzylacetone are higher than those of TeSADH on (rac)-2-butanol, making W110A TeSADH twice as efficient on benzylacetone as TeSADH is on (rac)-2-butanol.

#### **2.4.3 Effect of pH on enzyme activity**

Alcohol oxidation and ketone reduction assays were performed at different pH values in citrate and Tris buffers at overlapping pHs to determine how pH affects W110A TeSADH activity. Results show that the optimum pH was 4.9 for ketone reduction, and 8.8 for alcohol oxidation (Figure 2-7). These results show a significant difference from the TeSADH optimum pH of 6.5 for ketone reduction, and a slight difference from 9.0 for alcohol oxidation (3).

#### **2.4.4 W110A TeSADH's enantioselectivity**

GC analysis on a chiral column combined with optical rotation measurements showed a 99% conversion in the asymmetric reduction of benzylacetone

Substrate <sup>b</sup>	W110A ( $\mu\text{mol}/\text{min}\cdot\text{mg}$ protein)	Substrate <sup>b</sup>	TeSADH ( $\mu\text{mol}/\text{min}\cdot\text{mg}$ protein)
2-Butanol (10 mM)	3.65	2-Butanol (7.5 mM)	45.27
(rac)-1-Phenethyl alcohol (10 mM)	0.2429	(rac)-1-Phenethyl alcohol (10 mM)	0.15
Acetophenone (7.5 mM)	0.94	Acetophenone (7.5 mM)	0.90
(S)-1-Phenyl-2-propanol (7.5 mM)	14.62	(rac)-1-phenyl-2-propanol (10 mM)	0.142
(R)-1-Phenyl-2-propanol (7.5 mM)	0.51		
Phenylacetone (7.5 mM)	37.61	Phenylacetone (7.5 mM)	1.02
(S)-4-Phenyl-2-butanol (7.5 mM)	26.83	(rac)-4-Phenyl-2-butanol (7.5 mM)	0.29
(R)-4-Phenyl-2-butanol (10 mM)	0.26		
Benzylacetone (7.5 mM)	34.58	Benzylacetone (7.5 mM)	5.94

**Table 2-1. Specific activities of wild-type TeSADH and W110A TeSADH on multiple substrates.**

Enzyme assays were performed at 60°C for 1 min in 50 mM Tris-HCl pH 6.5 (reduction of ketones) or pH 8.0 (oxidation of alcohols), with 0.4 mM NADP(H).

<sup>b</sup> Substrate concentrations are indicated in parentheses.

Substrate	TeSADH			W110A TeSADH		
	$V_{\max}$ (app) ( $\mu\text{mol}/\text{min}\cdot\text{mg}$ )	$K_m$ (app) (mM)	$V_{\max}/K_m$ (ml/min·mg)	$V_{\max}$ (app) ( $\mu\text{mol}/\text{min}\cdot\text{mg}$ )	$K_m$ (app) (mM)	$V_{\max}/K_m$ (ml/min·mg)
(rac)-2-Butanol	37	0.51	0.072	$29.2 \pm 3.6$	$80.3 \pm 18$	0.00036
(S)-1-Phenyl-2-propanol	-	-	-	$16.2 \pm 2.2$	$0.75 \pm 0.1$	0.022
(S)-4-Phenyl-2-Butanol	-	-	-	$33.5 \pm 3.4$	$0.39 \pm 0.03$	0.086
Benzylacetone	-	-	-	$44.9 \pm 2.8$	$0.25 \pm 0.02$	0.18
Phenylacetone	-	-	-	$46.7 \pm 2.5$	$0.86 \pm 0.07$	0.054

**Table 2-2. Kinetic parameters of W110A TeSADH mutant on multiple substrates.** Enzyme assays were performed at 60°C for 1 min in 50 mM Tris-HCl pH 6.5 (reduction of ketones) or pH 8.0 (oxidation of alcohols), with 0.4 mM NADP(H).

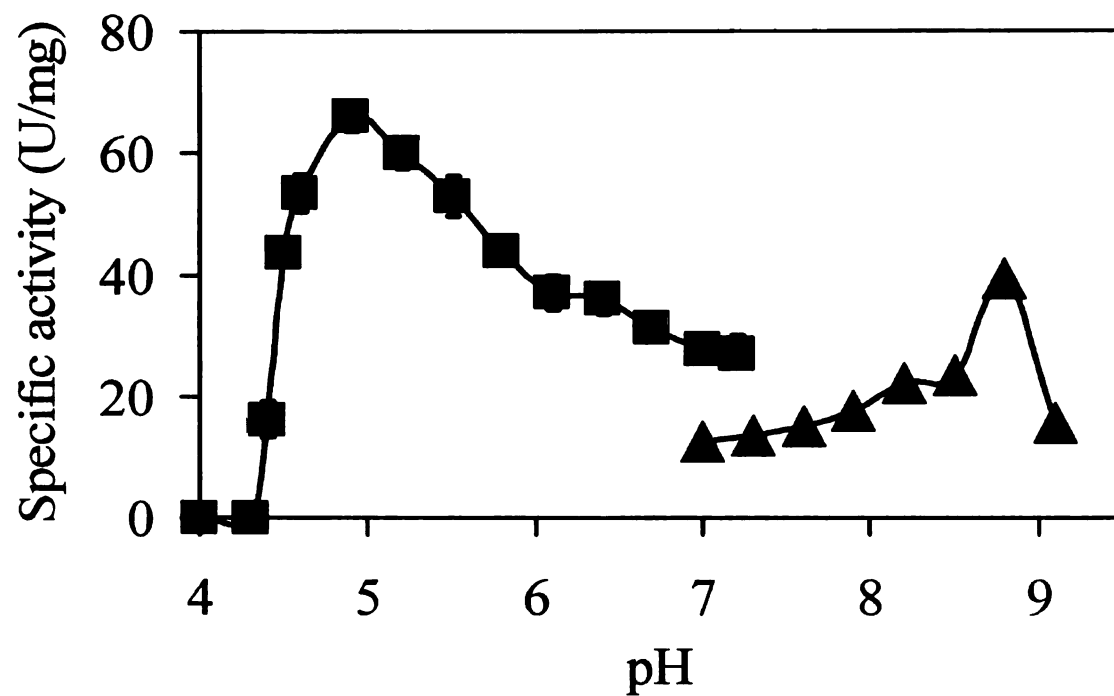


**Figure 2-7. Effect of pH on W110A TeSADH activity.** (■): Benzylacetone and citrate buffer (pH 4.0-7.2); (▲): (rac)-4-phenyl-2-butanol and Tris buffer (pH 7.0-9.1).

with W110A TeSADH. The alcohol produced had the (S) configuration, and it was produced with an ee above 99%. This result shows the applicable value of this enzyme for reducing or eliminating enantiomer separation steps. GC and optical rotation of products from phenylacetone reduction by W110A TeSADH showed a 95% conversion, but only a 37% ee of (S)-1-phenyl-2-propanol. Because this product has a low ee, separation steps would still be required to produce a pure enantiomer, reducing the value of this reaction.

#### **2.4.5 Effects of temperature on W110A TeSADH activity and stability**

Assays at temperatures ranging from 5°C to 97°C showed that W110A TeSADH activity increased from 5 to 87.5°C, with the enzyme showing maximal activity at 87.5°C, 2.5°C below the temperature for TeSADH maximum activity (90°C). Above 87.5°C, the activity dropped sharply, suggesting that this enzyme starts inactivating above this temperature (Figure 2-8). This small decrease in optimum temperature suggests that W110A TeSADH is destabilized in comparison to TeSADH, but that this destabilization is only marginal. W110A TeSADH kinetic inactivation data confirmed this result (Figure 2-9). Burdette et al. (5) initially described TeSADH's kinetic inactivation as being a one-step mechanism ( $R^2 = 0.9654$  – Figure 2-7 inset). In our hands, though, TeSADH inactivation at 90°C could not be fitted with a simple exponential decay function, but instead was best fitted by the sum of two exponentials ( $R^2 = 0.99318$ ) suggesting that W110A TeSADH goes through a two-stage decay process. This change in enzyme property may be due to an extra mutation (A168D) that was found both in the TeSADH we used as our control and in W110A TeSADH, but not

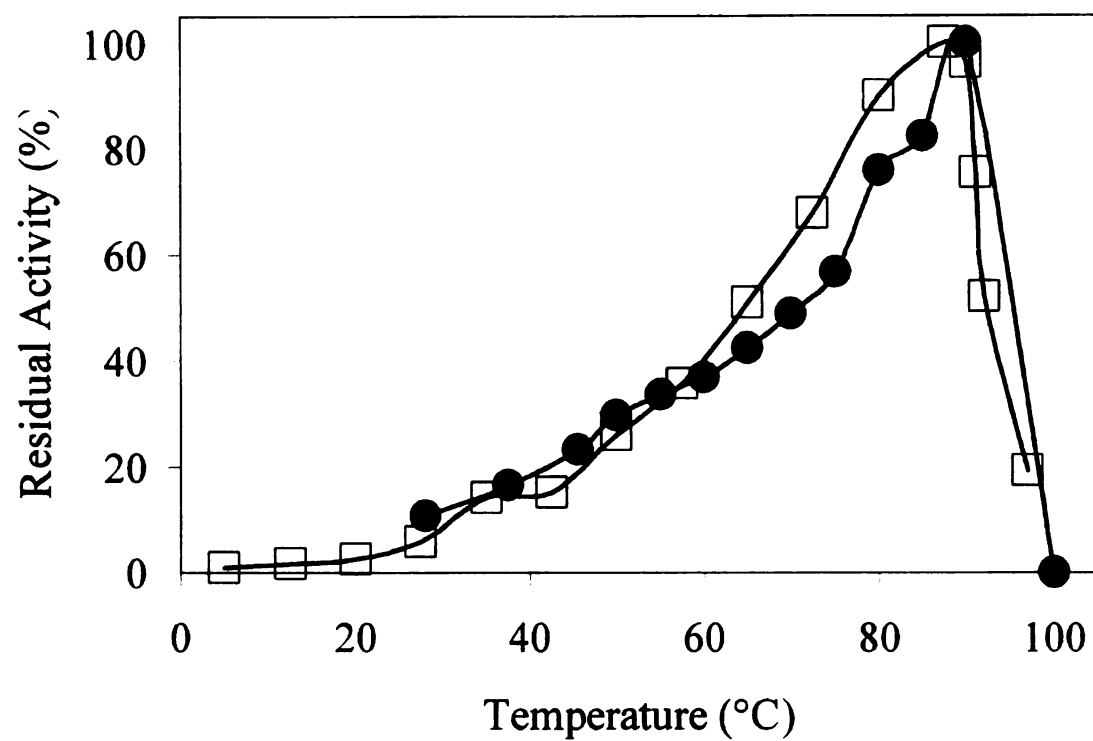


**Figure 2-8.** Temperature activity profiles of W110A TeSADH with (rac)-1-phenyl-2-propanol as the substrate (□) and of TeSADH with 2-butanol as the substrate (●).

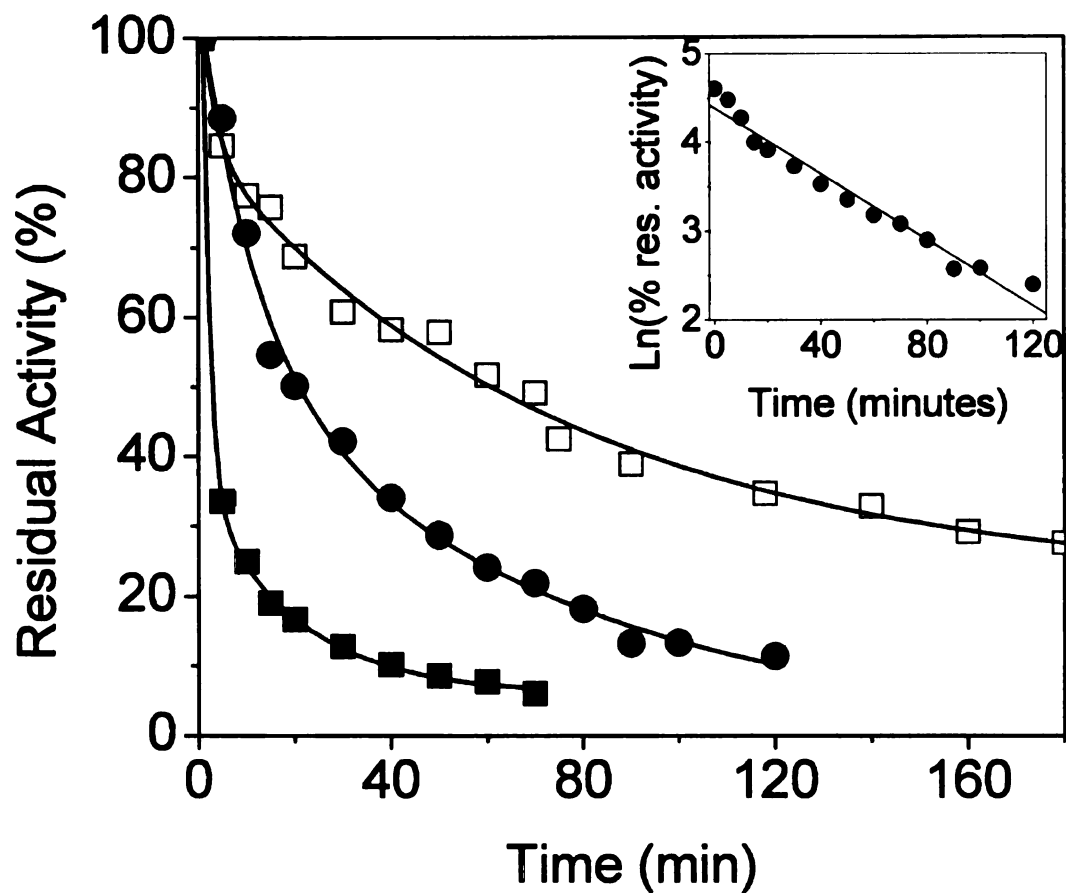


**Figure 2-9. Kinetic stability of W110A TeSADH versus TeSADH.** TeSADH inactivation at 90°C (●); W110A TeSADH inactivation at 85°C (□); W110A TeSADH inactivation at 90°C (■). Residual activity was measured on 5 mM (rac)-4-phenyl-2-butanol (W110A TeSADH) and 5 mM (rac)-2-butanol (TeSADH) at 60°C for 1 minute. Inactivation curves were fitted by the sum of two exponentials. Inset: Fitting of TeSADH inactivation at 90°C as a one-step inactivation mechanism.

reported to be present in the TeSADH initially tested (6). This Ala168 is a buried residue, and the extra bulk of the Asp side chain may cause a slight destabilization. W110A TeSADH was less stable than TeSADH at 90°C (W110A TeSADH and TeSADH lost 94% and 71% activity, respectively, after 70 min at 90°C), but W110A TeSADH was more stable at 85°C than TeSADH at 90°C. These results confirm that, although mutation W110A destabilizes TeSADH, the mutant enzyme remains highly thermostable.

#### **2.4.6 W110A TeSADH activity on aryl derivatives of phenylacetone and benzylacetone**

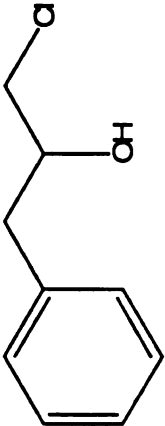
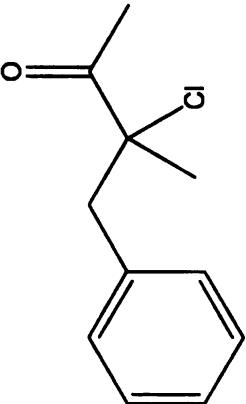
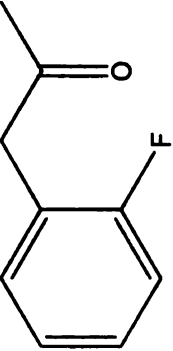
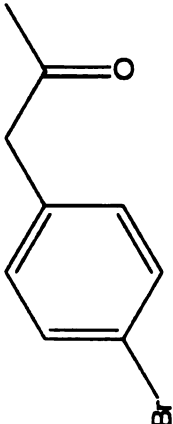
To determine the potential usefulness of W110A TeSADH in industrial syntheses, W110A TeSADH activity was tested on commercially available aryl derivatives of 1-phenyl-2-propanol, phenylacetone, and benzylacetone. W110A TeSADH showed significant levels of activity on 3-chloro-3-methyl-4-phenyl-2-butanone, (2-fluorophenyl) acetone, and 1-(4-bromophenyl) acetone, but showed no detectable activity on 1-chloro-3-phenyl-2-propanol (Table 2-3). Because only a small amount of 1-chloro-3-phenyl-2-propanol could be purchased from Sigma-Aldrich's Rare Chemical Library, the enantiomeric composition of this alcohol is unknown. It is not excluded that this alcohol is provided mostly in the (R) form. It could be one possible reason why W110A TeSADH is inactive on this substrate. Other ketones with side-chains containing phenol rings have been tested as substrates for W110A TeSADH. W110A TeSADH was able to convert 97% or more of 1-phenyl-1,3-butanedione, phenoxy-2-propanone, and 1-(4-methoxyphenyl)-2-propanone to the corresponding (S)-alcohol with greater than 99% e.e. (23).



**Table 2-3. Activity of W110A TeSADH on (1 mM) aryl derivatives.**

Enzyme assays were performed at 60°C for 1 min in 50 mM Tris-HCl pH~6.5 (reduction of ketones) or pH~8.0 (oxidation of alcohols), with 0.4 mM NADP(H).

<sup>b</sup> Substrates of W110A TeSADH that are the substructures for the aryl derivatives. ND: not detectable

Substrate	Derivative structure	Specific activity ( $\mu\text{mol}/\text{min}\cdot\text{mg}$ protein)
<i>1-Phenyl-2-propanol</i> <sup>b</sup> 1-Chloro-3-phenyl-2-propanol		$13.5 \pm 2.0$ ND
<i>Benzylacetone</i> <sup>b</sup> 3-Chloro-3-methyl-4-phenyl-2-butanone		$37.6 \pm 4.2$ $3.9 \pm 0.2$
<i>Phenylacetone</i> <sup>b</sup> (2-Fluorophenyl) acetone 1-(4-Bromophenyl) acetone	 	$39.8 \pm 1.2$ $14.8 \pm 0.2$ $43.8 \pm 1.9$

#### 2.4.7 Effect of solvent on W110A TeSADH stability

Most recently developed cofactor recycling systems for the enzymatic production of chiral alcohols are based on a two-enzyme approach in which one ADH performs the desired ketone reduction, and a second enzyme—often formate dehydrogenase—recycles the cofactor. With their usually broad substrate specificity, ADHs also allow a one-enzyme approach, in which the same ADH performs the desired ketone reduction and recycles the cofactor by oxidizing a cosubstrate. To shift the reaction equilibrium toward the production of the desired alcohol and to increase the substrate and product solubilities, the enzyme should be able to withstand high cosubstrate concentrations (9).

For example, an SADH from *Rhodococcus ruber* was recently isolated that shows activity at 30°C in the presence of 80% 2-propanol or 50% acetone (17). Because reaction products were analyzed only after a 12-h incubation, though, it is unclear how stable this enzyme is in the presence of high solvent concentrations.

Here, we opted instead to measure enzyme stability by measuring the remaining activity after incubation in the presence of solvent. W110A TeSADH solvent stability was tested in 30% 2-propanol at four different temperatures. The 2-propanol present in the inactivation solution was used as the substrate to measure residual activity (195 mM final assay concentration). Almost no decrease in W110A TeSADH activity was observed after incubations in the presence of 30% 2-propanol at up to 50°C. However, W110A TeSADH lost 80% activity after 120 min incubation at 60°C (Figure 2-10). These results are very similar to those observed with the wild-type TeSADH (Figure 2-10). These results indicate that, for long reaction times in the presence of solvents, W110A TeSADH would be best used at temperatures of 50°C or below. These solvent

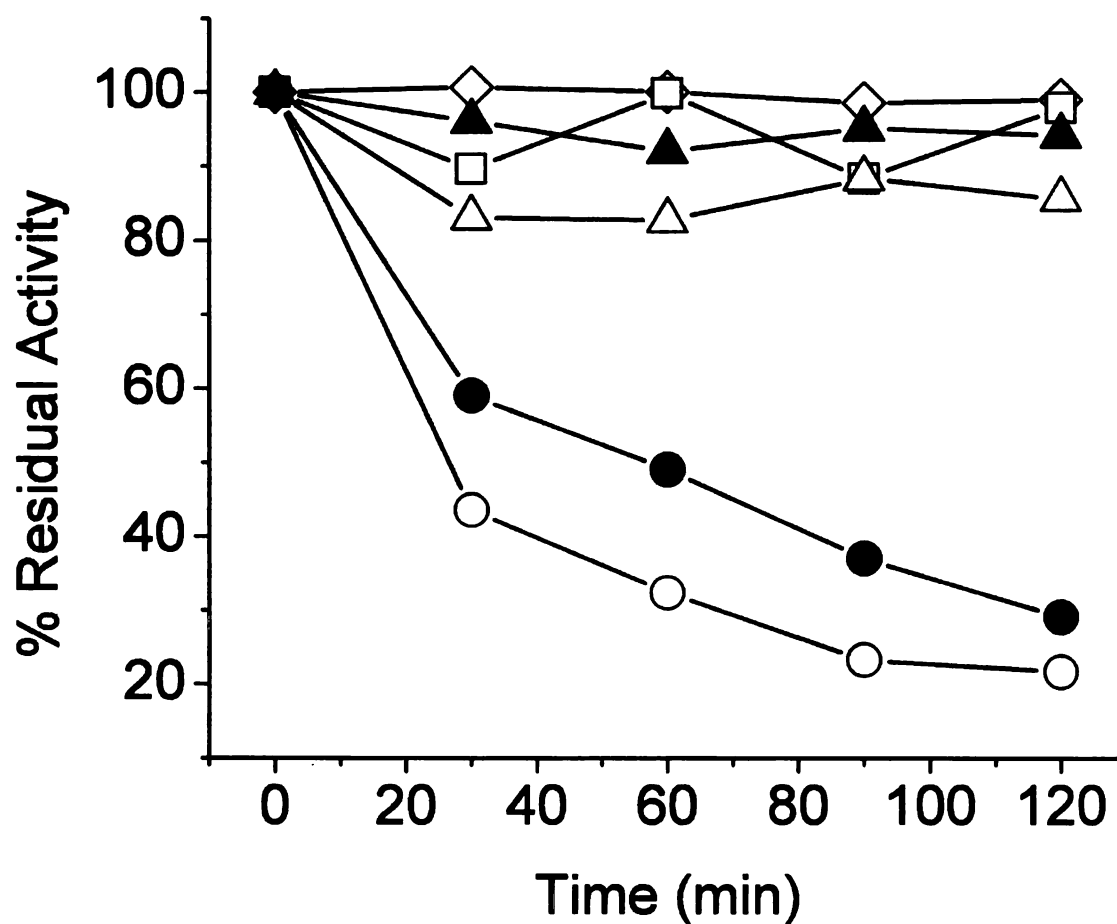


**Figure 2-10. Solvent stability of W110A TeSADH (30°C {◇}; 40°C {□}; 50°C {△}; and 60°C {○}) and TeSADH (50°C {▲} and 60°C {●}) in 30% 2-propanol at different temperatures.**

stability results are highly encouraging. Being able to operate at or below 50°C in the presence of 30% 2-propanol would allow for (i) higher concentrations of substrates that are only moderately soluble in water and (ii) for cofactor recycling using wild-type TeSADH as the coupling enzyme and 2-propanol as the recycling substrate.

#### **2.4.8 Validation of our modeling approach**

The facts that W110A TeSADH is active on (S)-1-phenyl-2-propanol and that Y267G TeSADH is not suggest that (S)-2-butanol's orientation in the TbSADH•(S)-2-butanol binary complex (PDB # 1BXZ) differs from its orientation in an active enzyme-substrate-cofactor ternary complex. Even though HLADH is a primary ADH and it shows only limited activity on secondary alcohols, the orientation of BRB in the HLADH•BRB•NAD<sup>+</sup> ternary complex seems to be an excellent indication of how the reactive oxygen (and the corresponding C–OH bond) in secondary alcohols should be positioned in TeSADH's catalytic site to yield an active ternary complex.

## 2.5 Conclusions

The W110A mutation significantly changed the substrate specificity of TeSADH to include a variety of phenyl-substituted alcohols and ketones. W110A TeSADH is active on benzylacetone, phenylacetone, (S)-1-phenyl-2-propanol, and (S)-4-phenyl-2-butanol; it shows almost no activity on the corresponding (R)-alcohols; and it produces (S)-4-phenyl-2-butanol at greater than 99% e.e. W110A TeSADH is now active on aryl derivatives of phenylacetone and benzylacetone. Its activity and enantiomeric specificity make W110A TeSADH a potentially useful catalyst for chiral synthesis of aryl derivatives of alcohols.

## **2.6 Acknowledgements**

This work was supported by NSF Award MCB-0445750 and by a grant from the Michigan Economic Development Corporation through its Michigan Technology Tri-Corridor Program.

## 2.7 References

1. **Agarwal, P. K., S. P. Webb, and S. Hammes-Schiffer.** 2000. Computational studies of the mechanism for proton and hydride transfer in liver alcohol dehydrogenase. *J. Am. Chem. Soc.* **122**:4803-4812.
2. **Bogin, O., M. Peretz, and Y. Burstein.** 1997. *Thermoanaerobacter brockii* alcohol dehydrogenase: characterization of the active site metal and its ligand amino acids. *Protein Sci.* **6**:450-458.
3. **Burdette, D., and J. G. Zeikus.** 1994. Purification of acetaldehyde dehydrogenase and alcohol dehydrogenases from *Thermoanaerobacter ethanolicus* 39E and characterization of the secondary-alcohol dehydrogenase (2° Adh) as a bifunctional alcohol dehydrogenase--acetyl-CoA reductive thioesterase. *Biochem. J.* **302**:163-170.
4. **Burdette, D. S., F. Secundo, R. S. Phillips, J. Dong, R. A. Scott, and J. G. Zeikus.** 1997. Biophysical and mutagenic analysis of *Thermoanaerobacter ethanolicus* secondary-alcohol dehydrogenase activity and specificity. *Biochem. J.* **326**:717-724.
5. **Burdette, D. S., V. V. Tchernajenko, and J. G. Zeikus.** 2000. Effect of thermal and chemical denaturants on *Thermoanaerobacter ethanolicus* secondary-alcohol dehydrogenase stability and activity. *Enzyme Microb. Technol.* **27**:11-18.
6. **Burdette, D. S., C. Vieille, and J. G. Zeikus.** 1996. Cloning and expression of the gene encoding the *Thermoanaerobacter ethanolicus* 39E secondary-alcohol dehydrogenase and biochemical characterization of the enzyme. *Biochem. J.* **316**:115-122.
7. **Choi, J. H., Y. K. Choi, Y. H. Kim, E. S. Park, E. J. Kim, M. J. Kim, and J. Park.** 2004. Aminocyclopentadienyl ruthenium complexes as racemization catalysts for dynamic kinetic resolution of secondary alcohols at ambient temperature. *J. Org. Chem.* **69**:1972-1977.
8. **Devaux-Basseguy, R., A. Bergel, and M. Comtat.** 1997. Potential applications of NAD(P)-dependent oxidoreductases in synthesis: A survey. *Enzyme Microb. Technol.* **20**:248-258.
9. **Edegger, K., C. C. Gruber, K. Faber, A. Hafner, and W. Kroutil.** 2006. Optimization of reaction parameters and cultivation conditions for biocatalytic hydrogen transfer employing overexpressed ADH-'A' from *Rhodococcus ruber* DSM 44541 in *Escherichia coli*. *Life Sci.* **6**:149-154.
10. **Eriksson, T., S. Björkman, and P. Höglund.** 2001. Clinical pharmacology of thalidomide. *Eur. J. Clin. Pharmacol.* **57**:365-376.



11. **Guex, N., and M. C. Peitsch.** 1997 SWISS-MODEL and the Swiss-PdbViewer: an environment for comparative protein modeling. *Electrophoresis* **18**:2714-2723.
12. **Heiss, C., M. Laivenieks, J. G. Zeikus, and R. S. Phillips.** 2001. Mutation of cysteine-295 to alanine in secondary alcohol dehydrogenase from *Thermoanaerobacter ethanolicus* affects the enantioselectivity and substrate specificity of ketone reductions. *Bioorg. and Med. Chem.* **9**:1659-1666.
13. **Hols, P., A. Ramos, J. Hugenholtz, J. Delcour, W. M. de Vos, H. Santos, and M. Kleerebezem.** 1999. Acetate utilization in *Lactococcus lactis* deficient in lactate dehydrogenase: a rescue pathway for maintaining redox balance. *J. Bacteriol.* **17**:5521-5526.
14. **Hummel, W.** 1997. New alcohol dehydrogenases for the synthesis of chiral compounds. *Adv. Biochem. Eng. Biotechnol.* **58**:145-184.
15. **Keinan, E., E. K. Hafeli, K. K. Seth, and R. Lamed.** 1986. Thermostable enzymes in organic synthesis. 2. Asymmetric reduction of ketones with alcohol dehydrogenase from *Thermoanaerobium brockii*. *J. Am. Chem. Soc.* **108**:162-169.
16. **Korkhin, Y., A. J. Kalb (Gilboa), M. Peretz, O. Bogin, Y. Burstein, and F. Frolow.** 1998. NADP-dependent bacterial alcohol dehydrogenases: crystal structure, cofactor-binding and cofactor specificity of the ADHs of *Clostridium beijerinckii* and *Thermoanaerobacter brockii*. *J. Mol. Biol.* **278**:967-981.
17. **Kosjek, B., W. Stampfer, M. Pogorevc, W. Goessler, K. Faber, and W. Kroutil.** 2004. Purification and characterization of a chemotolerant alcohol dehydrogenase applicable to coupled redox reactions. *Biotechnol. Bioeng.* **86**:55-62.
18. **Laemmli, U. K.** 1970. Cleavage of structural proteins during the assembly of the head of bacteriophage T4. *Nature* **227**:680-685.
19. **Lee, Y. E., M. K. Jain, C. Lee, S. E. Lowe, and J. G. Zeikus.** 1993. Taxonomic distinction of saccharolytic thermophilic anaerobes: description of *Thermoanaerobacterium xylanolyticum* gen. nov., sp. nov., and *Thermoanaerobacterium saccharolyticum* gen. nov., sp. nov.; reclassification of *Thermoanaerobium brockii*, *Clostridium thermosulfurogenes*, and *Clostridium thermohydrosulfuricum* E100-69 as *Thermoanaerobacter brockii* comb. nov., *Thermoanaerobacterium thermosulfurigenes* comb. nov., and *Thermoanaerobacter thermohydrosulfuricus* comb. nov., respectively; and transfer of *Clostridium thermohydrosulfuricum* 39E to *Thermoanaerobacter ethanolicus*. *Int. J. Syst. Bacteriol.* **43**:41-51.
20. **Liese, A., K. Seelbach, and C. Wandrey.** 2000. *Industrial Biotransformations*. Wiley-VCH, Weinheim, New York, Chichester, Brisbane, Singapore, Toronto.

21. **Machielsen, R., A. R. Uria, S. W. Kengen, and J. van der Oost.** 2006. Production and characterization of a thermostable alcohol dehydrogenase that belongs to the aldo-keto reductase superfamily. *Appl. Environ. Microbiol.* **72**:233-238.
22. **Miroliaei, M., and M. Nemat-Gorgani.** 2002. Effect of organic solvents on stability and activity of two related alcohol dehydrogenases: a comparative study. *Int. J. Biochem. Cell Biol.* **34**:169-75.
23. **Musa, M. M., K. I. Ziegelmann-Fjeld, C. Vieille, J. G. Zeikus, and R. S. Phillips.** Asymmetric reduction and enantioselective oxidation using W110A secondary alcohol dehydrogenase from *Thermoanaerobacter ethanolicus*. **Submitted.**
24. **Nakamura, K., Y. Inoue, T. Matsuda, and I. Misawa.** 1999. Stereoselective oxidation and reduction by immobilized *Geotrichum candidum* in an organic solvent. *J. Chem. Soc. Perkin Trans. 1*:2397-2402.
25. **Patel, R. N.** 2005. Biocatalysis: Synthesis of chiral intermediates for pharmaceuticals. *In* C. T. Hou (ed.), *Handbook of Industrial Biocatalysis*. Taylor & Francis Group, Boca Raton, FL.
26. **Peitsch, M. C.** 1995. Protein modeling by E-mail. *Bio/Technology* **13**:658-660.
27. **Schmid, A., J. S. Dordick, B. Hauer, A. Kiener, M. Wubbolts, and B. Witholt.** 2001. Industrial biocatalysis today and tomorrow. *Nature* **409**:258-268.
28. **Schwede, T., J. Kopp, N. Guex, and M. C. Peitsch.** 2003. SWISS-MODEL: an automated protein homology-modeling server. *Nucleic Acids Res.* **31**:3381-3385.
29. **Tripp, A. E., D. Burdette, J. G. Zeikus, and R. S. Phillips.** 1998. Mutation of serine-39 to threonine in thermostable secondary alcohol dehydrogenase from *Thermoanaerobacter ethanolicus* changes enantiospecificity. *J. Am. Chem. Soc.* **120**:5137-5141.
30. **Vondervoot, L. S., S. Bouttemy, J. M. Padron, J. Muzart, and P. L. Alster.** 2002. Chromium catalyzed oxidation of (homo-)allylic and (homo-)propargylic alcohols with sodium periodate to ketones or carboxylic acids. *Synlett* **2**:243-246.

## **CHAPTER III**

### **Molecular Design and Characterization of *Thermoanaerobacter ethanolicus* 39E Secondary Alcohol Dehydrogenase for Cofactor Specificity Change**

**Manuscript prepared according to guidelines for submission to *Protein Engineering, Design, and Selection***

### 3.1 Abstract

The secondary alcohol dehydrogenase from *Thermoanaerobacter ethanolicus* 39E (TeSADH) is an NADP(H) specific enzyme, it is highly thermostable and solvent-stable, and it is active on a broad range of substrates. This enzyme has previously been engineered to produce phenyl-substituted alcohols and their aryl derivatives with high enantioselectivity. For an enzyme to be an attractive industrial biocatalyst, though, its use must be economically feasible. TeSADH's specificity for NADP(H) is a limitation to its application in industrial reactions because of the much higher cost and lower stability of NADP(H) relative to NAD(H). The goal of this work was to change the cofactor specificity of TeSADH from NADP(H) to NAD(H). We used both site-directed mutagenesis and directed evolution to change the cofactor specificity and to attempt to optimize the activity of mutants with NAD(H). Triple mutant G198D/C203K/Y218P (GCY) was used as the parent for directed evolution because its  $V_{\max}$  was 14 times that of TeSADH with  $\text{NAD}^+$ , and comparable to the  $V_{\max}$  of TeSADH with  $\text{NADP}^+$ . The first generation directed evolution mutant had a single extra mutation, D186V, which decreased the  $K_m$  1.8 times and increased the catalytic efficiency 1.6 times compared to the parent, GCY. The second generation mutant (containing the additional mutations I49V/N54S/D315N) had almost the same kinetic properties as the first generation mutant.

## 3.2 Introduction

There is an ever growing interest in biocatalytic processes for industrial purposes (24). This interest is mainly due to the growing need for “cleaner” technologies that are more environmentally friendly, create less waste, and use fewer non-renewable resources (1).

Numerous industrial-scale chemical syntheses (i.e., for polymer intermediates, pharmaceuticals, agrochemicals, and specialty chemicals) are hindered by low-selectivity processes, and by the production of undesirable byproducts (9). Enzymatic processes are attractive because they work under mild reaction conditions such as ambient temperature and pressure and neutral pH, which can reduce the incidence of undesirable isomerization, racemization, epimerization, and rearrangement reactions. Enzymatic reactions can replace some classical organic chemical reactions that are difficult to conduct, or replace a multi-step chemical reaction with a single enzymatic reaction. Using enzyme catalysts also eliminates the need for expensive chemical catalysts, which can be difficult to produce, regenerate, and separate from the final product (16, 20).

Economic factors must also be taken into account in any industrial-scale process. High conversion rates, specificity and selectivity, catalyst stability, substrate cost, cofactor usage, and space-time yield must be considered during the scale-up of any reaction (27).

While many other enzymes have been developed into powerful industrial catalysts, the need for cofactors (NAD(H) and NADP(H)) for redox reactions has been a hurdle for the use of dehydrogenases in industrial-scale reactions. Chemical cofactor recycling methods have been developed, but they have only been used on a laboratory

scale. If the cofactor cannot be recycled then a stoichiometric amount of cofactor must be used. Due to the high cost of the cofactor, this use is not economically feasible. Advances in enzymatic cofactor recycling systems have shown promise for larger scale uses of dehydrogenases (27). Degussa-Hüls AG (Germany) developed an enzyme-membrane reactor in 1981, and has since modified it to accommodate L-amino acid dehydrogenase to produce the unnatural amino acid *L-tert*-leucine (L-Tle) by the reductive amination of the prochiral  $\alpha$ -keto acid, trimethyl pyruvate. L-Tle is an important product, because it is substituted for leucine in therapeutic peptides in which it is less prone to hydrolysis by serum proteases (27). In the Degussa reactor, *Candida boidinii* formate dehydrogenase is used to recycle the cofactor, NADH. Because L-Tle is an unnatural amino acid, its synthesis cannot be carried out by fermentation, so Degussa's enzyme membrane reactor produces L-Tle with an average conversion of 85% and a space-time yield of 638g/day, with the total cofactor turnover number of 125,000 over a two-month period. Degussa operates this reactor on an industrial scale to produce high quality L-Tle (16, 27, 28). This reactor demonstrates the possibility of an increased use of dehydrogenases in industrial settings.

Enzyme specificity for NADP(H) versus NAD(H) has been a limitation for use of certain redox enzymes in industrial processes. Per gram, NADPH is ten times as expensive as NADH (\$877/g NADPH vs. \$85.10/g NADH – Sigma online catalog March 2007). NADPH is also much less stable than NADH. For example, at 30°C from pH 2 to 4.5 NADPH degrades 80% faster than NADH, and at pH 6.0 at 41°C, NADH has a half-life of 400 min, while NADPH has a half-life of only 56 min (30). Luckily, recent advances in molecular biology, high-throughput screening, instrumentation, and

engineering have led to the ability to produce enzymes with customized activity and selectivity (19, 31), in particular with reversed cofactor specificity (17, 25, 26, 32).

Several groups have reported the change of enzyme cofactor specificity through rational design and mutagenesis. Both isocitrate dehydrogenase (IDH) and isopropylmalate dehydrogenase (IMDH) have been engineered to reverse their cofactor specificity, each using the other as the template for change. IDH and IMDH are homologous and structurally similar enzymes that are both involved in amino acid synthesis. The wild-type *Escherichia coli* IDH is a NADP(H)-dependent enzyme, and the wild-type *E. coli* and *Thermus thermophilus* IMDHs are both NAD(H)-dependent. First, the sequences and crystal structures (both with cofactor bound to the enzyme) of *E. coli* IDH and *T. thermophilus* IMDH were compared. This comparison showed that six residues are conserved in NADP(H)-dependent IDHs, but that only three are conserved in NAD(H)-dependent IMDHs and confer cofactor specificity. These three NAD(H)-dependent conserved residues were introduced into IDH (K344D, Y345I, and V351A), and two additional mutations of non-conserved residues (Tyr391 and Arg395) were made to remove interactions with the ribose phosphate of NADP(H). Crystal structures show that the mutant IDH binds NAD(H) in the same manner as the wild-type IMDH binds NAD(H), forming the same hydrogen bonds, and has comparable activity (17, 32).

Similar sequence and structural comparisons were used to change the cofactor specificity of *E. coli* IMDH from NAD(H) to NADP(H). In this case, the *E. coli* and *T. thermophilus* IMDHs were compared. Five additional mutations were introduced in the *E. coli* IMDH to mimic the IDH cofactor binding site (D236R, D289K, I290Y, A296V,

and G337Y). *E. coli* IMDH's cofactor specificity changed from a 100-fold preference for NAD(H) to a 200-fold preference for NADP(H) (17).

To investigate the minimal structure requirements for cofactor specificity reversal, three mutations were introduced into *Rana perezi* ADH8 (Western Palearctic water frog), which is the only known vertebrate NADP(H)-specific ADH. Mutations G223D, T224I, and H225N were chosen to mimic residues common to NAD(H)-specific vertebrate ADHs. Individually, single mutants still preferred NADP(H) to NAD(H), but double mutants G223D+T224I and T224I+H225N showed decreased catalytic efficiency with NADP(H). The triple mutant G223D+T224I+H225N showed complete cofactor specificity reversal, with a catalytic efficiency ( $k_{\text{cat}}/K_m$ ) on NADH of  $155,00 \text{ mM}^{-1} \text{ min}^{-1}$  versus a  $k_{\text{cat}}/K_m$  of  $760 \text{ mM}^{-1} \text{ min}^{-1}$  on NADPH starting from a  $k_{\text{cat}}/K_m$  for NADPH of  $133,330 \text{ mM}^{-1} \text{ min}^{-1}$  for the wild-type enzyme (22).

There is also an increasing interest in the use of thermostable enzymes for industrial processes. Mesophilic enzymes are often unstable under the conditions of industrial synthesis processes and so may not be suitable as catalysts (9). In contrast, thermostable enzymes are globally more stable, with increased stability at elevated temperatures, as well as at increased solvent and detergent concentrations, and they have increased shelf and reactor lives (6, 23).

The secondary ADH (EC 1.1.1.2) from the thermophilic bacterium *Thermoanaerobacter ethanolicus* 39E (TeSADH) was cloned and expressed in *E. coli* by Burdette et al. (5). TeSADH is a medium chain, zinc-containing enzyme, and has a requirement for a nicotinamide cofactor, specifically NADP(H). TeSADH is a tetrameric, 352-amino acids long enzyme with a total molecular mass of 160 kDa.



TeSADH was previously thought to differ from *Thermoanaerobacter brockii* SADH (TbSADH) by 3 amino acids (5), but recent sequencing results in our lab (Laivenieks, unpublished result) and *T. ethanolicus* 39E genome sequencing data (NCBI entry 2P\_00779753) show that the two enzymes are in fact identical (3).

We previously engineered TeSADH by site-directed mutagenesis (SDM), to produce phenyl-substituted secondary alcohols with high enantioselectivity (33). The W110A TeSADH is highly active on phenyl-substituted alcohols and ketones, and aryl derivatives of those new substrates, and has high enantiospecificity and enantioselectivity. For example it produces (S)-4-phenyl-2-butanol with >99% ee. W110A TeSADH is also highly active on (S)-1-phenyl-2-propanol and (S)-4-phenyl-2-butanol, but does not have measurable activity on the (R)-alcohols. Its catalytic and selectivity properties on these substrates make it an interesting enzyme for industrial syntheses, but its specificity for NADP(H) remains a limitation to its potential industrial uses.

Previous attempts have been made to change the cofactor specificity of TeSADH by SDM. Two mutations were chosen, G198D and Y218F (4, 12). The single mutants G198D TeSADH and Y218F TeSADH had very similar, improved kinetics with  $\text{NAD}^+$  as the cofactor (Table 3-1). Compared to the wild-type TeSADH activity with  $\text{NAD}^+$  the  $K_m$  of G198D TeSADH for  $\text{NAD}^+$  decreased 3 times and its  $V_{\max}$  increased 5.7 times, and the  $K_m$  of Y218F TeSADH for  $\text{NAD}^+$  decreased 2.5 times and its  $V_{\max}$  increased 5.2 times, leading to 17-fold (G198D) and 13-fold (Y218F) increases in catalytic efficiency with  $\text{NAD}^+$ . Despite these encouraging results, the two mutant enzymes have  $V_{\max}$  values with  $\text{NAD}^+$  that are still 3 times lower than the wild-type enzyme with  $\text{NADP}^+$ .

**Table 3-1. TeSADH and G198D and Y218F TeSADH kinetic parameters**

	<b>NADP<sup>+</sup></b>			<b>NAD<sup>+</sup></b>		
	<b>V<sub>max</sub>app</b>	<b>K<sub>m</sub>app</b>	<b>V<sub>max</sub>/K<sub>m</sub></b>	<b>V<sub>max</sub>app</b>	<b>K<sub>m</sub>app</b>	<b>V<sub>max</sub>/K<sub>m</sub></b>
	(U/mg)	(mM)		(U/mg)	(mM)	
TeSADH	72	0.016	4.5	4.4	2.3	0.002
G198D	18	3.6	0.005	25	0.76	0.033
Y218F	21	3.4	0.006	23	0.93	0.025

All values were determined at 60°C

V<sub>max</sub>/K<sub>m</sub> = catalytic efficiency

Their affinity for  $\text{NAD}^+$  is still 47 times (G198D) and 58 times (Y218F) lower than that of the wild-type for  $\text{NAD}^+$ . These numbers indicate that there is still a lot of room for optimizing the activity of TeSADH with NAD(H).

In this paper, we will use SDM and directed evolution (DE) in an attempt to change the cofactor specificity of TeSADH from NADP(H) to NAD(H). The purpose is to construct a TeSADH mutant that has kinetic parameters with  $\text{NAD}^+$  comparable to those of the wild-type enzyme with  $\text{NADP}^+$ .

### 3.3 Materials and methods

#### 3.3.1 Strains and plasmids

PCR products for SDM were subcloned into the pCR2.1-TOPO vector (Invitrogen, Carlsbad, CA) and transformed into Chemically Competent One Shot TOP10 *E. coli* cells (Invitrogen, Carlsbad, CA). The XL2 Blue(DE3) *E. coli* strain was constructed using the DE3 lysogenization kit (Novagen, Madison, WI). XL2 Blue(DE3) was used to screen the DE library because the XL2 Blue strain (Stratagene, La Jolla, CA) has an *hsdR* mutation that prevents the cleavage of nicked DNA by the *EcoK* endonuclease system, resulting in many more colonies per transformation. All mutated genes were subcloned into pET-24a(+) (Novagen, Madison, WI) for expression.

#### 3.3.2 Structural and sequence comparisons

The TeSADH, horse liver ADH (HLADH), and yeast ADHI (YADH) (HLADH and YADH are NAD(H)-dependent ADHs) were aligned using the ClustalW multiple sequence alignment program to compare the residues conveying cofactor specificity. Because TeSADH and TbSADH are identical, all structural comparisons of TeSADH and HLADH used the published structures of TbSADH (13). These comparisons were done on a Dell In computer using InsightII (Accelrys, San Diego, CA). Figures were made using PyMOL (DeLano Scientific LLC, Palo Alto, CA). The structures of the HLADH•NAD<sup>+</sup> (PDB #1HLD) and TbSADH•NADP<sup>+</sup> (PDB #1YKF) binary complexes were superimposed using residues surrounding the cofactor binding site, and the cofactor binding residues were compared. Three TeSADH residues (G198, C203, Y218) were

compared to HLADH residues and mutations were decided upon to mimic the HLADH cofactor binding site.

### 3.3.3 Site directed mutagenesis

SDM was performed as described (33) using the Expand High Fidelity PCR System (Roche, Indianapolis, IN) to construct the triple mutant G198D/C203K/Y218P (GCY TeSADH) in three steps. The wild-type *adhB* gene in the pADHB1M1-kan plasmid (a pBluescript II KS+kanamycin derivative) was used as the template for the first step (4, 5). All primers were synthesized by the Michigan State University Macromolecular Structure Facility.

Mutation G198D was introduced first. The 5'- and 3'-ends of the gene were amplified using primers: 5'-end (forward) 5'-ATCAATATGTCATATGATGAAAGGT-TTTGCAATGC (A, where CATATG encodes a 5' *NdeI* site) and (reverse) 5'-AACTGGTCTACTGTCTACGGCAAT (where GTC encodes the G198D mutation) ; 3'-end (forward) 5'-ATTGCCGTAGACAGTAGACCAGTT (where GAC encodes the G198D mutation) and (reverse) 5'-GTCATCTCGAGT-GCTAATATTACAACAGGTTTG (B, where CTCGAG encodes a 3' *XhoI* site). The two PCR products were then reassembled into the full *adhB* gene by PCR using primers A and B.

Once cloned into pET-24a(+), the G198D *adhB* mutant gene was then used as a template for the second SDM step. The C203K mutation was introduced with primers: 5'-end (forward) A and (reverse) 5'-TGCAGCATCTACTTTAACTGGTCTACT (where TTT encodes the C203K mutation); 3'-end (forward) 5'-AGTAGACCAGTTAAAGTA-

GATGCTGCA (where AAA encodes the C203K mutation) and (reverse) **B**. The two PCR products were then reassembled into the full *adhB* gene by PCR using primers **A** and **B**.

The G198D/C203K *adhB* mutant gene cloned in pET-24a(+) was used as the template for the third SDM step. The Y218P mutant was introduced with primers: 5'-end (forward) **A** and (reverse) 5'-AGGACCATCTTTAGGGTTTACAATATC (where AGG encodes the Y218P mutation); 3'-end (forward) 5'-GATATTGTAAACCCTAAAGATG-GTCCT (where CCT encodes the Y218P mutation) and (reverse) **B**. The two PCR products were then reassembled into the full *adhB* gene by PCR using primers **A** and **B**.

Each full gene was subcloned into PCR 2.1-TOPO. The recombinant plasmids purified from TOP10 cells were submitted for automated sequencing at the Michigan State University Genomics Facility. Mutant sequences were compared to the wild-type *adhB* sequence using the ClustalW multiple sequence alignment program. The genes containing only mutations G198D, C203K, Y218P, or a combination of these mutations, were then subcloned into pET24a(+) for expression. In these constructs, the TeSADH mutants were expressed as fusion proteins with a C-terminal His<sub>6</sub> tag as done previously (33).

#### **3.3.4 Error-prone PCR**

Error-prone PCR of the entire pET-24a(+)-*adhB* GCY construct was performed using Taq DNA polymerase, 2.5 mM MgCl<sub>2</sub>, 0.5 mM MnCl<sub>2</sub>, and uneven dNTP concentrations (0.35 mM dATP, 0.40 mM dTTP, 0.20 mM dGTP, 1.35 mM dCTP) in a 50 µl reaction mixture (10). Primers were constructed as 20-mers with a 4-bp overlap between the forward and reverse primers, and 0.6 mM of each of the following primers

were used: forward (covering the T7 promoter region) 5' – AATACGACTCACTATAG-GGG; and reverse (covering the lac operator) 5' – TTATCCGCTCACAATTCCCC. The initial denaturation step was 5 min at 95°C. Thirty-five amplification cycles were performed with denaturation for 1 min at 95°C, annealing for 1 min at 55°C, and elongation for 7 min at 72°C (1.1 min per kb). A final elongation was done for 10 min at 72°C. PCR reactions were then incubated at 37°C with 1 µl *DpnI* for 1 hour to digest the parental DNA.

### **3.3.5 Screening of TeSADH mutants' activity with NAD<sup>+</sup>**

Screening of TeSADH mutant libraries was done using a colorimetric method with phenazine methosulfate (PMS) and nitroblue tetrazolium (NBT), which react with NAD(P)H resulting in a blue-purple formazan dye (18). The screening process required multiple steps. Error-prone PCR products were transformed into XL2 Blue(DE3) and plated on LB medium (per liter: 10 g tryptone, 5 g yeast extract, 5 g NaCl) agar containing kanamycin (20 mg/l) (LB kan) at a cell density such that colonies would be numerous but well separated, and incubated at 37°C overnight. For best results, growth was stopped when the colonies reached about 1 mM in diameter. A nitrocellulose membrane was placed on the plates to pick up the colonies. After marking membrane orientation, the membrane was gently lifted and was placed, colonies up, on a fresh LB kan agar plate and incubated at 37°C for 2 hours to allow the cells to adhere to the membrane. The membrane was then placed onto a LB kan agar plate containing 1 mM IPTG (LB kan IPTG) and incubated at 37°C for 2 hours to induce protein expression. After induction, the plates+membranes were placed in a toluene vapor environment for

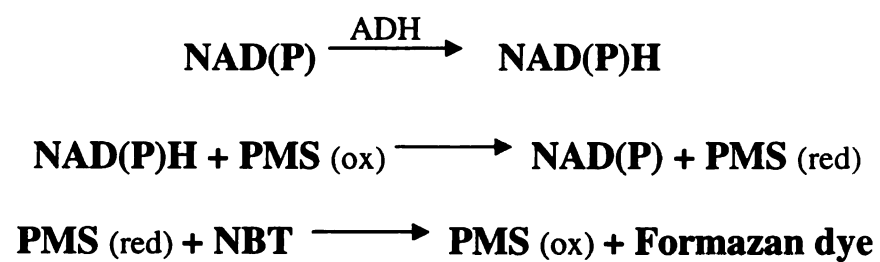
20 min to permeabilize the cells. The membrane was then transferred to an agar only plate (15 g/l agar in distilled water) and incubated at 80°C for 45 min to inactivate the mesophilic host proteins, while leaving the thermostable TeSADH intact. This heat treatment is critical to remove any background NAD(H)-dependent *E. coli* enzyme activities that could interfere with the screening.

After the heat treatment, 5 mL of 0.35% agarose containing substrate (5 mM 2-butanol), cofactor (varied concentrations of NAD<sup>+</sup>) and buffer (50 mM Tris-HCl, pH 8.0) was poured on top of the membrane+agar plate. The agarose was allowed to set fully, and the plates were incubated at 60°C for 45 min. A 5 ml 0.35% agarose layer containing 1.67 mg NBT, 0.05 mg PMS, and 50 mM potassium phosphate, pH 8.0 was then poured over the first top agar layer. The plates containing the membranes and the layers were incubated at room temperature overnight to allow the NADH produced during TeSADH oxidation of 2-butanol to react with PMS and NBT to produce the formazan dye (Scheme 3-1) (11). The colonies with the darkest purple color were picked from the master plate for further investigation.

### **3.3.6 Protein expression and purification**

For the determination of approximate activity, colonies were picked and grown overnight in 5 mL LB kan at 37°C. 1.5 ml of the overnight culture was spun down and resuspended in 0.5 ml fresh LB medium, which was used to inoculate 5 ml LB kan IPTG (1 mM), and shaken at 37°C for 3-5 hours. To prepare crude extracts, the 5 mL cultures were spun down (5,000 rpm for 5 min) and resuspended in 300 µl of 50 mM Tris-HCl, (pH 8.0). The cells were lysed by sonication, and heat treated at 75°C for 15 min to





**Scheme 3-1. NAD(P)(H), PMS and NBT reaction to produce formazan dye**

inactivate non-thermostable host proteins. The lysate was spun down (14,000 rpm for 10 min) to remove cell debris and inactivated enzymes. The supernatant was used for activity assays.

For specific activity determination the proteins were expressed in BL21(DE3) cells. The cultures were grown in 50 ml LB kan to 0.6-0.8 OD<sub>600</sub> before being induced with 1 mM IPTG at 37°C for 3-5 hours. The cells were spun down (5,000 rpm for 10 min), and the proteins were then purified on a HisSpin Trap column (GE Healthcare, Piscataway, NJ) according to the instructions with one additional washing step. This additional washing step, between the binding buffer and elution steps, used 400 µl of a modified elution buffer that contained 100 mM imidazole. This resulted in a purer protein sample.

For kinetic analysis, the GCY, ΩE3, and 2E proteins were again expressed in BL21(DE3). Cultures were grown, and proteins purified on a Ni-NTA (Qiagen, Valencia, CA) column using the Gibco BRL procedure for Protein Expression System, pRoEX-1 vector (cat. no. 10197-010, Gaithersburg, MD) as described (33). Purified proteins were aliquoted and frozen at -80°C.

All protein concentrations were determined using the BioRad Protein Dye with bovine serum albumin as the standard. All fractions from protein purifications were tested by SDS-PAGE (15).

### **3.3.7 Enzyme assays**

Enzyme activity in crude extracts and purified enzyme samples was measured as described (3) with 0.4 mM NAD<sup>+</sup> as the cofactor. All assays were done in 50 mM Tris-

HCl, (pH 8.0) with 5 mM (*rac*)-2-butanol as the substrate. Initial velocity was measured spectrophotometrically at 60°C by following NADH production at 340 nm in a Varian Cary 300 UV/vis spectrophotometer equipped with a Peltier heating system. All enzymes were incubated at 40°C for at least 5 min before being added to the assay. One unit of activity was defined as the amount of enzyme needed to consume or produce 1  $\mu$ mol of NADH per minute.

To determine the kinetic parameters, enzyme assays were performed with (*rac*)-2-butanol (0.005-20 mM),  $\text{NAD}^+$  (0.05–70 mM), or  $\text{NADP}^+$  (0.005-40 mM), in 50 mM Tris–HCl (pH 8.0) at 60°C for 1 min. The  $K_{m\text{app}}$  and  $V_{\text{maxapp}}$  for cofactor reduction were determined with 5 mM 2-butanol. The  $K_m$  and  $V_{\text{max}}$  for 2-butanol oxidation were determined with 40 mM  $\text{NAD}^+$  (GCY and 2E) or 50 mM  $\text{NAD}^+$  ( $\Omega$ E3). At least nine substrate concentrations were used for each data set and each set was performed in triplicate. The  $K_m$  and  $V_{\text{max}}$  values of GCY,  $\Omega$ E3, and 2E TeSADH for 2-butanol oxidation were calculated using the Non-Linear Curve Fit tool of Origin 6.1 (OriginLab Corporation, Northampton, MA).

The results of  $\text{NAD}^+$  reduction by GCY,  $\Omega$ E3, and 2E TeSADH and  $\text{NADP}^+$  reduction by 2E TeSADH were not conducive to non-linear curve fitting because the activity reached a maximum before it began to decrease (Figure 3-1). Instead, the  $K_{m\text{app}}$  and  $V_{\text{maxapp}}$  values for  $\text{NAD}^+$  reduction were estimated by using the maximum specific activity value achieved as the  $V_{\text{maxapp}}$  and defining the substrate concentration at half the  $V_{\text{maxapp}}$  as the  $K_{m\text{app}}$ . In these cases, the  $\text{NAD}^+$  (or  $\text{NADP}^+$ ) concentration used to determine the kinetic parameters for 2-butanol was the concentration at  $V_{\text{maxapp}}$ . This concentration was used, because at the standard of 10 times  $K_m$  the activity of the

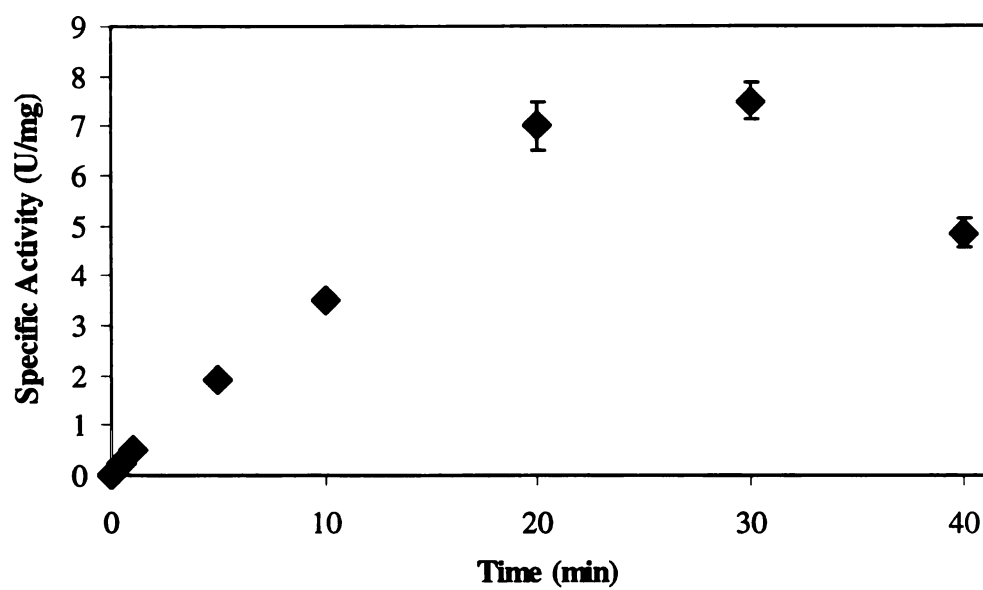


**Figure 3-1. Kinetics of NADP<sup>+</sup> reduction by 2E TeSADH with 2-butanol as the oxidation substrate at pH 8.0 and 60°C**

enzymes was greatly diminished.

### **3.3.8 Inhibition of TeSADH activity by $\text{NAD}^+$**

Inhibition of TeSADH activity by  $\text{NAD}^+$  was measured using five concentrations of  $\text{NAD}^+$  (0, 1, 2, 5, and 10 mM), and six concentrations of  $\text{NADP}^+$  (0.0032, 0.008, 0.016, 0.032, 0.08, and 0.16 mM). The  $K_i$  was calculated according to the Cornish-Bowden section on Inhibition by a Competing Substrate (8). All reactions contained 50 mM Tris-HCl (pH 8.0) and 5 mM 2-butanol, and were conducted at 60°C for 1.5 min.

### 3.4 Results and discussion

#### 3.4.1 TeSADH inhibition by $\text{NAD}^+$

Wild-type TeSADH is NADP(H) specific and has very low activity with NAD(H) (4). To determine whether NAD(H) and NADP(H) bind in the same site in TeSADH, inhibition experiments were performed using  $\text{NAD}^+$  as the inhibitor and  $\text{NADP}^+$  as the cofactor. The data was first plotted as a Lineweaver-Burke plot, but the data was not well fitted and the results were inconclusive (Figure 3-2). When plotted with a method from Cornish-Bowden (8),  $\text{NAD}^+$  appears to be an uncompetitive inhibitor of TeSADH's activity with  $\text{NADP}^+$ , with a  $K_{iu}$  of  $12 \pm 2$  mM (Figure 3-3). This uncompetitive inhibition by  $\text{NAD}^+$  would indicate that NAD(H) and NADP(H) bind in different sites. Uncompetitive inhibition of ADH's has been shown with other types of inhibitors (7, 21, 29). HLADH has been shown to have a nonspecific substrate/inhibitor binding site in close proximity to the zinc and properly bound coenzyme (2), which could indicate that the uncompetitive inhibition shown in TeSADH could be caused by nonspecific binding of NAD(H).

Previous attempts have been made to change TeSADH's cofactor specificity. Both the G198D and Y218F mutations were constructed by comparing the structure and sequence of NADP(H) specific TeSADH with that of the NAD(H)-specific HLADH, and assuming that the cofactors bind in the same site in the NADP(H)- and NAD(H)-dependent enzymes. Both TeSADH mutants showed increased activity with  $\text{NAD}^+$  in comparison to TeSADH with  $\text{NADP}^+$  suggesting that NAD(H) does bind in the same site as NADP(H).

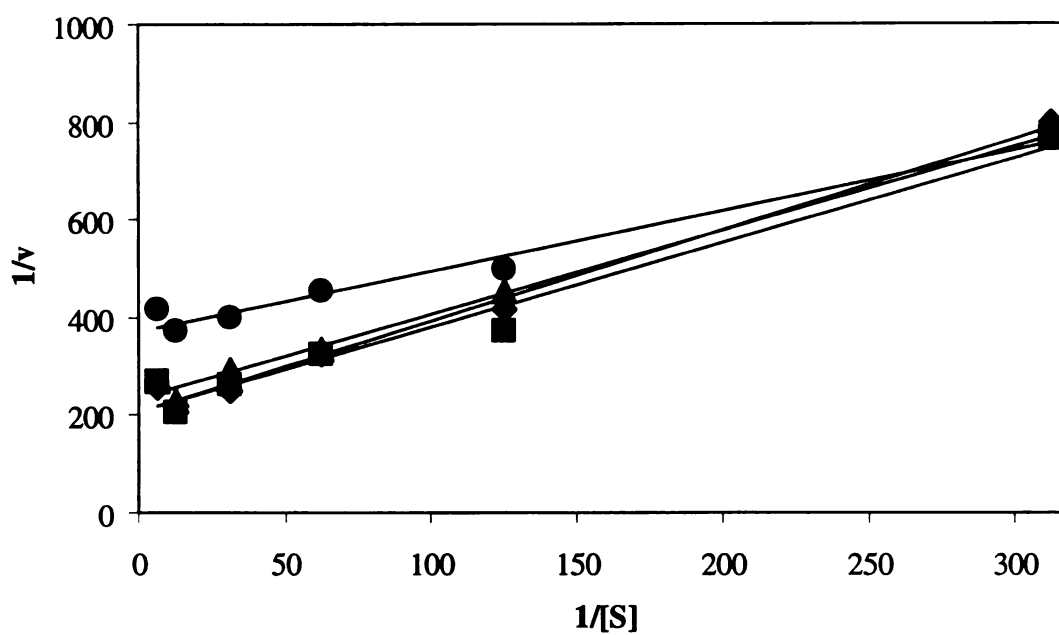


**Figure 3-2. Inhibition of TeSADH by NAD<sup>+</sup> shown as a Lineweaver-Burke plot with 0 mM NAD<sup>+</sup> (♦); 1 mM NAD<sup>+</sup> (■); 2 mM NAD<sup>+</sup> (▲); 10 mM NAD<sup>+</sup> (●)**

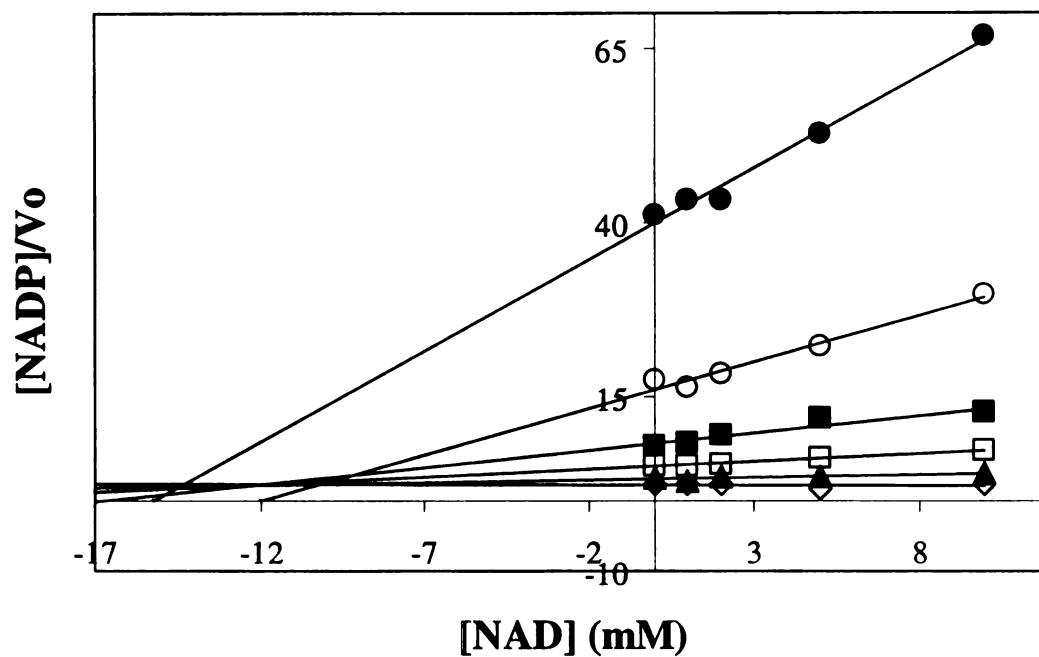


**Figure 3-3. Inhibition of TeSADH by  $NAD^+$  with 0.0032 mM  $NADP^+$  ( $\diamond$ ); 0.008 mM  $NADP^+$  ( $\blacktriangle$ ); 0.016 mM  $NADP^+$  ( $\square$ ); 0.032 mM  $NADP^+$  ( $\blacksquare$ ); 0.08 mM  $NADP^+$  ( $\circ$ ); 0.16 mM  $NADP^+$  ( $\bullet$ )**



### **3.4.2 Construction and characterization of a TeSADH G198D/Y218F double mutant**

Based on previous attempts at changing TeSADH's cofactor specificity from NADP(H) to NAD(H) (4, 12), we constructed the double mutant G198D/Y218F. We were hoping that the effects of these two mutations on cofactor specificity would be cumulative, and that the double mutant would have higher specificity for NAD(H). To our surprise, G198D/Y218F TeSADH showed only 0.17 U/mg specific activity with NAD<sup>+</sup>, suggesting that the two mutations are not compatible with each other with respect to cofactor specificity. To be sure of this decrease in activity, the  $K_m$  and  $V_{max}$  values should be measured.

### **3.4.3 Structural and sequence comparisons**

It has been reported that TbSADH residues Gly198, Ser199, Arg200, and Tyr218 are responsible for cofactor specificity (14). From our structural comparisons, we felt that Cys203 and Gly243 would be important as well. Mutation C203K would decrease the size of the active site in a way that excludes the NADP(H) phosphate moiety, and mutation G243I, which would also decrease the binding site size, presumably would cause a shift in the position of the cofactor to mimic the position of NAD(H) in HLADH.

Based on the sequences and structures of TeSADH and HLADH (Figures 3-4 and 3-5) we chose to construct mutations G198D, S199I, R220N, C203K, Y128P, and G243I. We also compared HLADH and TeSADH to the YADH sequence to see which residues were conserved in the two NAD(H) specific enzymes. HLADH and YADH had conserved residues at positions analogous to TeSADH G198 and C203.

TeSADH	VAGDKLRGAGRIIAV <b>GS</b> RPV <b>C</b> VDAAKYYGA	212
HLADH	IMGCKAAGAARIIGV <b>DINKD</b> <b>K</b> FAKAKEVGA	237
YADH	VQYAKAMG-YRVLGI <b>DGGEG</b> <b>K</b> EELFRSIGG	215
	: * * * : : : . : *	
TeSADH	TDIVN <b>Y</b> KD--GPIESQIMNLTEGKGVDAAI	240
HLADH	TECVN <b>P</b> QDYKKPIQEVLTMSNG-GVDFS	266
YADH	EVFID <b>F</b> TK-EKDIVGAVLKATDG-GAHGVI	243
	: : . * : : : * * . :	
TeSADH	IA <b>G</b> GNADIMATAVKIVKPG-GTIANVNYFG	269
HLADH	EV <b>I</b> GRLDTMVAALSCCQEAYGVSVIVGVPP	296
YADH	NV <b>S</b> VSEAAIEASTRYVRAN-GTTVLVGMPA	272
	. : : : * . . *	

**Figure 3-4. Comparison of the TeSADH, YADH, and HLADH NAD(P)(H) binding residues**

**Figure 3-5. Superimposed TeSADH and HLADH cofactor binding sites**

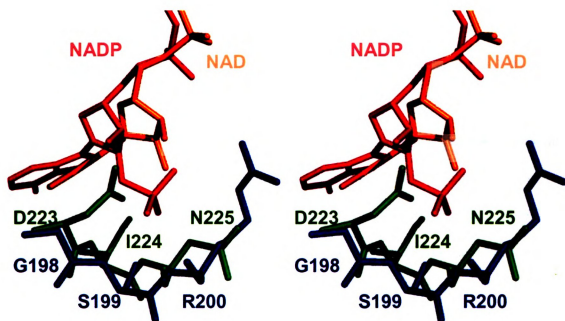
Green: HLADH residues, blue: TeSADH residues, red,:  $\text{NADP}^+$  in TeSADH, orange:  $\text{NAD}^+$  in HLADH

**A:** TeSADH residues 198-200, and HLADH residues 223-225

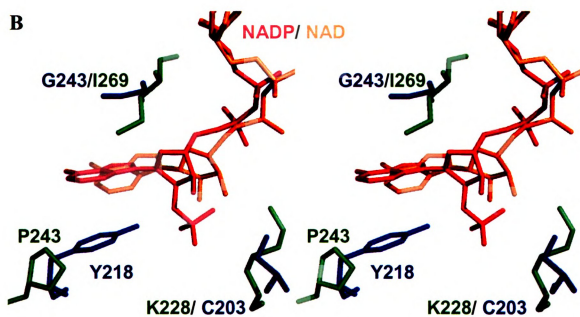
**B:** TeSADH residues 203,218,and 243; and HLADH residues 228,243, and 269

Figure is shown in stereo mode

A



B



#### 3.4.4 Site-directed mutagenesis

Mutations G198D, S199I, R220N, C203K, Y128P, and G243I were introduced in TeSADH individually or in combination. A total of forty-six mutants (Table 3-2) were constructed and their activity was tested in heat-treated crude extracts. Most were inactive, a few had very low activity with  $\text{NAD}^+$ , and a few retained some activity with  $\text{NADP}^+$  (data not shown). Though mutant GCY had an increased  $K_m$  compared to TeSADH and G198D TeSADH, its  $V_{\max}$  was increased 3 times compared to G198D TeSADH and 17.5 times compared to wild-type TeSADH with  $\text{NAD}^+$ , and became comparable to that of the wild-type TeSADH with  $\text{NADP}^+$  (Table 3-3).

#### 3.4.5 Directed evolution

Because of its high  $V_{\max}$  with  $\text{NAD}^+$ , GCY TeSADH was chosen as the parent for DE. Our goal was to decrease the  $K_m$  of DE mutants while maintaining the high  $V_{\max}$  value of GCY TeSADH. From the sequence and structural comparisons, we hypothesized that these three mutations were key to the path of developing an NAD(H)-specific enzyme. Mutations G198D and C203K mimic the residues that are conserved in YADH and HLADH, and mutation Y218P mimics HLADH, removing a hydroxyl group that could hydrogen bond with the phosphate group of NADP(H). The first generation DE mutant,  $\Omega\text{E3}$ , contained a single mutation in addition to the parental mutations. The second generation DE mutant, 2E, had three mutations in addition to the parent mutations (Table 3-4). The locations of the mutations varied, from buried to surface residues, none of which were near the cofactor binding site (Table 3-5 and Figure 3-6).

**Table 3-2. All mutants constructed by SDM and tested for activity**

<b>Single mutants</b>	<b>Triple mutants</b>
R200N	S199I + R200N + Y218P
S199I	G198D + S199I + C203K
C203K	G198D + R200N + C203K
Y218P	G198D + R200N + Y218P
<b>Double mutants</b>	G198D + S199I + G243I
G198D + Y218P	G198D + S199I + C203K
G198D + R200D	G198D+R200D+C203K
G198D + C203K	<b>Quadruple mutants</b>
S199I + C203K	S199I + R200N +C203K + Y218P
S199I + Y218P	G198D + R200D + C203K + Y218P
S199I + R200N	G198D + S199I + R200N + Y218P
S199I + G243I	G198D + C203K + Y218P + G243I
C203K + Y218P	G198D + R200N + C203K + Y218P
G198D + Y218F	G198D + S199I + R200N + C203K
R200N + C203K	G198D + S199I + R200D + C203K
R200N + Y218P	G198D + C203K + Y218F + G243I
G198D + G243I	G198D + S199I + C203K + Y218P
G198D + S199I	<b>Quintuple mutants</b>
G198D + R200N	G198D + S199I + R200N + Y218F + G243I
<b>Triple mutants</b>	G198D + S199I + R200N + C203K + Y218F
G198D + S199 I+ S317P	G198D + S199I + R200N + Y218P + G243I
S199I + C203K + Y218P	G198D + S199I + R200N + C203K + Y218P
G198D + R200N + Y218F	S199I + R200N + C203K + Y218P + G243I
G198D + C203K + Y218P	<b>Sextuple mutants</b>
G198D + S199I + Y218P	G198D + S199I + R200N + C203K + Y218P + G243I
G198D + R200D + Y218P	

**Table 3-3. Kinetic parameters of TeSADH, G198D TeSADH, GCY TeSADH, and TeSADH DE mutants  $\Omega$ E3 and 2E for NAD<sup>+</sup> and 2-butanol**

	Parent	2-butanol		NAD <sup>+</sup>			
		V <sub>max</sub> (U/mg)	K <sub>m</sub> (mM)	V <sub>max</sub> /K <sub>m</sub>	V <sub>max</sub> app (U/mg)	K <sub>m</sub> app (mM)	V <sub>max</sub> /K <sub>m</sub>
Wild-type	-	37	0.51	0.073	4.4	2.3	0.002
G198D		-	-	-	25	0.76	0.033
GCY	-	135	2	0.067	77	15	0.005
$\Omega$ E3	GCY	118	3.8	0.031	63	11.3	0.006
2E	$\Omega$ E3	77	3.7	0.029	51	7.6	0.007

**Table 3-4. Mutations in the DE parent and resulting enzymes**

Mutant	Parent	Mutations
GCY	-	G198D/C203K/Y218P
$\Omega$ E3	GCY	GCY + D186V
2E	$\Omega$ E3	$\Omega$ E3 + I49V/N54S/D315N

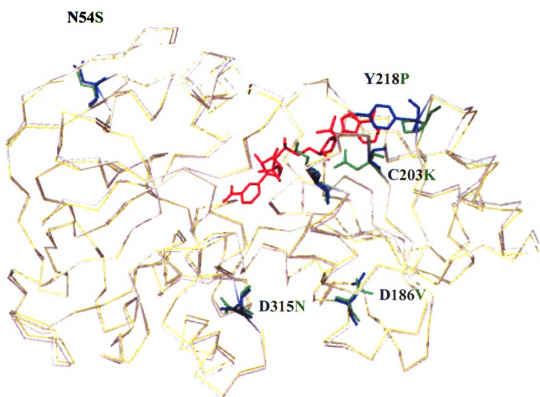
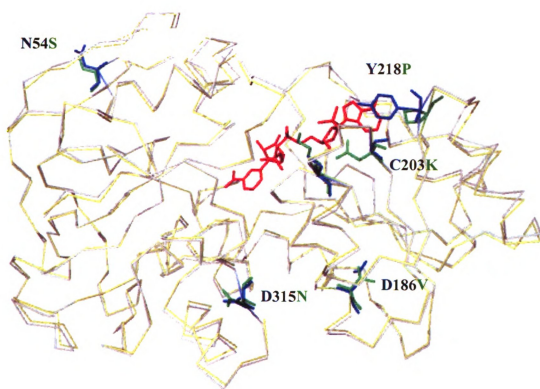
**Table 3-5. Locations of mutated residues in DE mutants**

<b>Mutation</b>	<b>Location</b>
D186V	Buried
I49V	Near active site residues Y267 (3.45 Å) and W110 (3.63 Å)
N54S	Surface – away from cofactor and substrate binding sites
D315N	Surface – away from cofactor and substrate binding sites



**Figure 3-6. Locations of all mutations in DE mutant 2E**

White: TeSADH backbone; yellow: 2E backbone; blue: TeSADH residues;  
green: 2E mutant residues; red: NADP<sup>+</sup>  
Figure is shown in stereo.



### 3.4.6 Enzyme activity

The specific activity of mutant  $\Omega$ E3 was 3.1 times higher than that of the parent, GCY (Table 3-6). The specific activity of mutant 2E was 3.1 times higher than that of its parent,  $\Omega$ E3, and 9.6 times higher than that of GCY.

Kinetic parameters were determined for GCY,  $\Omega$ E3, and 2E with 2-butanol and  $\text{NAD}^+$ , and for 2E with  $\text{NADP}^+$  (Tables 3-3 and 3-7) (3, 4). The  $K_m$  of GCY for 2-butanol increased 3.9 times compared to TeSADH, but the  $V_{\max}$  increased by 3.6 times. The  $K_m$  of GCY for  $\text{NAD}^+$  increased 6.5 times compared to TeSADH with  $\text{NAD}^+$ , but its  $V_{\max}$  increased 17.5 times compared to TeSADH with  $\text{NAD}^+$ , and is comparable to TeSADH with  $\text{NADP}^+$ .

Curiously, the  $K_m$  of  $\Omega$ E3 for 2-butanol increased 7.5 times, and the  $V_{\max}$  increased 3.2 times compared to those of TeSADH. Despite its 3.1-fold increase in specific activity the  $K_m$  of  $\Omega$ E3 increased 1.9 times and the  $V_{\max}$  decreased 1.1 times compared to GCY on 2-butanol. Kinetic parameters of  $\Omega$ E3 were slightly better than those of its parent, GCY, for  $\text{NAD}^+$ . Its  $K_m$  for  $\text{NAD}^+$  decreased 1.3 times and its  $V_{\max}$  decreased only 1.2 times compared to GCY.

The  $K_m$  of 2E for 2-butanol increased 7.3 times and the  $V_{\max}$  increased 2 times compared to TeSADH. However, despite an apparent 3.1 times increase compared to  $\Omega$ E3, and nearly 10 times increase compared to GCY, the  $K_m$  of 2E for 2-butanol increased 1.9 times, and the  $V_{\max}$  decreased by 1.8 times compared to GCY. Kinetic parameters of 2E were slightly better than those of its parent,  $\Omega$ E3, for  $\text{NAD}^+$ . Its  $K_m$  for  $\text{NAD}^+$  decreased 1.5 times and its  $V_{\max}$  decreased only 1.2 times compared to  $\Omega$ E3, and its  $K_m$  decreased 2-fold compared to GCY.

**Table 3-6. Specific activities of TeSADH, SDM mutant GCY, and DE mutants  $\Omega$ E3 and 2E**

	Parent	Specific Activity (U/mg)	Activity Increase (per generation)	Activity Increase (total)
GCY (NAD <sup>+</sup> )	-	0.25 $\pm$ 0.03	-	-
$\Omega$ E3 (NAD <sup>+</sup> )	GCY	0.78 $\pm$ 0.09	3.1x	3.1x
2E (NAD <sup>+</sup> )	$\Omega$ E3	2.41 $\pm$ 0.28	3.1x	9.6x

**Table 3-7. Kinetic parameters of TeSADH for NAD<sup>+</sup>, and TeSADH DE mutant 2E for NAD<sup>+</sup> and NADP<sup>+</sup>**

	NADP <sup>+</sup>			NAD <sup>+</sup>		
	V <sub>maxapp</sub> (U/mg)	K <sub>mapp</sub> (mM)	V <sub>max</sub> /K <sub>m</sub>	V <sub>maxapp</sub> (U/mg)	K <sub>mapp</sub> (mM)	V <sub>max</sub> /K <sub>m</sub>
Wild-type	72	0.016	4.5	-	-	-
2E	7.5	10.6	0.0007	51	7.6	0.007

The  $K_m$  of 2E for  $NADP^+$  increased by 662.5 times, and the  $V_{max}$  decreased by 16 times compared to wild-type TeSADH (Table 3-7). 2E has a 6.8-fold higher  $V_{max}$  with  $NADP^+$ . These results show that the cofactor preference of 2E TeSADH has changed from  $NADP^+$  to  $NAD^+$ .

### 3.5 Conclusions

These data show that we have SDM and DE mutants with  $V_{\max}$  values with  $\text{NAD}^+$  comparable to that of wild-type TeSADH with  $\text{NADP}^+$ , and that the  $K_m$  values of our DE mutants for  $\text{NAD}^+$  decreased by half compared to the parent, GCY TeSADH, leading to a 1.5-fold increase in catalytic efficiency for 2E compared to GCY TeSADH. The cofactor specificity of 2E TeSADH has been changed. It now shows a preference for  $\text{NAD}^+$  over  $\text{NADP}^+$ , with a 7.3 times higher catalytic efficiency and a 7.6 times higher  $V_{\max}$  with  $\text{NAD}^+$  compared to  $\text{NADP}^+$ .

### 3.6 References

1. **Ahuja, S. K., G. M. Ferreira, and A. R. Moreira.** 2004. Utilization of enzymes for environmental applications. *Crit. Rev. Biotechnol.* **24**:125-154.
2. **Becker, N. N., and J. D. Roberts.** 1984. Structure of the liver alcohol dehydrogenase-NAD<sup>+</sup>-pyrazole complex as determined by <sup>15</sup>N NMR spectroscopy. *Biochemistry* **23**:3336-3340.
3. **Burdette, D., and J. G. Zeikus.** 1994. Purification of acetaldehyde dehydrogenase and alcohol dehydrogenases from *Thermoanaerobacter ethanolicus* 39E and characterization of the secondary-alcohol dehydrogenase (2° Adh) as a bifunctional alcohol dehydrogenase--acetyl-CoA reductive thioesterase. *Biochem. J.* **302**:163-170.
4. **Burdette, D. S., F. Secundo, R. S. Phillips, J. Dong, R. A. Scott, and J. G. Zeikus.** 1997. Biophysical and mutagenic analysis of *Thermoanaerobacter ethanolicus* secondary-alcohol dehydrogenase activity and specificity. *Biochem. J.* **326**:717-724.
5. **Burdette, D. S., C. Vieille, and J. G. Zeikus.** 1996. Cloning and expression of the gene encoding the *Thermoanaerobacter ethanolicus* 39E secondary-alcohol dehydrogenase and biochemical characterization of the enzyme. *Biochem. J.* **316**:115-122.
6. **Bustard, M. T., J. G. Burgess, V. Meeyoo, and P. C. Wright.** 2000. Novel opportunities for marine hyperthermophiles in emerging biotechnology and engineering industries. *J. Chem. Technol. Biotechnol.* **75**:1095-1109.
7. **Chadha, V. K., K. G. Leidal, and B. V. Plapp.** 1983. Inhibition by carboxamides and sulfoxides of liver alcohol dehydrogenase and ethanol metabolism. *J. Med. Chem.* **26**:916-922.
8. **Cornish-Bowden, A.** 1995. Inhibition by a competing substrate, p. 105-111, *Fundamentals of enzyme kinetics*. Portland press, London.
9. **Demirjian, D. C., F. Moris-Varas, and C. S. Cassidy.** 2001. Enzymes from extremophiles. *Curr. Opin. Chem. Biol.* **5**:144-151.
10. **Drummond, D. A., B. L. Iverson, G. Georgiou, and F. H. Arnold.** 2005. Why high-error-rate random mutagenesis libraries are enriched in functional and improved proteins. *J. Mol. Biol.* **350**:806-816.
11. **Glieder, A., and P. Meinhold.** 2003. High-throughput screens based on NAD(P)H depletion, p. 157-159. *In* F. H. Arnold and G. Georgiou (ed.), *Directed enzyme evolution: Screening and selection methods*, vol. 230. Humana Press Inc., Totowa, NJ.

12. **Hassler, B. L., M. Dennis, M. Laivenieks, J. G. Zeikus, and R. M. Worden.** 2007. Mutation of Tyr-218 to Phe in *Thermoanaerobacter ethanolicus* secondary alcohol dehydrogenase: effects on bioelectronic interface performance. Appl. Biochem. Biotechnol. **In press**.
13. **Korkhin, Y., F. Frolow, O. Bogin, M. Peretz, A. J. Kalb(Gilboa), and Y. Burstein.** 1996. The crystal structure of the thermostable alcohol dehydrogenase from *Thermoanaerobium Brockii*: the role of prolines in thermal stability Perspectives on protein engineering, "from folds to functions", 5Th International Conference, Montpellier, France.
14. **Korkhin, Y., A. J. Kalb (Gilboa), M. Peretz, O. Bogin, Y. Burstein, and F. Frolow.** 1998. NADP-dependent bacterial alcohol dehydrogenases: crystal structure, cofactor-binding and cofactor specificity of the ADHs of *Clostridium beijerinckii* and *Thermoanaerobacter Brockii*. J. Mol. Biol. **278**:967-981.
15. **Laemmli, U. K.** 1970. Cleavage of structural proteins during the assembly of the head of bacteriophage T4. Nature **227**:680-685.
16. **Liese, A., K. Seelbach, and C. Wandry.** 2000. Industrial Biotransformations. Wiley-VCH, Weinheim, New York, Chichester, Brisbane, Singapore, Toronto.
17. **Lunzer, M., S. P. Miller, R. Felsheim, and A. M. Dean.** 2005. The biochemical architecture of an ancient adaptive landscape. Science **310**:499-501.
18. **Mayer, K. M., and F. H. Arnold.** 2002. A colorimetric assay to quantify dehydrogenase activity in crude cell lysates. J. Biomol. Screen. **7**:135-140.
19. **Musa, M. M., K. I. Ziegelmann-Fjeld, C. Vieille, J. G. Zeikus, and R. S. Phillips.** 2007. Asymmetric reduction and oxidation of aromatic ketones and alcohols using W110A secondary alcohol dehydrogenase from *Thermoanaerobacter ethanolicus*. J. Org. Chem. **72**:30-34.
20. **Patel, R. N.** 2005. Biocatalysis: Synthesis of chiral intermediates for pharmaceuticals, p. Chapter 26. In C. T. Hou (ed.), Handbook of Industrial Biocatalysis. Taylor & Francis Group, Boca Raton, FL.
21. **Plapp, B. V., and K. B. Berst.** 2003. Specificity of human alcohol dehydrogenase 1C\*2 (  $\gamma_2\gamma_2$ ) for steroids and simulation of the uncompetitive inhibition of ethanol metabolism. Chem. Biol. Interact. **143-144**:183-193.
22. **Rosell, A., E. Valencia, W. F. Ochoa, I. Fita, X. Pares, and J. Farres.** 2003. Complete reversal of coenzyme specificity by concerted mutation of three consecutive residues in alcohol dehydrogenase. J. Biol. Chem. **278**:40573-40580.
23. **Salazar, O., P. C. Cirino, and F. H. Arnold.** 2003. Thermostabilization of a cytochrome p450 peroxxygenase. Chembiochem. **4**:891-893.



24. **Schoemaker, H. E., D. Mink, and M. G. Wubbolts.** 2003. Dispelling the myths-biocatalysis in industrial synthesis. *Science* **299**:1694-7.
25. **Serov, A. E., A. S. Popova, V. V. Fedorchuk, and V. I. Tishkov.** 2002. Engineering of coenzyme specificity of formate dehydrogenase from *Saccharomyces cerevisiae*. *Biochem. J.* **367**:841-847.
26. **Tishkov, V. I., and V. O. Popov.** 2004. Catalytic mechanism and application of formate dehydrogenase. *Biochemistry (Moscow)* **69**:1252-1267.
27. **Wandrey, C.** 2004. Biochemical reaction engineering for redox reactions. *The Chemical Record* **4**:254-265.
28. **Wöltinger, J., K. Drauz, and A. S. Bommarius.** 2001. The membrane reactor in the fine chemicals industry. *Applied Catalysis A: General* **221**:171-185.
29. **Wratten, C. C., and W. W. Cleland.** 1965. Kinetic studies with liver alcohol dehydrogenase. *Biochemistry* **4**:2442-2451.
30. **Wu, J. T., L. H. Wu, and J. A. Knight.** 1986. Stability of NADPH: effect of various factors on the kinetics of degradation. *Clin. Chem.* **32**:314-319.
31. **Zaks, A.** 2001. Industrial biocatalysis. *Curr. Opin. Chem. Biol.* **5**:130-136.
32. **Zhu, G., G. B. Golding, and A. M. Dean.** 2005. The selective cause of an ancient adaptation. *Science* **307**:1279-1282.
33. **Ziegelmann-Fjeld, K. I., M. M. Musa, R. S. Phillips, J. G. Zeikus, and C. Vieille.** 2007. A *Thermoanaerobacter ethanolicus* secondary alcohol dehydrogenase mutant derivative highly active and stereoselective on phenylacetone and benzylacetone. *Protein Eng. Des. Sel.* **20**:47-55.

## **CHAPTER IV**

### **Conclusions and directions for future research**

The use of enzymes in industry is continually gaining interest in order to create a more environmentally friendly, less costly option to traditional chemical syntheses (1, 8). This has increased the need for enzymes tailored to produce specific products and for the technology needed to carry out the enzyme engineering (5, 11). Enzymes have been engineered for many purposes. For example, the cofactor specificity of formate dehydrogenase was changed from NAD(H) to NADP(H) to allow formate dehydrogenase's use for NADP(H) cofactor recycling (9, 10) and the activity of isolated galactose oxidase was increased (3). This change of enzyme characteristics can be done with either site-directed mutagenesis (SDM) or directed evolution (DE) (3, 7).

In this thesis we focused on engineering substrate and cofactor specificities in *Thermoanaerobacter ethanolicus* secondary alcohol dehydrogenase (TeSADH). We used structure-based SDM to alter TeSADH's substrate specificity to include phenyl-substituted alcohols, ketones, and their aryl derivatives. We used SDM and DE to change TeSADH's cofactor specificity from NADP(H) to NAD(H) to make the industrial use of this enzyme more cost effective.

## **4.1 W110A TeSADH**

The W110A mutation introduced in TeSADH to increase the size of the large substrate binding pocket (Chapter II) (12). This mutation was designed based on modeling the phenylacetone molecule in the TeSADH catalytic site and removing the Trp110 bulky residue, whose side-chain was overlapping with the substrate. The W110A mutation changed the substrate specificity of TeSADH to accommodate phenyl-substituted alcohols and ketones. W110A TeSADH is active on (S)-1-phenyl-2-propanol,

(S)-4-phenyl-2-butanol, phenylacetone, benzylacetone, and a variety of aryl derivatives of these substrates, and it shows little activity with the (R)-alcohols. W110A TeSADH produces (S)-4-phenyl-2-butanol with high enantioselectivity (>99%). W110A TeSADH also produces a variety of aryl-substituted alcohols with high enantioselectivity (98-99%). Although W110A TeSADH does not produce (S)-1-phenyl-2-propanol with high ee (37%), it has been shown that the addition of a single methoxy group to the phenyl ring can increase the ee to >99% (Appendix A) (5).

W110A TeSADH is shown to retain most of the thermostability characteristics of the wild-type enzyme. It is only slightly destabilized compared to TeSADH. W110A TeSADH also showed a solvent stability similar to that of TeSADH. At 50°C or below the W110A TeSADH maintains full activity for at least 120 min in the presence of 30% 2-propanol. However, at the same solvent concentration, 80% of the enzyme activity is lost after 120 min at 60°C.

W110A TeSADH has also been shown to be active in 100% organic solvent (Appendix B) (6). When encapsulated in porous silicate classes, a type of non-covalent immobilization, W110A TeSADH reduced benzylacetone to (S)-4-phenyl-2-butanol in 100% hexane with an 80% conversion and 96% ee, and in 100% diisopropyl ether with a 40% conversion and 97% ee.

## **4.2 Future work with W110A TeSADH**

For use in an industrial environment it is essential that an enzyme be stable for long periods of time in the reaction conditions. When using substrates with low solubility in water this may mean using an organic co-solvent to increase the solubility of

the substrate. In this case the enzyme must be stable in the determined concentration of organic solvent.

Our solvent stability determinations were done over a time of only 120 min, which is a much shorter time than the months that would be necessary for use in industry. Therefore, further stability assays should be done to determine the long-term effects of solvent on W110A TeSADH stability. Studies should also be done to determine the effect of higher solvent concentrations in order to determine at what concentration of solvent activity starts to decrease.

After determination of W110A TeSADH solvent stability under multiple conditions W110A TeSADH should be engineered to increase its solvent stability at temperatures above 50°C and at high solvent concentrations. This can be done by DE using a nitroblue tetrazolium/phenazine methosulfate-based plate screening procedure.

### **4.3 Changing TeSADH cofactor specificity**

Prior work had been done to change TeSADH's cofactor specificity from NADP(H) to NAD(H). The two mutants that were constructed (G198D and Y219F) showed a decrease in  $K_m$  and an increase in  $V_{max}$  compared to TeSADH with  $NAD^+$ . However, these improvements in activity with  $NAD^+$  were not sufficient to bring the level of activity to that of TeSADH with  $NADP^+$  (2, 4).

In our work, we used both SDM and DE to increase the specificity of TeSADH for  $NAD^+$  (Chapter III). Our goal was to engineer TeSADH to have similar catalytic parameters with  $NAD^+$  as the wild-type enzyme does with  $NADP^+$ . We constructed a triple mutant by structure-based SDM using mutations that we thought would be essential

for NAD<sup>+</sup> specificity. Mutant G198D/C203K/Y218P (GCY) had an 9-fold increased K<sub>m</sub> with NAD<sup>+</sup> compared to TeSADH with NAD<sup>+</sup>, but its V<sub>max</sub> was comparable to TeSADH with NADP<sup>+</sup>, so we used it as a parent in DE in order to increase its specificity for NAD<sup>+</sup>.

Two rounds of DE were performed. The first round produced a enzyme with a single extra mutation (D186V) compared to the parent GCY. The GCY/D186V mutant ( $\Omega$ E3) was used as the parent for the second round of DE, which produced an enzyme with three extra mutations I49V, N54S, and D315N. Kinetic parameters of  $\Omega$ E3 were better than those of its parent, GCY, for NAD<sup>+</sup>. Its K<sub>m</sub> for NAD<sup>+</sup> decreased 1.3 times and its V<sub>max</sub> decreased only 1.2 times compared to GCY.

Kinetic parameters of 2E were slightly better than those of its parent,  $\Omega$ E3, for NAD<sup>+</sup>. Its K<sub>m</sub> for NAD<sup>+</sup> decreased 1.5 times and its V<sub>max</sub> decreased only 1.2 times compared to  $\Omega$ E3, and its K<sub>m</sub> decreased 2-fold compared to GCY. However, the K<sub>m</sub> of 2E for NADP<sup>+</sup> increased by 662.5 times, and the V<sub>max</sub> decreased by 16 times compared to wild-type TeSADH (Table 3-7). 2E has a 6.8-fold higher V<sub>max</sub> with NAD<sup>+</sup> than with NADP<sup>+</sup>, and a 10-fold higher catalytic efficiency with NAD<sup>+</sup> than with NADP<sup>+</sup>. These results show that the cofactor preference of 2E TeSADH has changed from NADP<sup>+</sup> to NAD<sup>+</sup>.

#### **4.4 Future work to increase NAD(H) specificity of TeSADH**

The SDM mutant GCY and both DE mutants' V<sub>max</sub> with NAD<sup>+</sup> are comparable to that of the wild-type enzyme with NADP<sup>+</sup>, but the K<sub>m</sub> is higher, indicating that continued work is needed to optimize TeSADH activity with NAD<sup>+</sup>.

After the second generation DE mutant, no further mutants were found that showed apparent higher activity with  $\text{NAD}^+$ . Problems arose with the screening procedure, such as all colonies on the plate being a uniform color (either light or dark) or no colonies that were deemed ideal for testing. We will work to optimize the screening procedure by decreasing the incubation time and/or temperature with the substrate and cofactor. Additionally, during the color formation step, the plates should be checked at 30 min to 1 hour, rather than being left overnight, to determine which colonies to pick and test for activity. Additionally, because the goal is to decrease the  $K_m$  of successive mutants, we will optimize the system with decreased concentrations of cofactor.

For TeSADH to be industrially attractive, it must be both enantioselective for desirable products, be stable, and be economical to use. Therefore, the ultimate goal of this project should be to combine a solvent stable W110A TeSADH with the mutations of a TeSADH that is specific for  $\text{NAD}^+$ .

## 4.5 References

1. **Ahuja, S. K., G. M. Ferreira, and A. R. Moreira.** 2004. Utilization of enzymes for environmental applications. *Crit. Rev. Biotechnol.* **24**:125-154.
2. **Burdette, D. S., F. Secundo, R. S. Phillips, J. Dong, R. A. Scott, and J. G. Zeikus.** 1997. Biophysical and mutagenic analysis of *Thermoanaerobacter ethanolicus* secondary-alcohol dehydrogenase activity and specificity. *Biochem. J.* **326**:717-724.
3. **Delagrave, S., D. J. Murphy, J. L. Pruss, A. M. Maffia, III., B. L. Marrs, E. J. Bylina, W. J. Coleman, C. L. Grek, M. R. Dilworth, M. M. Yang, and D. C. Youvan.** 2001. Application of a very high-throughput digital imaging screen to evolve the enzyme galactose oxidase. *Protein Eng.* **14**:261-267.
4. **Hassler, B. L., M. Dennis, M. Laivenieks, J. G. Zeikus, and R. M. Worden.** 2007. Mutation of Tyr-218 to Phe in *Thermoanaerobacter ethanolicus* secondary alcohol dehydrogenase: effects on bioelectronic interface performance. *Appl. Biochem. Biotechnol.* **In press**.
5. **Musa, M. M., K. I. Ziegelmann-Fjeld, C. Vieille, J. G. Zeikus, and R. S. Phillips.** 2007. Asymmetric reduction and oxidation of aromatic ketones and alcohols using W110A secondary alcohol dehydrogenase from *Thermoanaerobacter ethanolicus*. *J. Org. Chem.* **72**:30-34.
6. **Musa, M. M., K. I. Ziegelmann-Fjeld, C. Vieille, J. G. Zeikus, and R. S. Phillips.** 2007. Xerogel-encapsulated W110A secondary alcohol dehydrogenase from *Thermoanaerobacter ethanolicus* performs asymmetric reduction of hydrophobic ketones in organic solvents. *Angew. Chem. Int. Ed. Engl.* .
7. **Patel, R. N.** 2005. Biocatalysis: Synthesis of chiral intermediates for pharmaceuticals, p. Chapter 26. *In* C. T. Hou (ed.), *Handbook of Industrial Biocatalysis*. Taylor & Francis Group, Boca Raton, FL.
8. **Schoemaker, H. E., D. Mink, and M. G. Wubbolts.** 2003. Dispelling the myths-biocatalysis in industrial synthesis. *Science* **299**:1694-7.
9. **Serov, A. E., A. S. Popova, V. V. Fedorchuk, and V. I. Tishkov.** 2002. Engineering of coenzyme specificity of formate dehydrogenase from *Saccharomyces cerevisiae*. *Biochem. J.* **367**:841-847.
10. **Tishkov, V. I., and V. O. Popov.** 2004. Catalytic mechanism and application of formate dehydrogenase. *Biochemistry (Moscow)* **69**:1252-1267.
11. **Zaks, A.** 2001. Industrial biocatalysis. *Curr. Opin. Chem. Biol.* **5**:130-136.
12. **Ziegelmann-Fjeld, K. I., M. M. Musa, R. S. Phillips, J. G. Zeikus, and C. Vieille.** 2007. A *Thermoanaerobacter ethanolicus* secondary alcohol



dehydrogenase mutant derivative highly active and stereoselective on phenylacetone and benzylacetone. *Protein Eng. Des. Sel.* **20**:47-55.

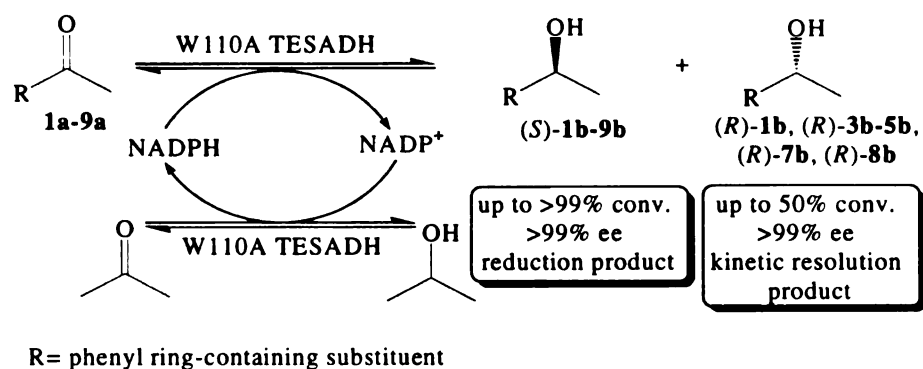
## **APPENDICIES**

## APPENDIX A

### **Asymmetric reduction and oxidation of aromatic ketones and alcohols using W110A secondary alcohol dehydrogenase from *Thermoanaerobacter ethanolicus***

**Research presented in this appendix was published as the following manuscript:**

Musa, M.M., K.I. Ziegelmann-Fjeld, C. Vieille, J.G. Zeikus, and R.S. Phillips.  
Asymmetric reduction and enantioselective oxidation using W110A secondary alcohol dehydrogenase from *Thermoanaerobacter ethanolicus*. *J. Org. Chem.* 2007; 72(1); 30-34.  
DOI: 10.1021/jo0616097



## A.1 Abstract

An enantioselective asymmetric reduction of phenyl ring-containing prochiral ketones to yield the corresponding optically active secondary alcohols was achieved with W110A secondary alcohol dehydrogenase from *Thermoanaerobacter ethanolicus* (W110A TESADH) in Tris buffer using 2-propanol (30%, v/v) as cosolvent and cosubstrate. This concentration of 2-propanol was crucial not only to enhance the solubility of hydrophobic phenyl ring-containing substrates in the aqueous reaction medium, but also to shift the equilibrium in the reduction direction. The resulting alcohols have *S*-configuration, in agreement with Prelog's rule, in which the nicotinamide-adenine dinucleotide phosphate (NADPH) cofactor transfers its *pro*-R hydride to the *re* face of the ketone. A series of phenyl ring-containing ketones, such as 4-phenyl-2-butanone (**1a**) and 1-phenyl-1,3-butadione (**2a**), were reduced with good to excellent yields and high enantioselectivities. On the other hand, 1-phenyl-2-propanone (**7a**) was reduced with lower ee than 2-butanone derivatives. (*R*)-Alcohols, the *anti*-Prelog products, were obtained by enantiospecific oxidation of (*S*)-alcohols through

oxidative kinetic resolution of the *rac*-alcohols using W110A TESADH in Tris buffer/acetone (90:10, v/v).

## A.2 Introduction

Tremendous efforts have been made in recent years to establish enantioselective routes to enantiomerically pure compounds, due to their importance in pharmaceutical, agricultural, and food industries.<sup>1</sup> Recent developments in medicine have shown that a single enantiomer is biologically active in most chiral drugs.<sup>2</sup> Optically active alcohols are one of the most important synthons. They can be produced from their corresponding prochiral ketones via asymmetric reduction, or from their racemic alcohols via enantiospecific kinetic resolution (KR).<sup>3,4</sup> Chiral metal complexes have been used as catalysts for these purposes,<sup>5</sup> however, these methods produce toxic residual metals that create environmental problems. Enzymes are recognized to be among the most effective catalysts for producing optically active alcohols. Among their advantages are their chemo-, regio-, and stereoselectivities due to the strict recognition of a particular substrate by a given enzyme. Biocatalytic processes also are less hazardous and energy consuming than conventional chemistry methodologies. They are normally carried out under mild conditions, which minimize problems of product isomerization, racemization, or epimerization. Biocatalysts are easily produced at low cost and with minimum waste, and they can be decomposed in the environment after use. Unfortunately, they do have some disadvantages. For example, many enzymes are thermally unstable. Another disadvantage is the limited solubility of most organic substrates in water; this leads to larger reaction volumes, a need for cosolvents, and complicated product recovery.<sup>6</sup>

Alcohol dehydrogenases (ADHs, EC 1.1.1.X, X=1 or 2) are enzymes that catalyze the reversible reduction of ketones and aldehydes to the corresponding alcohols. The asymmetric reduction of ketones using the commercially available yeast ADH and

horse liver ADH is limited not only due to their temperature sensitivity, but also due to their sensitivity towards organic solvents and their loss of activity upon immobilization. An additional disadvantage of horse liver ADH is its low affinity for acyclic ketones.<sup>7,1b</sup> Secondary ADH from *Thermoanaerobacter ethanolicus* (TESADH, EC 1.1.1.2), a highly thermostable enzyme, has been isolated and characterized.<sup>8</sup> NADPH is required by this enzyme, from which the hydride is transferred to the carbonyl carbon. Since NADPH is a costly cofactor, alcohols like 2-propanol or ketones like acetone are used as hydrogen source or hydrogen sink to regenerate the cofactor and therefore make both processes catalytic. This enzyme is stable at temperatures up to 80°C and it exhibits high activity in the asymmetric reduction of ketones.<sup>9</sup> Because of its thermostability, resistance to organic solvents, and reactivity for a wide variety of substrates, it is a useful biocatalyst for synthetic applications.<sup>10</sup>

A series of ethynyl ketones and ethynylketoesters were reduced enantioselectively to the corresponding non-racemic propargyl alcohols using wild-type TESADH.<sup>10a</sup> The behavior of TESADH has been shown to be similar to results obtained from reductions with a very highly homologous (99% identity),<sup>8b</sup> NADPH-dependent, *Thermoanaerobium brockii* ADH (TBADH).<sup>11</sup> For TBADH, Keinan *et al.* suggested that the two alkyl groups of substrates occupy two hydrophobic sites which differ from one another in volume and also in their affinities toward the alkyl groups (Figure 1).<sup>11</sup> It was also shown that the small site, which has higher affinity toward the alkyl groups of the Ketone, can accommodate up to three carbon substituents, like the isopropyl group.<sup>10a,b,</sup>

11

We have recently reported a new mutant of TESADH, where tryptophan-110 was

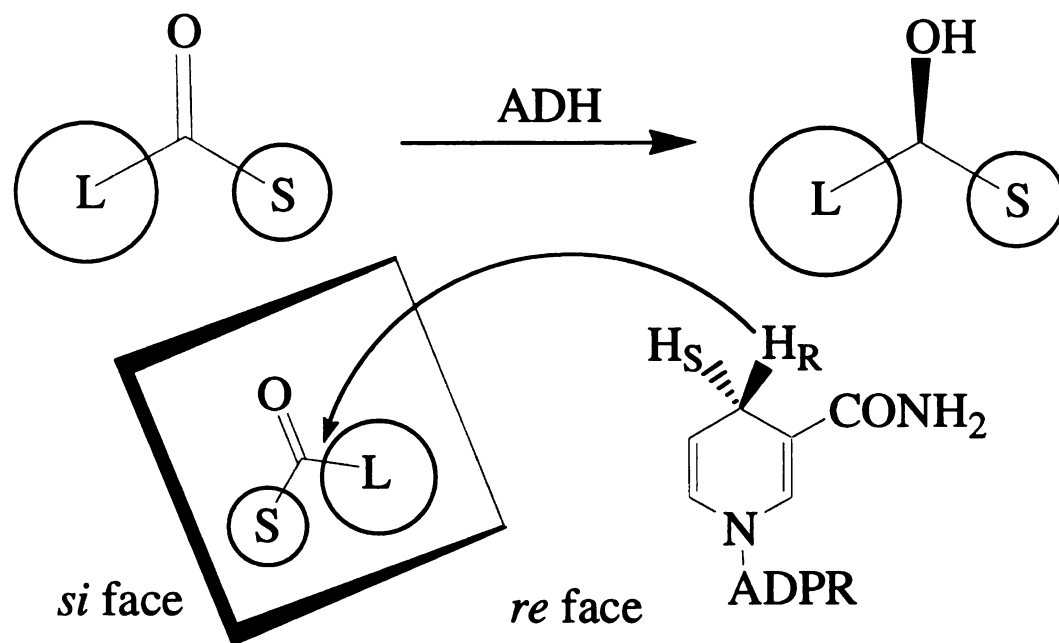


**Figure A-1. Prelog's rule for predicting the stereochemistry of alcohols formed from their corresponding ketones by asymmetric reduction with ADHs**



substituted by alanine, (W110A TESADH).<sup>12</sup> This replacement makes the large pocket able to accommodate phenyl ring-containing substrates that are not substrates for wild-type TESADH.<sup>10b</sup> Its modified substrate range makes this mutant enzyme useful for the enantioselective reduction of phenyl ring-containing ketones such as 4-phenyl-2-butanone (**1a**) and, in the reverse direction, for the enantioselective oxidation via KR of racemic phenyl ring-containing secondary alcohols.

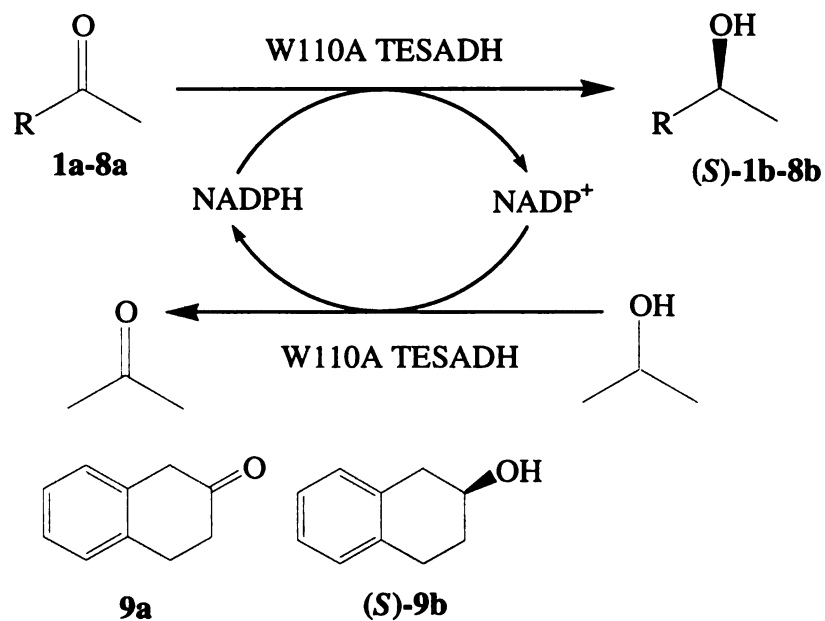
### A.3 Results and discussion

A series of phenyl ring-containing ketones, which could not be reduced by wild-type TESADH, were reduced by W110A TESADH to produce the corresponding non-racemic alcohols with good yields and high optical purities (Table 1). The reductions were carried out in Tris buffer containing 30% (v/v) 2-propanol, which serves as both cosolvent and hydride source to reduce the oxidized coenzyme. The use of such a high percentage of 2-propanol was crucial not only to enhance the solubility of the hydrophobic phenyl ring-containing ketone substrates in aqueous media, but also to shift the equilibrium into the reduction direction. The produced alcohols had *S* configuration, in agreement with Prelog's rule, in which the NADPH cofactor transfers its *pro*-R hydride to the *re* face of the ketone (Figure 1).<sup>13,1b,c</sup>

Phenyl ring-containing 2-butanone derivatives were reduced to the corresponding (*S*)-alcohols with excellent stereoselectivities and moderate to excellent yields (Table 1). 4-Phenyl-2-butanone (**1a**) was reduced stereoselectively to produce (*S*)-4-phenyl-2-butanol ((*S*)-**1b**) with excellent chemical and optical yields. The  $\beta$ -diketone 1-phenyl-1,3-butanedione (**2a**) was reduced regio- and stereoselectively to furnish the monohydroxy ketone (*S*)-3-hydroxy-1-phenyl-1-butanone ((*S*)-**2b**) with excellent yield and ee, leaving the other keto group at C-1 intact. (*E*)-4-Phenyl-3-butene-2-one (**3a**) was reduced with moderate yield and excellent optical purity to produce the allylic alcohol (*S*)-4-phenyl-3-butene-2-ol ((*S*)-**3b**). The presence of the methoxy group at the para position of the phenyl ring in 4-(4-methoxyphenyl)-2-butanone (**4a**) affected the ee of the produced (*S*)-4-(4-methoxyphenyl)-2-butanol ((*S*)-**4b**) (91% ee), which is lower than for (*S*)-**1b**. Phenoxy-2-propanone (**5a**) was reduced with very high yield and optical purity to

**Table A-1. Asymmetric Reduction of Phenyl Ring-Containing Ketones Using W110A TESADH**

<sup>a</sup> The absolute configurations of the products were determined by comparison of the signs of the optical rotation with those reported previously. <sup>b</sup> % conversion was determined by GC. <sup>c</sup> Isolated yield. <sup>d</sup> Unless otherwise mentioned, ee was determined by chiral stationary phase GC for the produced alcohol. <sup>e</sup> ee was determined for the corresponding acetate derivative (see the Supporting Information).



Substrate	R	product <sup>a</sup>	conv (%) <sup>b</sup>	ee (%) <sup>d</sup>
<b>1a</b>	PhCH <sub>2</sub> CH <sub>2</sub>	<b>(S)-1b</b>	99	>99
<b>2a</b>	Ph(C=O)CH <sub>2</sub>	<b>(S)-2b</b>	98	>99
<b>3a</b>	( <i>E</i> )-Ph-HC=CH	<b>(S)-3b</b>	64	>99
<b>4a</b>	<i>p</i> -MeOC <sub>6</sub> H <sub>4</sub> (CH <sub>2</sub> ) <sub>2</sub>	<b>(S)-4b</b>	87	91
<b>5a</b>	PhOCH <sub>2</sub>	<b>(S)-5b</b>	>99	>99 <sup>e</sup>
<b>6a</b>	<i>p</i> -ClC <sub>6</sub> H <sub>4</sub> CH <sub>2</sub> CHCl	<b>(2<i>S</i>,3<i>R</i>)-6b</b>	83 <sup>c</sup>	>99
<b>7a</b>	PhCH <sub>2</sub>	<b>(S)-7b</b>	95	37 <sup>e</sup>
<b>8a</b>	<i>p</i> -MeOC <sub>6</sub> H <sub>4</sub> CH <sub>2</sub>	<b>(S)-8b</b>	97	>99 <sup>e</sup>
<b>9a</b>		<b>(S)-9b</b>	>99	71 <sup>e</sup>

produce the corresponding (*S*)-phenoxy-2-propanol ((*S*)-**5b**). When the  $\alpha$ -chloroketone, 3-Chloro-4-(4-chlorophenyl)-2-butanone (**6a**), was reduced with W110A TESADH, (+)-(2*S*,3*R*)-3-chloro-4-(4-chlorophenyl)-2-butanol ((+)-(2*S*,3*R*)-**6b**) was produced with high enantioselectivity (>99% ee) and diastereoselectivity (92:8 mixture of *anti* and *syn*- $\alpha$ -chlorohydrins). The absolute configuration of (+)-(2*S*,3*R*)-**6b** was confirmed by comparing the sign of the optical rotation with that reported previously for the very similar compound, (+)-(2*S*,3*R*)-4-phenyl-3-bromo-2-butanol ( $[\alpha]_D^{20} +29.2$ ,  $c$  2.08, CHCl<sub>3</sub>; lit.<sup>14</sup>  $[\alpha]_D^{25} +37$ ,  $c$  0.06, CHCl<sub>3</sub>, 95% ee). In a separate experiment, reduction of **6a** with NaBH<sub>4</sub>, which is expected to give mainly the *syn* product,<sup>15</sup> afforded a mixture of four diastereomers (( $\pm$ )-**6b**) (88:12 mixture of *syn*- and *anti*- $\alpha$ -chlorohydrins), in which the *syn*-**6b** had a different retention time than (+)-(2*S*,3*R*)-**6b** by injection in a chiral column GC (Figure 2a,b). Reduction of **6a** to almost a single stereoisomer, (+)-(2*S*,3*R*)-**6b**, using W110A TESADH indicated that the process involves a KR, and this should be combined with isolation of (*S*)-**6a** as unreacted enantiomer and a maximum yield of 50% of the produced  $\alpha$ -chlorohydrin. We have noticed that the yield is higher than 50%, and the isolated unreacted **6a** is a racemic mixture. This indicates that the reduction of **6a** with W110A TESADH proceeds by dynamic kinetic resolution via a facile buffer-catalyzed enolization, which enables the unreacted enantiomer (*S*)-**6a** to racemize after the depletion of (*R*)-**6a** starts.<sup>16</sup> The  $\alpha$ -chlorohydrin (+)-(2*S*,3*R*)-**6b** was then converted quantitatively to the corresponding epoxide, (-)-(2*S*,3*S*)-4-(4-chlorophenyl)-2,3-epoxybutane ((-)-(2*S*,3*S*)-**6c**), without racemization using 1,8-diazabicyclo[5.4.0]undec-7-ene (DBU) (Scheme 1, Figure 2c).<sup>3d</sup> The absolute configuration of (-)-(2*S*,3*S*)-**6c** was

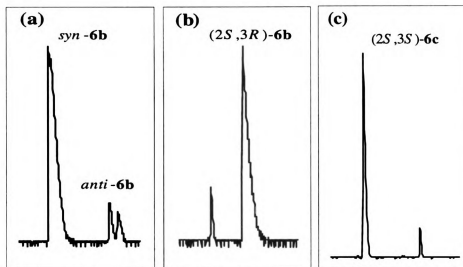
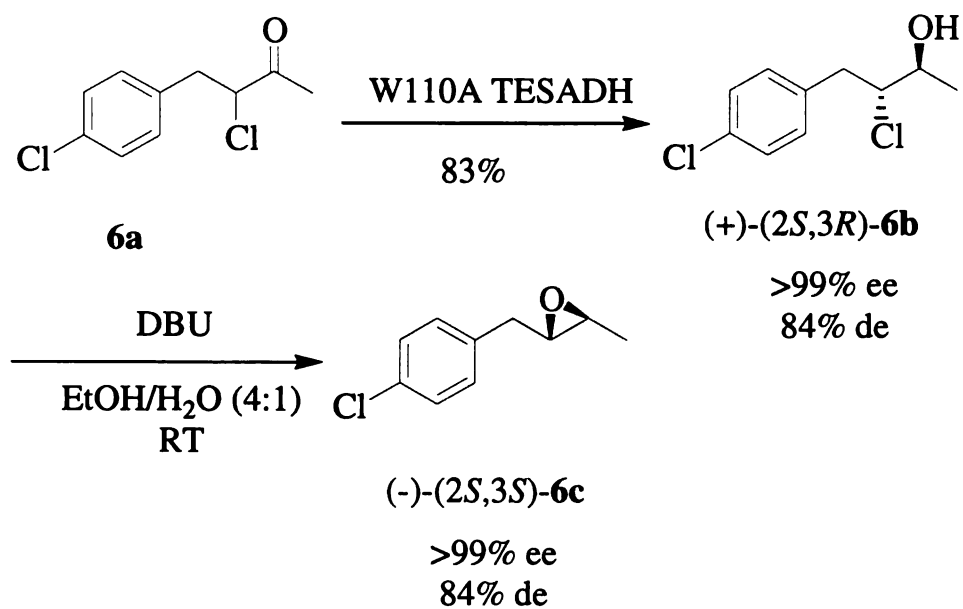


**Figure A-2.** GC chromatograms illustrating: a: the products of  $\text{NaBH}_4$  reduction of 6a. b: the products of W110A TESADH reduction of 6a. c: (-)-(2*S*,3*S*)-6c produced from (+)-(2*S*,3*R*)-6b.



**Scheme A-1. Conversion of (+)-(2*S*,3*R*)-6b into (-)-(2*S*,3*S*)-6c.**

confirmed by the comparison of the sign of optical rotation with that reported for the very similar compound (-)-(2*S*,3*S*)-4-phenyl-2,3-epoxybutane ( $[\alpha]_{\text{D}}^{20}$  -26.2, *c* 2.32, CHCl<sub>3</sub>; lit.<sup>14</sup>  $[\alpha]_{\text{J}}^{25}$  -27, *c* 0.04, CHCl<sub>3</sub>, >98% ee).

Unexpectedly, 1-phenyl-2-propanone (**7a**) was reduced to produce (*S*)-1-phenyl-2-propanol ((*S*)-**7b**) with poor enantioselectivity, indicating that **7a** can fit in alternative modes in the active site within the large pocket allowing the NADPH cofactor to deliver its *pro*-R hydride from either *re* or *si* faces. 1-(4-Methoxyphenyl)-2-propanone (**8a**) was reduced to produce (*S*)-1-(4-methoxyphenyl)-2-propanol ((*S*)-**8b**) with excellent chemical yield and ee, which means that the sterically bulky para methoxy substituent in **8a** restricts the substrate to only a single binding mode within the active site. The cyclic ketone 2-tetralone (**9a**) was reduced with high yield and moderate stereopreference to produce (*S*)-2-tetralol ((*S*)-**9b**). Enzymatic asymmetric reduction of substrates with sterically hindered groups on both sides of the carbonyl, like **9a**, is of great interest because these substrates are typically either poor or non-substrates for ADHs, therefore very few ADHs are able to achieve such asymmetric reductions.<sup>1b,3c</sup>

Oxidation via KR of phenyl ring-containing *rac*-alcohols was used to produce their (*R*)-alcohols, the *anti*-Prelog configured alcohols, as unreacted enantiomers with moderate to high enantiomeric ratios using W110A TESADH. The reactions were carried out in Tris buffer containing 10% (v/v) acetone. The amount of acetone needed was less than the amount of 2-propanol used in the reduction pathway simply because alcohols are more soluble than their corresponding hydrophobic ketones in aqueous media. As with all KRs, these reactions suffer from the limitation that the maximum theoretical yield with high enantiomeric ratio of a single enantiomer, (*R*) in this case, is 50% (Table 2). As



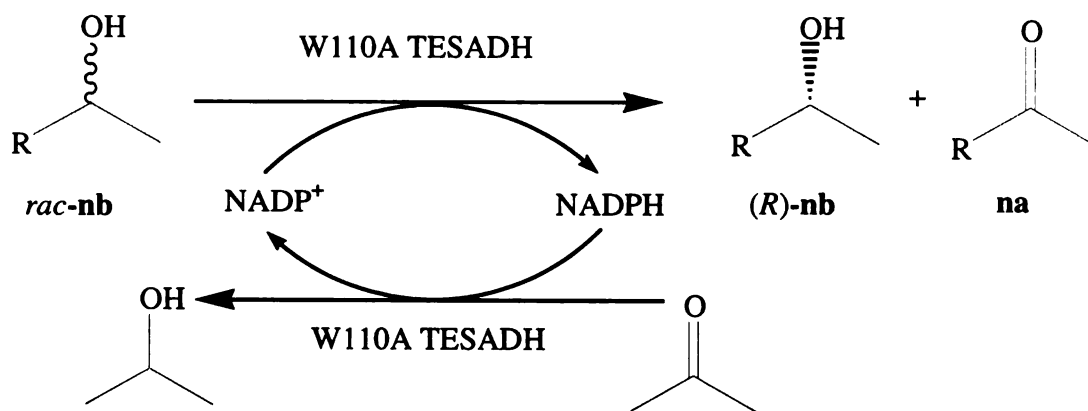
**Table A-2. Enantiospecific Kinetic Resolution of Phenyl Ring-Containing *rac*-Alcohols Using W110A TESADH**

<sup>a</sup> The absolute configurations of the unreacted alcohols were confirmed by coinjection in a chiral column GC with their *S* enantiomers prepared by the asymmetric reduction of the corresponding ketones employing W110A TESADH (Table 1).

<sup>b</sup> % conversion was determined by GC.

<sup>c</sup> Unless otherwise mentioned, ee was determined by a chiral stationary phase GC for the alcohols.

<sup>d</sup> ee was determined for the corresponding acetate derivative (see the Supporting Information).



**n = 1, 3-5, 7, 8**

substrate	R	product <sup>a</sup>	conv. (%) <sup>b</sup>	ee (%) <sup>c</sup>
<i>rac</i> -1b	PhCH <sub>2</sub> CH <sub>2</sub>	( <i>R</i> )-1b	50	>99
<i>rac</i> -3b	( <i>E</i> )-Ph-HC=CH	( <i>R</i> )-3b	50	>99
<i>rac</i> -4b	<i>p</i> -MeOC <sub>6</sub> H <sub>4</sub> (CH <sub>2</sub> ) <sub>2</sub>	( <i>R</i> )-4b	75	77 <sup>d</sup>
<i>rac</i> -5b	PhOCH <sub>2</sub>	( <i>R</i> )-5b	19	25
<i>rac</i> -7b	PhCH <sub>2</sub>	( <i>R</i> )-7b	49	39 <sup>d</sup>
<i>rac</i> -8b	<i>p</i> -MeOC <sub>6</sub> H <sub>4</sub> CH <sub>2</sub>	( <i>R</i> )-8b	48	92 <sup>d</sup>

expected, the substrates reduced with high ee showed high stereospecificities in the oxidation pathway and *vice versa*.

The enantiospecific oxidation via KR using W110A TESADH exclusively oxidized the *S* enantiomers of *rac*-**1b** and *rac*-**3b** to the corresponding ketones **1a** and **3a**, respectively, leaving their (*R*)-alcohols as unreacted enantiomers with excellent enantiomeric ratios (Table 2). The production of optically active **1b** is important as it is a precursor for antihypertensive agents, such as bufeniodide and labetalol.<sup>3b,17</sup> For *rac*-**4b**, it was resolved by oxidative KR to furnish (*R*)-**4b** with moderate stereopreference (77% ee at 75% conversion). Under the same conditions, KR of *rac*-**5b** furnished (*R*)-**5b** with 25% ee at only 19% conversion, indicating that the KR of this alcohol takes place with high enantiomeric discrimination. Even with addition of more enzyme and acetone, we were not able to push the reaction to higher yield. The racemic 1-phenyl-2-propanol (*rac*-**7a**) was resolved, as expected, with low enantiospecificity because it was reduced with low ee. (*S*)-1-(4-Methoxyphenyl)-2-propanol ((*S*)-**8b**) was oxidized with excellent enantioselectivity to its corresponding ketone **8a** leaving (*R*)-**8b** as enantiomerically pure unreacted enantiomer. Although **9a** was reduced with high yield and moderate ee, *rac*-**9b** was not oxidized by W110A TESADH. The same results for *rac*-**9b** were obtained by Stampfer *et al.* using *Rhodococcus ruber* DSM 44541.<sup>3b</sup>

Resistance of TESADH to organic cosolvents allowed the redox reactions in both directions to be carried out at relatively high substrate concentration (35 mM in the reduction pathway and 70 mM in the oxidation pathway). The design of new TESADH mutants such as W110A TESADH in addition to TESADH's resistance to organic

solvents and high concentrations of substrates make this enzyme useful for synthetic applications.

## A.4 Conclusion

We have been able to produce both enantiomers of a series of phenyl ring-containing secondary alcohols by asymmetric reduction and enantioselective oxidation via KR using W110A TESADH. (*S*)-alcohols were produced via asymmetric reduction with high chemical and moderate to high optical yields using 2-propanol as a cosubstrate for coenzyme regeneration and as a cosolvent. A number of racemic phenyl ring-containing alcohols were resolved with W110A TESADH using acetone as a hydrogen acceptor and a cosolvent. These reactions produced a mixture of (*R*)-alcohols as unreacted enantiomer with good enantiomeric ratios and the corresponding ketones, which could be recycled. The use of 2-propanol (30%, v/v) and acetone (10% v/v) in high concentration in the reduction and oxidation pathways was crucial not only to enhance the solubility of hydrophobic phenyl ring-containing substrates, but also to shift the equilibrium to the desired direction. It is of great interest to produce optically active alcohols of both enantiomers using the same enzyme because the two enantiomers are often of equal importance and only a few *anti*-Prelog enzymes are available. W110A TESADH will be of great interest to organic chemists for the preparation of optically active phenyl ring-containing alcohols because of its thermal stability and high tolerance to organic cosolvents.

## **A.5 Experimental section**

### **A.5.1 General procedures**

Capillary gas chromatographic measurements were performed on a GC equipped with a flame ionization detector and a Supelco  $\beta$ -Dex 120 chiral column (30 m, 0.25 mm [i.d.], 0.25  $\mu$ m film thickness) using Helium as the carrier gas.  $^1\text{H}$  NMR and  $^{13}\text{C}$  NMR spectra were recorded on 400 MHz spectrometer at room temperature in  $\text{CDCl}_3$  using either solvent peak or tetramethylsilane as internal standard. Column chromatographies were carried out on standard grade silica gel (60Å, 32-63 $\mu$ m) with ethyl acetate in hexane as eluent.

### **A.5.2 Materials**

Commercial grade solvents were used without further purification.  $\text{NADP}^+$ , Novozyme 435, and  $\text{NaBH}_4$  were used as purchased from commercial sources. Substrates **1a-6a**, **9a**, *rac*-**1b**, *rac*-**7b**, (*R*)-**7b**, and (*S*)-**7b** were used as purchased from commercial suppliers. **7a** and **8a** were prepared as described previously.<sup>18</sup> *rac*-**3b**, *rac*-**4b**, *rac*-**5b**, *rac*-**8b**, and *rac*-**9b** were prepared by reducing the corresponding ketones with  $\text{NaBH}_4$ .<sup>19</sup>

### **A.5.3 Gene expression and purification of W110A TESADH**

W110A TESADH was expressed in recombinant *E. coli* HB101(DE3) cells and purified as described.<sup>12</sup>

### **A.5.4 General procedure for asymmetric reduction of phenyl ring-containing ketones with W110A TESADH**

Reactions were conducted with 0.34 mmol of substrate, 2 mg NADP<sup>+</sup>, and 0.75 mg of W110A TESADH in 10.0 mL of 50 mM Tris-buffer (pH 8.0)/2-propanol (70:30, v/v). The reaction mixture was stirred at 50°C for 10 h then it was extracted with 3 × 5 mL CH<sub>2</sub>Cl<sub>2</sub>. The combined organic layers were dried with Na<sub>2</sub>SO<sub>4</sub> and concentrated under vacuum. The remaining residue was analyzed by chiral column GC to determine the percent conversion and ee of the produced alcohols then purified with silica gel using hexane/ethyl acetate (85/15) (95/5 for **6b**).

#### A.5.5 (+)-(2*S*,3*R*)-3-Chloro-4-(4-chlorophenyl)-2-butanol ((+)-(2*S*,3*R*)-**6b**)

$[\alpha]_D^{20} +29.2$  (*c* 2.08, CHCl<sub>3</sub>) >99% ee, 84% de; <sup>1</sup>H NMR,  $\delta$ : 1.33 (d, 3H, *J*= 6.4 Hz), 1.91 (brs, 1H), 2.91 (dd, 1H, *J*= 14.6 Hz, *J*= 9.8 Hz), 3.10 (dd, 1H, *J*=14.6 Hz, *J*= 4.2 Hz), 3.96 (qd, 1H, *J*= 6.4, *J*= 4.0), 4.14 (td, 1H, *J*= 9.6, *J*= 4.0), 7.17 (d, 2H, *J*= 8.0), 7.29 (d, 2H, *J*= 8.0); <sup>13</sup>C NMR,  $\delta$ : 18.8, 39.2, 69.4, 70.3, 128.9, 130.8, 132.9, 136.3; HRMS calcd for C<sub>10</sub>H<sub>12</sub>OCl<sub>2</sub> [M + H]<sup>+</sup>, 219.0343; found, 219.0347.

#### A.5.6 General procedure for kinetic resolution of phenyl ring-containing racemic alcohols with W110A TESADH

Reactions were conducted with 0.34 mmol of substrate, 1 mg NADP<sup>+</sup>, and 0.38 mg of W110A TESADH in 5.0 mL of 50 mM Tris-buffer/acetone (90:10) (v/v). The reaction mixture was stirred at 50°C for 12 h then it was extracted with 3 × 5 mL CH<sub>2</sub>Cl<sub>2</sub>. The combined organic layers were dried with Na<sub>2</sub>SO<sub>4</sub> and concentrated under vacuum. The remaining residue was analyzed by chiral stationary phase GC to determine the percent conversion to ketone and ee of the unreacted (*R*)-alcohol.

#### A.5.7 Synthesis of (-)-(2*S*,3*S*)-4-(4-chlorophenyl)-2,3-epoxybutane ((-)-(2*S*,3*S*)-6c)

It was prepared from (2*S*,3*R*)-6b using a previously reported procedure for epoxidation.<sup>3d</sup>  $[\alpha]_{\text{D}}^{20}$  -26.2 (*c* 2.32, CHCl<sub>3</sub>) >99% ee, 84% de; <sup>1</sup>H NMR,  $\delta$ : 1.23 (d, 3H, *J*= 5.2 Hz), 2.71-2.80 (m, 4H), 7.10 (d, 2H, *J*= 8.4), 7.20 (d, 2H, *J*= 8.8); <sup>13</sup>C NMR,  $\delta$ : 17.1, 37.9, 54.6, 59.6, 128.8, 130.5, 132.6, 136.1; HRMS calcd for C<sub>10</sub>H<sub>11</sub>OCl [M + H]<sup>+</sup>, 183.0576; found, 183.0571.

#### A.5.8 Determination of absolute configuration

The absolute configurations of the following compounds were determined by comparing of the sign of the optical rotation with that reported in the literature: (*S*)-1b,<sup>20</sup> (*S*)-2b,<sup>21</sup> (*S*)-3b,<sup>22</sup> (*S*)-4b,<sup>23</sup> (*S*)-5b,<sup>24</sup> (*S*)-7b,<sup>25</sup> (*S*)-8b,<sup>26</sup> and (*S*)-9b.<sup>3b</sup> The absolute configuration of (*S*)-7b was also demonstrated by coinjection on a chiral column GC with commercially available (*R*)-7b and (*S*)-7b. The absolute configuration of (*S*)-1b was confirmed by coinjection on a chiral column GC with (*R*)-1b, which was prepared by KR of *rac*-1b using Novozyme 435.<sup>27</sup> The absolute configurations of (*R*)-1b, (*R*)-3b, (*R*)-4b, (*R*)-5b, (*R*)-7b, and (*R*)-8b were elucidated by coinjection on GC using a chiral stationary phase with their *S* enantiomers prepared from asymmetric reduction of the corresponding ketones using W110A TESADH.



## **A.6 Acknowledgment**

Financial support from National Science Foundation (Grant number 0445511) to RSP, JGZ, and CV is gratefully acknowledged.

## A.7 Supporting information

Chiral GC chromatogram for both enantiomers of the acetate derivatives of alcohols **1b-5b** and **7b-9b**. Optical rotation values for (*S*)-**1b-5b** and (*S*)-**7b-9b**. <sup>1</sup>H NMR and <sup>13</sup>C NMR spectra for compounds (*S*)-**1b-5b**, (*S*)-**7b-9b**, (+)-(2*S*,3*R*)-**6b** and (-)-(2*S*,3*S*)-**6c**. This material is available free of charge via the Internet at <http://pubs.acs.org>.

## A.8 References

- (1) (a) García-Urdiales, E.; Alfonso, I.; Gotor, V. *Chem. Rev.* **2005**, *105*, 313-354. (b) Kroutil, W.; Mang, H.; Edegger, K.; Faber, K. *Curr. Opin. Chem. Biol.* **2004**, *8*, 120-126. (c) Nakamura, K.; Yamanaku, R.; Matsuda, T.; Harada, T. *Tetrahedron: Asymmetry* **2003**, *14*, 2659-2681. (d) Nakamura, K.; Matsuda, T.; Harada, T. *Chirality* **2002**, *14*, 703-708. (e) Phillips, R. S. *Can. J. Chem.* **2002**, *80*, 680-685.
- (2) Ariens, E. *J. Med. Res. Rev.* **1986**, *6*, 451-466.
- (3) (a) Zhu, D.; Yang, Y.; Hua, L. *J. Org. Chem.* **2006**, *71*, 4202-4205. (b) Stampfer, W.; Kosjek, B.; Faber, K.; Kroutil, W. *J. Org. Chem.* **2003**, *68*, 402-406. (c) Yadav, J. S.; Nanda, S.; Reddy, P. T.; Rao, A. B. *J. Org. Chem.* **2002**, *67*, 3900-3903. (d) Schubert, T.; Hummel, W.; Müller, M. *Angew. Chem. Int. Ed.* **2002**, *41*, 634-636. (e) Stampfer, W.; Kosjek, B.; Moitzi, C.; Kroutil, W.; Faber, K. *Angew. Chem. Int. Ed.* **2002**, *41*, 1014-1017. (f) Nakamura, K.; Inoue, Y.; Matsuda, T.; Misawa, I. *J. Chem. Soc. Perkin Trans. 1* **2000**, 2397-2402. (g) Bortolini, O.; Fantin, G.; Fogagnolo, M.; Giovannini, P. P.; Guerrini, A.; Medici, A. *J. Org. Chem.* **1997**, *62*, 1854-1856. (h) Grunwald, J.; Wirz, B.; Scollar, M. P.; Kilbanov, A. M. *J. Am. Chem. Soc.* **1986**, *108*, 6732-6734.
- (4) (a) Birman, V. B.; Jiang, H. *Org. Lett.* **2005**, *7*, 3445-3447. (b) Ghanem, A.; Aboul-enein, H. Y. *Chirality* **2005**, *17*, 1-15. (c) Martin-Matute, B.; Edin, M.; Bogar, K.; Bachväll, J. E. *Angew. Chem. Int. Ed.* **2004**, *43*, 6535-6539. (d) Birman, V. B.; Uffman, E. W.; Jiang, H.; Li, X.; Kilbane, C. J. *J. Am. Chem. Soc.* **2004**, *126*, 12226-12227. (e) Nakamura, K.; Matsuda, T.; Harada, T. *Chirality* **2002**, *14*, 703-708. (f) Kim, K.; Song, B.; Choi, M.; Kim, M. *Org. Lett.* **2001**, *3*, 1507-1509.
- (5) (a) Weinert, C. S.; Fanwick, P. E.; Rothwell, I. P. *Organometallics* **2005**, *24*, 5759-5766. (b) Noyori, R.; Okhuma, T. *Angew. Chem. Int. Ed.* **2001**, *40*, 40-73. (c) Blake, A. J.; Cunningham, A.; Ford, A.; Teat, S. J.; Woodward, S. *Chem. Eur. J.* **2000**, *6*, 3586-3594.
- (6) (a) Gervais, T. R.; Carta, G.; Gianer, J. L. *Biotechnol. Prog.* **2003**, *49*, 389-395. (b) Cao, L.; Langen, L. V.; Sheldon, R. A. *Curr. Opin. Biotechnol.* **2003**, *14*, 387-394. (c) Kilbanov, A. M. *Nature* **2001**, *409*, 241-246. (d) Koeller, M. K.; Wong, C. H. *Nature* **2001**, *409*, 232-240. (e) Riva, S.; Carrea, G. *Angew. Chem. Int. Ed.* **2000**, *39*, 2226-2254.
- (7) (a) Kovalenko, G. A.; Sokolovskii, V. D. *Biotechnol. Bioeng.* **1983**, *25*, 3177-3184. (b) Pollak, A.; Blumenfeld, H.; Wax, M.; Baughn, R. L.; Whitesides, G. M. *J. Am. Chem. Soc.* **1980**, *102*, 6324-6336.

- (8) (a) Burdette, D.; Zeikus, J. G. *Biochem. J.* **1994**, *302*, 163-170. (b) Burdette, D. S.; Vieille, C.; Zeikus, J. G. *Biochem. J.* **1996**, *316*, 115-122.
- (9) (a) Pham, V. T.; Phillips, R. S. *J. Am. Chem. Soc.* **1990**, *112*, 3629-3632. (b) Pham, V. T.; Phillips, R. S.; Ljugdahl, L. G. *J. Am. Chem. Soc.* **1989**, *111*, 1935-1936.
- (10) (a) Heiss, C.; Phillips, R. S. *J. Chem. Soc. Perkin Trans. 1* **2000**, 2821-2825. (b) Heiss, C.; Laivenieks, M.; Zeikus, J. G.; Phillips, R. S. *Bioorg. Med. Chem.* **2001**, *9*, 1659-1666. (c) Heiss, C.; Laivenieks, M.; Zeikus, G.; Phillips, R. S. *J. Am. Chem. Soc.* **2001**, *123*, 345-346. (d) Tripp, A. E.; Burdette, D. S.; Zeikus, J. G.; Phillips, R. S. *J. Am. Chem. Soc.* **1998**, *120*, 5137-5141.
- (11) Keinan, E.; Hafeli, E. K.; Seth, K. K.; Lamed, R. *J. Am. Chem. Soc.* **1986**, *108*, 162-169.
- (12) Ziegelmann-Fjeld, K. I.; Musa, M. M.; Phillips, R. S.; Zeikus, J. G.; Vieille, C.; In press.
- (13) Prelog, V. *Pure Appl. Chem.* **1964**, *9*, 119-130.
- (14) Besse, P.; Fernard, M. F.; Veschambre, H. *Tetrahedron: Asymmetry* **1994**, *5*, 1249-1268.
- (15) (a) Usami, Y.; Ueda, Y. *Chem. Lett.* **2005**, *34*, 1062-1063. (b) Hamamoto, H.; Mamedov, V. A.; Kitamoto, M.; Hayashi, N.; Tsuboi, S. *Tetrahedron: Asymmetry* **2000**, *11*, 4485-4497. (c) Tsuboi, S.; Sakamoto, J.; Yamashita, H.; Sakai, T.; Utaka, M. *J. Org. Chem.* **1998**, *63*, 1102-1108. (d) Tsuboi, S.; Yamafuji, N.; Utaka, M. *Tetrahedron: Asymmetry* **1997**, *8*, 375-379. (e) Duhamel, P.; Leblond, B.; biodois-Sery, L.; Poirier, J. J. *J. Chem. Soc. Perkin Trans. 1* **1994**, 2265-2271. (f) Tsuboi, S.; Sakamoto, J.; Sakai, T.; Utaka, M.; *Chem. Lett.* **1989**, *8*, 1427-1428. (g) Satoh, T.; Sugimoto, A.; Yamakawi, K. *Chem. Pharm. Bull.* **1989**, *37*, 184-186.
- (16) (a) Feske, B. D.; Kaluzna, I. A.; Stewart, J. D. *J. Org. Chem.* **2005**, *70*, 9654-9657. (b) Poessl, T. M.; Kosjek, B.; Ellmer, U.; Grubber, C. C.; Edegger, K.; Faber, K.; Hildebrandt, P.; Bornscheuer, U. T.; Kroutil, W. *Adv. Synth. Catal.* **2005**, *347*, 1827-1834.
- (17) Johnson, J. A.; Akers, W. S.; Herring, V. L.; Wolf, M. S.; Sullivan, J. M. *Pharmacotherapy* **2000**, *20*, 622-628.
- (18) King, J. A.; McMillan, F. H. *J. Am. Chem. Soc.* **1951**, *73*, 4911-4915.
- (19) Yadav, V. K.; Babu, K. G. *Tetrahedron* **2003**, *59*, 9111-9116.

- (20) Nakamura, K.; Inoue, Y.; Matsuda, T.; Misawa, I. *J. Chem. Soc. Perkin Trans. 1* **1999**, 2397-2402.
- (21) Ahmad, K.; Koul, S.; Taneja, S. C.; Singh, A. P.; Kapoor, M.; Riyaz-ul-Hassan; Verma, V.; Qazi, G. N. *Tetrahedron: Asymmetry* **2004**, *15*, 1685-1692.
- (22) Mastranzo, V. M.; Quintero, L.; Parrodi, C. A.; Juaristi, E.; Walsh, P. J. *Tetrahedron* **2004**, *60*, 1781-1789.
- (23) Donzelli, F.; Fuganti, C.; Mendoza, M.; Pedrocchi-Fantoni, G.; Servi, S.; Zucchi, G. *Tetrahedron: Asymmetry* **1996**, *7*, 3129-3134.
- (24) Nakamura, K.; Takenaka, K.; Fujii, M.; Ida, Y. *Tetrahedron Lett.* **2002**, *43*, 3629-3631.
- (25) Erdélyi, B.; Szabó, A.; Seres, G.; Birincsik, L.; Ivanics, J.; Szatzker, G.; Poppe, L. *Tetrahedron: Asymmetry* **2006**, *17*, 268-274.
- (26) Ferrabochi, P.; Grisenti, P.; Manzocchi, A.; Santaniello, E. *J. Chem. Soc. Perkin Trans. 1* **1990**, 2469-2474.
- (27) Choi, J. H.; Choi, Y. K.; Kim, Y. H.; Park, E. S.; Kim, E. J.; Kim, M.; Park, J. J. *Org. Chem.* **2004**, *69*, 1972-1977.

## **APPENDIX B**

### **Xerogel-Encapsulated W110A Secondary Alcohol Dehydrogenase from *Thermoanaerobacter ethanolicus* Performs Asymmetric Reduction of Hydrophobic Ketones in Organic Solvents**

**Research presented in this appendix was published as the following manuscript:**

Musa, M.M., Ziegelmann-Fjeld, K.I., Vieille, C., Zeikus, J.G., and R.S. Phillips. Xerogel-encapsulated W110A secondary alcohol dehydrogenase from *Thermoanaerobacter ethanolicus* performs asymmetric reduction of hydrophobic ketones in organic solvents. *Angewandte Chemie*. Early View DOI: 10.1002/anie.200604615

## B.1 Introduction, results and discussion

The use of biocatalysts in organic synthesis has become an effective and sometimes preferable alternative to normal chemical methodologies for the production of optically active compounds.<sup>[1,2]</sup> The asymmetric reduction of ketones and the kinetic resolution (KR) of racemic alcohols are the most important reactions for producing optically active alcohols, which then can be used to synthesize industrially important compounds like natural products.

A practical technique to improve enzyme performance is enzyme immobilization.<sup>[3]</sup> Most enzyme immobilization methods involve covalent attachment of the enzyme to an activated group on a solid or gel support, which may result in significant loss of activity. A simple and efficient non-covalent immobilization method is enzyme encapsulation in transparent porous silicate glasses prepared by the sol-gel method.<sup>[4]</sup> The resulting glasses allow the transport of small molecules, but not enzyme molecules, into and out of the glasses pores.<sup>[5]</sup> The sol-gel encapsulation of enzymes has a lot of advantages, such as ease of recycling, broad applicability, cost effectiveness, and safety.<sup>[3]</sup>

Alcohol dehydrogenases (ADHs) are enzymes that catalyze the reversible reduction of aldehydes and ketones to the corresponding alcohols.<sup>[6]</sup> However, ADHs have not been widely used for synthetic purposes in organic chemistry laboratories, in part because they require aqueous media, in which many ketone and alcohol substrates are poorly or not soluble; this leads to large reaction volumes and complicated product recovery.<sup>[2c,e]</sup> An obvious solution for this problem, using organic solvents,<sup>[7]</sup> was first demonstrated by Klivanov and co-workers.<sup>[8]</sup>

Secondary ADH (EC 1.1.1.2) from *Thermoanaerobacter ethanolicus* (TeSADH), a nicotinamide-adenine dinucleotide phosphate (NADP<sup>+</sup>)-dependent thermostable enzyme,<sup>[9,10]</sup> is a useful biocatalyst for synthetic applications because it tolerates organic solvents, and it accepts ketones and alcohols as substrates with high activities.<sup>[11,12]</sup> TeSADH obeys Prelog's rule, in which the coenzyme NADPH delivers its *pro*-R hydride from the *re* face of ketone substrates.<sup>[13]</sup> Recently, we have reported a new mutant of TeSADH, in which tryptophan-110 was replaced with alanine, W110A TeSADH.<sup>[14]</sup> Although this mutant is able to reduce phenyl ring-containing ketones at concentrations of 35 mM to produce their corresponding (*S*)-alcohols in Tris buffer/2-propanol (70:30, v/v), higher substrate concentrations are required for practical production of optically active alcohols.

Herein, we report the use of encapsulated W110A TeSADH in sol-gel glasses to overcome the aforementioned limitation. In 2003, Gröger *et al.* reported a practical asymmetric enzymatic reduction of poorly water-soluble ketones using an ADH-compatible biphasic reaction medium.<sup>[15]</sup> One problem associated with using mixed aqueous and organic solvents, water-miscible or immiscible, for enzymatic reactions is the tendency of these solutions to form emulsions in the workup, which causes problems of product separation. If the water, necessary for enzyme activity, is entrapped with the enzyme within the sol-gel, the workup procedure can be simplified by using water-immiscible organic solvents, and therefore emulsion formation can be avoided.

Sol-gel encapsulated W110A TeSADH was prepared as previously reported,<sup>[5,16]</sup> with some modifications. The sol-gel was kept in Tris buffer medium until it was used as wet sol-gel (hydrogel). The asymmetric reduction of 4-phenyl-2-



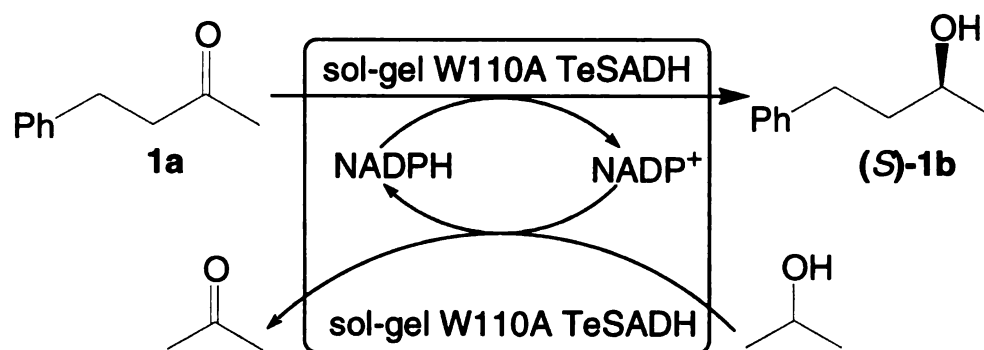
butanone (**1a**) to (*S*)-4-phenyl-2-butanol ((*S*)-**1b**), a precursor for the synthesis of bufeniode and labetalol, antihypertensive agents,<sup>[17]</sup> was used as a model in the screening reactions in this study. The hydrogel-encapsulated W110A TeSADH was used to reduce **1a** to (*S*)-**1b** in several different solvent systems (Table 1). The reduction carried out in aqueous buffer gave almost the same yield as with the free enzyme.<sup>[14a]</sup> However, the same sol-gel was reused three more times to give 56%, 30%, and 10% conversion, respectively. It was necessary to add 2.0 mg of NADP<sup>+</sup> for every new reaction because NADP<sup>+</sup> molecules either escape from the pores of the sol-gel glasses or become inactivated during turnover.<sup>[18a]</sup> The asymmetric reduction of **1a** was also carried out in Tris buffer/acetonitrile/2-propanol (41:41:18, v/v) to produce (*S*)-**1b** in good yield (81%). When the same sol-gel was reused, the yield was lower (43%). This indicates that W110A TeSADH is not inactivated by polar solvents. In all cases (*S*)-**1b** was produced with high enantioselectivity (>96% *ee*).

The asymmetric reduction of **1a** to (*S*)-**1b** was also performed in hexane and diisopropyl ether to give good to moderate conversions (80% and 40%, respectively) using hydrogel-encapsulated W110A TeSADH (Table 1). Although **1a** was reduced with higher yield in aqueous medium using sol-gel-encapsulated W110A TeSADH, using organic solvents makes the process more efficient by allowing the use of high concentrations of substrates (~140 mM). It also makes this asymmetric reduction accessible to hydrophobic substrates.

The W110A TeSADH hydrogel was dried in air for 24 h to form a xerogel (SiO<sub>2</sub>·nH<sub>2</sub>O). When this xerogel was used for asymmetric reduction of **1a** in Tris buffer/2-propanol (70:30, v/v), it gave the same conversion as that achieved by the hydrogel (Table 1). Asymmetric reduction of **1a** using the xerogel-encapsulated

**Table B-1.** Asymmetric reduction of **1a** using sol-gel encapsulated W110A TeSADH in different media.<sup>[a]</sup>

- [a] Unless otherwise stated, all reactions were performed at 50° C using sol-gel samples containing W110A TeSADH (0.43 mg) and NADP<sup>+</sup> (3.0 mg), **1a** (0.34 mmol), 2-propanol (600 µL), and 2.0 mL solvent.
- [b] 50 mM Tris buffer pH 8.0 (3.5 mL) and 2-propanol (1.5 mL).
- [c] 50 mM Tris buffer pH 8.0 (1.5 mL), CH<sub>3</sub>CN (1.5 mL) and 2-propanol (600 µL).
- [d] % conversion was determined by GC. [e] *ee* was determined by chiral stationary phase GC for the corresponding acetate derivative.<sup>[24]</sup>



Solvent	Hydrogel		Xerogel	
	Conv. [%] <sup>[d]</sup>	ee [%] <sup>[e]</sup>	Conv. [%] <sup>[d]</sup>	ee (%) <sup>[e]</sup>
50 mM Tris buffer pH 8.0 <sup>[b]</sup>	93 (1st)	98	92	98
	56 (2nd)	98		
	30 (3rd)	98		
	10 (4th)	98		
50 mM Tris buffer/CH <sub>3</sub> CN (1:1) <sup>[c]</sup>	81 (1st)	97	-	-
	43 (2nd)	97		
hexane diisopropyl ether	80	96	74	97
	40	97		

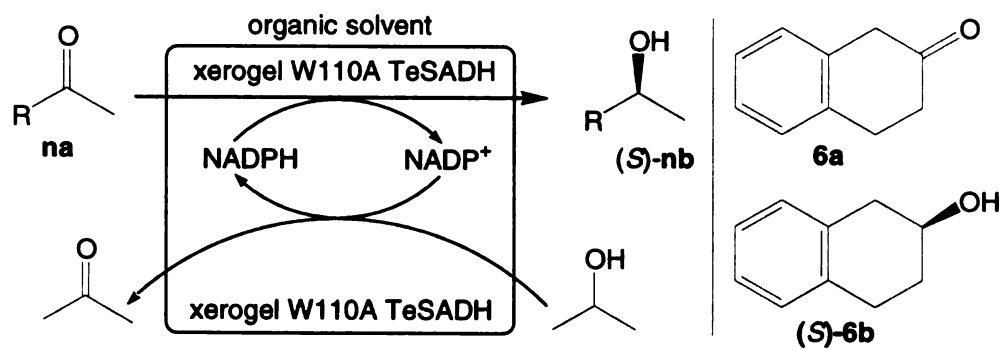
W110A TeSADH in hexane gave 74% conversion, compared to 80% with the hydrogel form. These results indicate that the xerogel retains the essential water molecules required for enzyme activity.<sup>[18b]</sup> Using the xerogel instead of hydrogel is preferable as it simplifies the work up procedure.<sup>[18c]</sup>

The lower yield for the asymmetric reduction using sol-gel encapsulated enzyme, compared to the reduction using free enzyme,<sup>[14a]</sup> could be due to the slow diffusion of substrate, product, and cosubstrate into and out of the sol-gel glasses. Regardless, the use of sol-gel encapsulated ADHs is of great advantage for several reasons beside the ease of workup. First, it makes these enzymes more stable than the free form, which makes them more attractive to organic chemists. Second, it allows the reuse of the enzyme. Third, it might allow these redox reactions to be mixed in situ with other organic reactions.

A series of phenyl ring-containing ketones were reduced using xerogel-encapsulated W110A TeSADH in hexane as a solvent and 2-propanol as a cosubstrate to produce their corresponding (*S*)-alcohols with good yields and high enantioselectivities (Table 2). All reactions were performed at 140 mM substrate concentrations. 1-Phenoxy-2-propanone (**2a**) was reduced with very high yield and enantioselectivity to produce (*S*)-1-phenoxy-2-propanol, (*S*)-**2b**. (*S*)-4-(4-Methoxyphenyl)-2-butanol, (*S*)-**3b**, was obtained from the enantioselective reduction of 4-(4-methoxyphenyl)-2-butanone (**3a**) with moderate yield and higher enantioselectivity, compared to the same alcohol produced by asymmetric reduction using free W110A TeSADH in Tris buffer (Table 2).<sup>[14a]</sup> Although 1-phenyl-2-propanone (**4a**) was reduced to (*S*)-1-phenyl-2-propanol, (*S*)-**4b**, with high yield but rather low *ee* (37%) in aqueous media,<sup>[14a]</sup> we were pleased to obtain good yield and

**Table B-2. Asymmetric reduction of phenyl ring-containing ketones using xerogel W110A TeSADH in organic solvents.**<sup>[a],[b]</sup>

- [a] All reactions were performed at 50°C using xerogel samples containing W110A TeSADH (0.43 mg), and NADP<sup>+</sup> (3.0 mg), substrate (0.34 mmol), 2-propanol (600 µL), and 2.0 mL hexane.
- [b] The absolute configuration was determined as described previously.<sup>[14a]</sup>
- [c] Results of reduction with free W110A TeSADH in 50 mM Tris buffer (pH 8.0)/2-propanol (70:30, v/v) are given in parentheses.<sup>[14a]</sup>
- [d] % conversion was determined by GC.
- [e] *ee* was determined by chiral stationary phase GC for the corresponding acetate derivative.<sup>[24]</sup>



<i>n</i>	R, (solvent)	Conv. [%] <sup>[c],[d]</sup>	<i>ee</i> [%] <sup>[c],[e]</sup>
1	Ph(CH <sub>2</sub> ) <sub>2</sub>	74 (99)	97 (>99)
2	PhOCH <sub>2</sub>	>99 (>99)	>99 (>99)
3	<i>p</i> -MeOC <sub>6</sub> H <sub>4</sub> (CH <sub>2</sub> ) <sub>2</sub>	61 (87)	94 (91)
4	PhCH <sub>2</sub> , (hexane)	80 (95)	69 (37)
	PhCH <sub>2</sub> , (toluene)	24	55
	PhCH <sub>2</sub> , (diisopropyl ether)	37	73
	PhCH <sub>2</sub> , ( <i>tert</i> -butyl alcohol)	38	63
5	<i>p</i> -MeOC <sub>6</sub> H <sub>4</sub> CH <sub>2</sub>	67 (97)	>99 (>99)
6		94 (>99)	76 (71)

significantly improved enantioselectivity (69% *ee*) using xerogel W110A TeSADH in hexane. The asymmetric reduction of **4a** was also performed using xerogel W110A TeSADH in toluene, *tert*-butyl alcohol, and diisopropyl ether to produce (*S*)-**4b** with 55, 63, and 73% *ee*, respectively. This indicates that the solvent can affect the enzyme enantioselectivity.<sup>[19]</sup> The lower yield in toluene (Table 2) may be due to competitive inhibition of aromatic ketone binding by toluene. The enantioselectivity of the reduction of **4a** by W110A TeSADH correlates neither with hydrophobicity nor with dipole moment of the solvent. This is consistent with the recent study of ADH-catalyzed reactions in biphasic systems by Filho *et al.*,<sup>[20]</sup> who reported that a single physicochemical parameter does not predict the biocompatibility of organic solvents but rather the solvent functionality would be of great significance. 1-(4-Methoxyphenyl)-2-propanone (**5a**) was reduced using the xerogel W110A TeSADH with a lower yield but the same *ee* compared to that using the free enzyme, producing (*S*)-1-(4-methoxyphenyl)-2-propanol ((*S*)-**5b**). The cyclic ketone, 2-tetralone (**6a**), was reduced to the corresponding (*S*)-2-tetralol ((*S*)-**6b**) by the xerogel with comparable yield to that produced using free W110A TeSADH in aqueous medium, but the *ee* of (*S*)-**6b** was improved in hexane using the xerogel (Table 2).

The low enantioselectivity observed in the reduction of **4a** and **6a** is a result of binding of these substrates in alternative ways within the large pocket of the active site,<sup>[14a]</sup> allowing NADPH to deliver its *pro*-R hydride to either the *re* face or the *si* face of the substrate. The improvement in enantioselectivity observed when these substrates are reduced by the xerogel W110A TeSADH in organic solvents is likely due to differences in solvation of the enzyme active site.<sup>[21]</sup> In an aqueous environment, the binding of a large substrate must displace solvent water from the

active site. The binding of the substrate in the “wrong” orientation may actually displace more water, making it favorable entropically.<sup>[22]</sup> In a non-aqueous medium, this entropic advantage would be diminished. We have previously proposed that active site solvation plays a significant role in the stereospecificity of aliphatic secondary alcohols by TeSADH.<sup>[23]</sup>

To our knowledge, this is the first report of a preparative scale asymmetric reduction using xerogel-encapsulated ADH in pure organic solvent media. This study clearly demonstrates that the misconception that practical nonaqueous enzymology is limited to hydrolases is false.

In summary, the tolerance of TeSADH to high concentrations of organic solvents allows asymmetric reduction of phenyl ring-containing hydrophobic ketones using xerogel-encapsulated W110A TeSADH. Sol-gel immobilization is a convenient method not only for reusing the enzyme but also for making the enzyme accessible to a wide variety of water-insoluble substrates by switching the traditional aqueous medium to organic media. This new method allows for the use of high concentrations of substrates that are crucial for large-scale synthetic applications. Reusable catalysts for chemo-, regio-, and enantioselective asymmetric reduction may be of industrial interest.



## B.2 Experimental Section

Commercial grade solvents were used without further purification. NADP<sup>+</sup>, tetramethyl orthosilicate (TMOS), **1a-3a**, and **6a** were used as purchased from commercial suppliers. **4a** and **5a** were prepared as described previously.<sup>[25]</sup>

Gene expression and purification of W110A TeSADH: W110A TeSADH was expressed in recombinant *Escherichia coli* HB101(DE3) cells and purified as described.<sup>[14b]</sup>

Preparation of sol-gel encapsulated W110A TeSADH: The silica sol was prepared by mixing TMOS (2.10 g), distilled water (0.47 g) and HCl (0.04 M, 3 drops). The mixture was then sonicated until one layer was formed. The gels were prepared by mixing 1.0 mL of the above sol with 1.0 mL of enzyme stock in a 10-mL round bottomed flask. The enzyme stock was prepared in 50 mM Tris buffer (pH 8.0) such that the concentration of the enzyme was 0.43 mg/mL and that of NADP<sup>+</sup> was 3.0 mg/mL. The sol-gel was then left in the same flask closed with Parafilm at RT for 48 h to allow gel aging. It was then used as is in the case of hydrogel. The hydrogel was dried at RT in air for 24 h to give hydrated silica SiO<sub>2</sub>.nH<sub>2</sub>O, the so-called xerogel.

Asymmetric reduction using xerogel-encapsulated W110A TeSADH in organic solvents: Unless otherwise mentioned, all reactions were performed using W110A TeSADH (0.43 mg) and NADP<sup>+</sup> (3.0 mg) encapsulated in sol-gel, substrate (0.34 mmol), 2-propanol (600  $\mu$ L), and 2.0 mL of organic solvent in a 10 mL round bottomed flask equipped with a magnetic stirrer. The reaction mixture was stirred at 50°C for 12 h. The sol-gel was then removed by filtration and washed with ethyl acetate (2 $\times$ 2 mL). The combined organic solvent was then concentrated under vacuum,

and the remaining residue was analyzed by a chiral column GC to determine the yield.

The residue was then converted to the corresponding acetate ester derivative to determine the *ee* of the product alcohol by GC.<sup>[23]</sup>

Capillary GC measurements were performed on a Varian 3300 GC equipped with a flame ionization detector and a Supelco  $\beta$ -Dex 120 chiral column (30 m, 0.25 mm [i.d], 0.25  $\mu$ m film thickness) using He as the carrier gas. All products were isolated and characterized as described previously.<sup>[14a]</sup> Their absolute configurations were determined by coinjection on a chiral column GC with their (*S*)- or (*R*)-alcohols, which were prepared by asymmetric reduction of the corresponding ketones or KR for the corresponding racemates using free W110A TeSADH.<sup>[14a]</sup>

### B.3 References

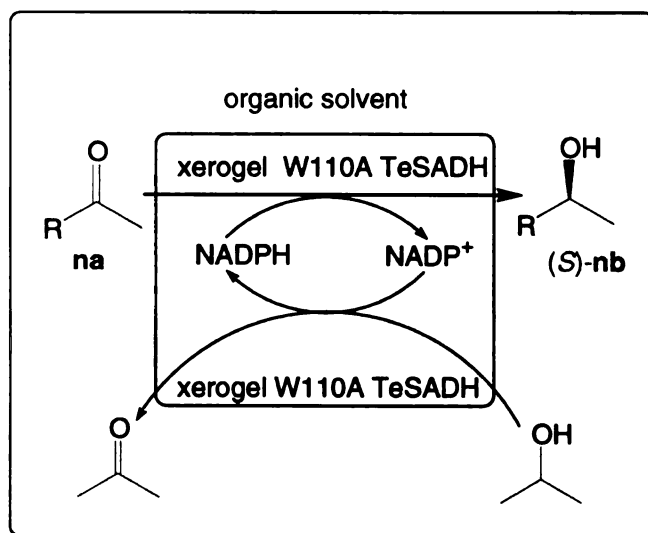
- [1] A. M. Thayer, *Chem. Eng. News* **2006**, 84 (33) 15-25.
- [2] a) E. Garcia-Urdiales, I. Alfonso, V. Gotor, *Chem. Rev.* **2005**, 105, 313-354; b) W. Kroutil, H. Mang, K. Edegger, K. Faber, *Curr. Opin. Chem. Biol.* **2004**, 8, 120-126; c) K. Nakamura, R. Yamanaku, T. Matsuda, T. Harada, *Tetrahedron: Asymmetry* **2003**, 14, 2659-2681; d) G. Carrea, S. Riva, *Angew. Chem. Int. Ed.* **2000**, 39, 2226-2254.
- [3] a) L. Cao, L. V. Langen, R. A. Sheldon, *Curr. Opin. Biotechnol.* **2003**, 14, 387-394; b) T. R. Gervais, G. Carta, J. L. Gainer, *Biotechnol. Prog.* **2003**, 19, 389-395.
- [4] a) L. E. Vera-Avila, E. Morales-Zamudio, M. P. Garcia-Camacho, *J. Sol-Gel Sci. Technol.* **2004**, 30, 197-204; b) F. Gelman, J. Blum, D. Avnir, *J. Am. Chem. Soc.* **2002**, 124, 14460-14463; c) M. T. Reetz, A. Zonta, J. Simpelkamp, *Biotechnol. Bioeng.* **1996**, 49, 527-534.
- [5] L. M. Ellerby, C. R. Nishida, F. Nishida, S. A. Yamanaka, B. Dunn, J. S. Valentine, J. I. Zink, *Science* **1992**, 255, 1113-1115.
- [6] a) D. Zhu, Y. Yang, L. Hua, *J. Org. Chem.* **2006**, 71, 4202-4205; b) W. Stampfer, B. Kosjek, K. Faber, W. Kroutil, *J. Org. Chem.* **2003**, 68, 402-406; c) J. S. Yadav, S. Nanda, P. T. Reddy, A. B. Rao, *J. Org. Chem.* **2002**, 67, 3900-3903; d) T. Schubert, W. Hummel, M. Müller, *Angew. Chem. Int. Ed.* **2002**, 41, 634-636; e) C. Heiss, R. S. Phillips, *J. Chem. Soc. Perkin Trans. 1* **2000**, 2821-2825.
- [7] a) A. M. Klibanov, *Curr. Opin. Biotechnol.* **2003**, 14, 427-431; b) A. M. Klibanov, *Nature* **2001**, 409, 241-246; c) Å. Jönsson, E. Wehtje, P. Adlercreutz, B. Mattiasson, *Biophys. Biochem. Acta* **1999**, 1430, 313-322.
- [8] J. Grunwald, B. Wirz, M. P. Scollar, A. M. Klibanov, *J. Am. Chem. Soc.* **1986**, 108, 6732-6734.
- [9] a) D. Burdette, J. G. Zeikus, *Biochem. J.* **1994**, 302, 163-170; b) D. C. Burdette, C. Vieille, J. G. Zeikus, *Biochem. J.* **1996**, 316, 115-122.
- [10] In unpublished results, Laivenieks *et al.* showed that TeSADH is identical to that from *Thermoanaerobium Brockii* (TBADH).
- [11] a) V. T. Pham, R. S. Phillips, *J. Am. Chem. Soc.* **1990**, 112, 3629-3632; b) V. T. Pham, R. S. Phillips, L. G. Ljugdahl, *J. Am. Chem. Soc.* **1989**, 111, 1935-1936.

- [12] a) C. Heiss, R. S. Phillips, *J. Chem. Soc. Perkin Trans. I* **2000**, 2821-2825; b) C. Heiss, M. Laivenieks, J. G. Zeikus, R. S. Phillips, *Bioorg. Med. Chem.* **2001**, 9, 1659-1666.
- [13] V. Prelog, *Pure Appl. Chem.* **1964**, 9, 119-130.
- [14] a) M. M. Musa, K. I. Ziegelmann-Fjeld, C. Vieille, J. G. Zeikus, R. S. Phillips, *J. Org. Chem.* **2007**, 72, 30-34; b) K. I. Ziegelmann-Fjeld, M. M. Musa, R. S. Phillips, J. G. Zeikus, C. Vieille, *Protein Eng. Des. Sel.* **2007**, 20, 47-55.
- [15] H. Gröger, W. Hummel, S. Buchholz, K. Drauz, T. V. Nguyen, C. Rollmann, H. Hüsken, K. Abokitse, *Org. Lett.* **2003**, 5, 173-176.
- [16] R. Obert, B. C. Dave, *J. Am. Chem. Soc.* **1999**, 121, 12192-12193.
- [17] J. A. Johnson, W. S. Akers, V. L. Herring, M. S. Wolf, J. M. Sullivan, *Pharmacotherapy* **2000**, 20, 622-628.
- [18] a) When the same sol-gel sample was reused without adding NADP<sup>+</sup>, only 10% conversion was achieved in the second reaction compared to 56% when new NADP<sup>+</sup> was added. b) About 65% by weight of the xerogel is water after 24 h drying in air. c) It was noticed that the xerogel loses its activity after drying for longer time (i.e. more than four days). However, the hydrogel is stable at room temperature for longer times as this enzyme has long-term stability.
- [19] P. A. Fitzpatrick, A. M. Klibanov, *J. Am. Chem. Soc.* **1991**, 113, 3166-3171.
- [20] M. V. Filho, T. Stillger, M. Müller, A. Liese, C. Wandrey *Angew. Chem. Int. Ed.* **2003**, 42, 2993-2996.
- [21] J. L. Schmitke, L. J. Stern, A. M. Klibanov, *Proc. Nat. Acad. Sci.* **1998**, 95, 12918-12923.
- [22] R. S. Phillips, *J. Mol. Cat. B* **2002**, 19-20, 103-107.
- [23] C. Heiss, M. Laivenieks, J. G. Zeikus, R. S. Phillips, *J. Am. Chem. Soc.* **2001**, 123, 345-346.
- [24] A. Ghanem, V. Schuring, *Tetrahedron: Asymmetry* **2003**, 14, 57-62.
- [25] J. A. King, F. H. McMillan, *J. Am. Chem. Soc.* **1951**, 73, 4911-4915.

## B.4 Asymmetric Synthesis

M. M. Musa, K. I. Ziegelmann-Fjeld, C. Vieille, J. G. Zeikus, and R. S. Phillips\*  
Xerogel-Encapsulated W110A Secondary Alcohol Dehydrogenase from  
*Thermoanaerobacter ethanolicus* Performs Asymmetric Reduction of Hydrophobic  
Ketones in Organic Solvents

**To gel well:** The asymmetric reduction of hydrophobic ketones by xerogel immobilized W110A secondary alcohol dehydrogenase from *Thermoanaerobacter ethanolicus* in organic solvents afforded their (S)-alcohols in comparable yields to these achieved using the free enzyme, and, in some cases, with higher enantioselectivities (see scheme). The use of xerogel ADH is a facile method as it allows the reuse of the enzyme, it makes it more stable, and it can affect its enantioselectivity by switching to organic solvents.



R= Phenyl ring-containing substituent

MICHIGAN STATE UNIVERSITY LIBRARIES



3 1293 03063 0762